

REGULATORY MECHANISMS IN INNATE IMMUNITY

APPROVED BY SUPERVISORY COMMITTEE

Zhijian J. Chen, Ph.D.

Eric Olson, Ph.D. (Chair)

Bruce Beutler, M.D.

Lora Hooper, Ph.D.

DEDICATION

I would like to thank my grandparents and my parents for their endless love and selfless support throughout my life.

I would also like to thank my mentor, Dr. James Chen, who is a great and brilliant scientist with rigorous attitude toward science, for his support during my whole Ph.D. life and for being a role model in pursuing science. I thank my thesis committee, Dr. Eric Olson, Dr. Lora Hooper, and Dr. Bruce Beutler, for their support and professional advice. I thank all the present and past lab members in Chen lab for being a united and productive family.

Last but not least, I thank my beloved fiancée, Xiaohong Li, for her love, support, and commitment to be with me for the rest of my life.

MECHANISM OF IRF5 ACTIVATION AND REGULATION OF CGAS ACTIVITY

by

JUNYAO REN

DISSERTATION

Presented to the Faculty of the Graduate School of Biomedical Sciences

The University of Texas Southwestern Medical Center at Dallas

In Partial Fulfillment of the Requirements

For the Degree of

DOCTOR OF PHILOSOPHY

The University of Texas Southwestern Medical Center at Dallas

Dallas, Texas

August 2018

Copyright

by

JUNYAO REN, 2018

All Rights Reserved

MECHANISM OF IRF5 ACTIVATION AND REGULATION OF CGAS ACTIVITY

JUNYAO REN, Ph.D.

The University of Texas Southwestern Medical Center at Dallas, 2018

Supervising Professor: Zhijian J. Chen, Ph.D.

Innate immunity is the frontline for the host to defend against infections. This process entails the cooperation among pathogen recognition receptors, adaptor proteins, kinases, and transcription factors that elicit the production of effector cytokines. As an important transcription factor, IRF5 was known to be essential for the host cytokine production in response to various ligands and SNPs in IRF5 have been closely related to autoimmune diseases. However, the mechanism by which IRF5 is activated is not well understood. In the first part of this dissertation, I presented evidence that the kinase IKK2 phosphorylates IRF5 on Serine 445, leading to its dimerization and nuclear translocation.

cGAMP is the first cyclic di-nucleotide discovered in metazoan. It is produced by the cytosolic DNA sensor cGAS in response to pathogen or self DNA as a second messenger to activate STING. cGAMP has been proven to be very important in anti-viral response and anti-tumor process. In the second part of the dissertation, I used next-generation sequencing techniques and presented that STING is the predominant receptor for cGAMP and innate immune response.

As the essential and general DNA sensor, cGAS was purified and identified from cellular cytosols. Upon DNA binding, cGAS utilize ATP and GTP to synthesize cGAMP. However, the regulation of cGAS activity in cells is still poorly understood. Here I presented that certain RNA species that is interferon inducible could inhibit cGAS catalytic activity in vitro and probably regulate cGAS mediated immune response in cells. Besides, I have discovered that during the cell cycle, cGAS is recruited and co-localize with chromosome and in actively dividing cells, cGAS remains in the nucleus. I further presented evidence that certain protein(s) in the nucleus can inhibit cGAS activity thus prevent cGAS from being activated by host DNA in the nucleus.

TABLE OF CONTENTS

TITLE	i
CHAPTER ONE: INTRODUCTION.....	1
CHAPTER TWO: IKKB IS AN IRF5 KINASE THAT INSTIGATES INFLAMMATION...	22
RESULTS	22
CONCLUSTION AND DISCUSSION.....	43
MATERIAL AND METHODS.....	45
CHAPTER THREE: STING IS THE PREDOMINANT RECEPTOR FOR CGAMP.....	50
RESULTS	50
CONCLUSTION AND DISCUSSION	83
MATERIAL AND METHODS	85
CHAPTER FOUR: CHARACTERIZATION AND PURIFICATION OF CGAS	
INHIBITOR(S)	89
CERTAIN RNA AS CGAS INHIBITOR	
RESULTS	89
CONCLUSTION AND DISCUSSION	102
CGAS INHIBITOR(S) FROM NUCLEUS	
RESULTS	104
CONCLUSTION AND DISCUSSION	114
MATERIAL AND METHODS	116
BIBLIOGRAPHY	121

PRIOR PUBLICATIONS

- Ren, J., Chen, X. and Chen, Z.J., 2014. IKK2 is an IRF5 kinase that instigates inflammation. Proceedings of the National Academy of Sciences, 111(49), pp.17438-17443.
- Liu, S., Cai, X., Wu, J., Cong, Q., Chen, X., Li, T., Du, F., Ren, J., Wu, Y.T., Grishin, N.V. and Chen, Z.J., 2015. Phosphorylation of innate immune adaptor proteins MAVS, STING, and TRIF induces IRF3 activation. Science, 347(6227), p.aaa2630.
- Yang, H., Wang, H., Ren, J., Chen, Q. and Chen, Z.J., 2017. cGAS is essential for cellular senescence. Proceedings of the National Academy of Sciences, p.201705499.

LIST OF FIGURES

FIGURE ONE	33
FIGURE 1-1.....	33
FIGURE 1-2.....	36
FIGURE 1-3.....	38
FIGURE 1-4.....	40
FIGURE 1-5.....	43
FIGURE 1-6.....	45
FIGURE 1-7.....	48
FIGURE 1-8.....	50
FIGURE 1-9.....	52
FIGURE TWO	62
FIGURE 2-1.....	62
FIGURE 2-2.....	66
FIGURE 2-3.....	68
FIGURE 2-4.....	70
FIGURE 2-5.....	71
FIGURE 2-6.....	73
FIGURE 2-7.....	75
FIGURE 2-8.....	76
FIGURE 2-9.....	79
FIGURE 2-10.....	82

FIGURE 2-11.....	84
FIGURE 2-12.....	86
FIGURE 2-13.....	88
FIGURE 2-14.....	90
FIGURE 2-15.....	92
FIGURE THREE	101
FIGURE 3-1.....	101
FIGURE 3-2.....	103
FIGURE 3-3.....	105
FIGURE 3-4.....	109
FIGURE 3-5.....	111
FIGURE 3-6.....	116
FIGURE 3-7.....	119
FIGURE 3-8.....	122

LIST OF TABLES

TABLE ONE	42
TABLE 1-1	42
TABLE 1-2	42
TABLE 1-3	44
TABLE TWO	64
TABLE 2-1	64
TABLE 2-2	67
TABLE 2-3	77
TABLE 2-4	98

CHAPTER ONE

INTRODUCTION

Innate immunity and adaptive immunity

The immune system consists of two major components: innate immunity, which provides early, general reactions to infections, and adaptive immunity, which later recognizes and reacts to microbial and non-microbial substances in a specific manner.

Once infection events are detected, the host quickly, usually within minutes to hours, initiate innate immune response as the first lines to defend. Cells involved in these lines include macrophages, natural killer (NK) cells, neutrophils and dendritic cells. These cells are recruited and migrate to the battlefield, the infection site where macrophages are activated and produce a large amount of effector chemokines (such as IL-8, IP-10, and CXCL-10) and cytokines (such as TNF-a, IL-6, IL-12, and type-I interferons) (Aderem 2001). These chemokines and cytokines lead to the effect of inflammation at the infection site, including vascular permeability increase, dendritic cells maturation, and neutrophil recruitment. To defend against infection, the innate immunity utilizes generally two methods. One is by the production of cationic antimicrobial peptides, including defensins and cathelicidins. Working together with conventional antibiotics, other peptides, and lysozyme, these peptides can kill bacteria very rapidly and can be effective against antibiotic-resistant infections (Hancock and Scott 2000). The other mechanism to defend infection is to kill by macrophages and neutrophils that have migrated to the site of infection. These cells can intake and eliminate pathogen particles either by phagocytosis or by receptor-mediated endocytosis.

The adaptive immune response usually takes place at least one day or several days after the initial contact with a pathogen. Lymphocytes, including B cells and T cells, are the major players in adaptive immunity and they provide the host with specific protection with memory. After in contact with antigens that have been processed and presented by dendritic cells and other antigen presenting cells, naïve B cells become activated and expand. Meanwhile, somatic hypermutation and affinity maturation processes increase the affinity of the antibodies produced by mature B cells for specific antigens. Antibodies are secreted and are able to recognize and bind to antigens presented on the surface of pathogens, such as virus and bacteria. The antibody-antigen binding would then initiate pathogen clearance responses. On the other hand, T lymphocytes play a central role in cell-mediated immunity and are consist of two major subtypes: CD4+ helper T cells (Th) and CD8+ cytotoxic T lymphocytes (CTL). CD4+ T cells produce various types of cytokines to assist other cell types in processes including the activation of macrophages and CTL, maturation of B lymphocytes and eliminate pathogens or tumors. CD8+ T cells, also called T-killer cells, are responsible to destroy compromised cells, including bacteria or virus-infected cells as well as tumor cells.

The general model for innate immune response

The innate immunity is a critical immune response that protects the host from infections immediately after they occur. The detection of the threats from viruses or bacteria is through a series of germline-encoded receptors, called pattern recognition receptors (PRRs). These receptors usually detect pathogen molecules that are much conserved evolutionarily, termed

as pathogen-associated molecular patterns (PAMPs). PAMPs are very specific to pathogens thus provide a mechanism for the immune receptors to differentiate non-self from self. One of the most famous PAMP is lipopolysaccharide (LPS) that is recognized by TLR4 together with an accessory protein MD2 (Kim et al. 2007). Upon ligand binding and activation, the alert signals are usually transmitted from the receptor to its downstream adaptor proteins. TLRs usually dependent on myeloid differentiation primary-response gene 88 (MyD88) (Burns et al. 1998) or TIR domain-containing adaptor inducing IFN- β (TRIF) (O'Neill and Bowie 2007) as adaptor proteins (Akira and Takeda 2004). RIG-I and MDA5 that sense RNA utilize mitochondrial antiviral-signaling protein (MAVS) for downstream signaling transduction (Seth et al. 2005). The newly discovered cytosolic DNA sensor, cGAS, synthesizes a secondary small messenger molecule, cGAMP, to activate its adaptor protein STING (Sun et al. 2013, Ishikawa, Ma, and Barber 2009). The activation of these adaptor proteins serves as a platform for the recruitment and activation of kinases, including TRAF family member-associated NF-kB activator (TANK)-binding kinase 1 (TBK1) (Fitzgerald et al. 2003), I κ B kinase (IKK) (Wang et al. 2001), IL-1 receptor (IL-1R)-associated kinase (IRAK) (Burns et al. 1998), Janus kinases (JAKs) (Der et al. 1998), and mitogen-activated protein kinases (MAPKs) (Chang and Karin 2001). These kinases, along with the adaptor proteins, activate transcription factors, including interferon regulatory factor (IRF) (Kawai and Akira 2007), NF-kB, activator protein 1 (AP1) (Kawai and Akira 2007), and signal transducers and activators of transcription (STATs) (Baetz et al. 2004). These transcription factors would translocate into the nucleus and, together with transcriptional co-factors, like

p200 and CBP, to promote the production of type-I interferons, inflammatory cytokines, and other effector proteins to eliminate infectious threats.

IRF5 signaling and autoimmune disease

The IRF family of transcription factors plays a pivotal role in the development of immune cells and induction of cytokines that are important in immune and inflammatory responses (Honda and Taniguchi 2006, Tamura et al. 2008). The mammalian IRF family consists of nine members, IRF1-9 (Ikushima, Negishi, and Taniguchi 2013). Among these, IRF3 and IRF7 have been extensively studied and shown to be important for the induction of type-I interferons (IFNs) and other cytokines in response to a variety of stimuli, such as virus infection. For example, infection with RNA viruses leads to the activation of RIG-I like receptors (RLRs), which in turn activate the mitochondrial adaptor protein MAVS(Kawai et al. 2005, Meylan et al. 2005, Seth et al. 2005, Xu et al. 2005, Yoneyama et al. 2004). MAVS then activates the kinase TBK1, which phosphorylates IRF3 and IRF7, causing these transcription factors to homodimerize and enter the nucleus to turn on type-I IFNs. MAVS also activates the kinase IKK β , which activates NF- κ B to induce pro-inflammatory cytokines. Stimulation of some Toll-like receptors (TLRs), especially those localized on the endosomal membranes such as TLR3, 4, 7, 8 and 9, also leads to strong activation of IRF3 and IRF7 to induce type-I IFNs(Noppert, Fitzgerald, and Hertzog 2007, Ikushima, Negishi, and Taniguchi 2013).

Compared to IRF3 and IRF7, much less is known about how IRF5 is activated. However, genetic studies have provided compelling evidence for an essential role of IRF5 in the production of inflammatory cytokines, such as TNF- α and IL-6, in response to TLR ligands

such as lipopolysaccharides (LPS) (Takaoka et al. 2005). IRF5 also functions together with IRF3 and IRF7 to mediate type-I interferon production in response to viral infections (Lazear et al. 2013). In addition, IRF5 plays important roles in M1 macrophage polarization (Krausgruber et al. 2011) and IgG class switching in B cells(Lien et al. 2010). Polymorphisms in the IRF5 gene have been linked to human autoimmune diseases, including systemic lupus erythematosus (Graham et al. 2006) and Sjogren's syndrome (Miceli-Richard et al. 2007). Thus, IRF5 is critical for regulating immune and inflammatory responses in health and disease(Lazzari and Jefferies 2014).

Similar to IRF3 and IRF7, IRF5 contains a DNA binding domain (DBD), an IRF association domain (IAD) and a Serine-rich region (SRR) at the C-terminus(Barnes, Moore, and Pitha 2001, Barnes et al. 2002). The SRR is phosphorylated in response to TLR stimulation or virus infection. The crystal structure of a human IRF5 mutant, S430D, which was proposed to mimic IRF5 phosphorylation, showed that IRF5 formed a dimer (Chen et al. 2008). However, the physiological phosphorylation sites of IRF5 had not yet been identified or validated. The kinase that mediates IRF5 phosphorylation was also unknown.

Toll-like receptor-mediated nucleic acid sensing

As the essential genetic information carrier for almost all life forms, nucleic acids are very important pathogen-associated molecular pattern (PAMP) molecules for innate immunity recognition. But at the same time, it is very important for the immune system to reduce the risk of recognizing self-nucleic acids, which might lead to autoimmune diseases(Ablasser, Hertrich, et al. 2013).

There are basically two groups of receptors that could sense DNA/RNA, determined by their localization in cells. Toll-like receptors (TLRs) are those localized on the endosome membrane and are expressed in dendritic cells, macrophages and B cells. The other group of receptors stay in the cytoplasm of cells and detect DNA and RNA molecules derived from pathogens that are exposed in the cytosol.

Most of the TLRs that recognize nucleic acids, including TLR3, TLR7, TLR8, TLR9, and TLR13, are exclusively expressed in intracellular membrane organelles, such as endoplasmic reticulum, endosome, and endolysosome. After ligand is taken by cells and processed, TLRs bind with the ligands, dimerize and undergo conformational changes that would recruit adaptor proteins, like MyD88, TRIF, TRAM, and TICAM1, to the TIR domain of the TLRs (Akira, Uematsu, and Takeuchi 2006). The adaptor proteins would then activate downstream signaling cascade and elicit the production of type-I interferons and proinflammatory cytokines.

The ectodomain of TLR3 can bind with double-stranded RNA (dsRNA) (Choe, Kelker, and Wilson 2005). The ligand for TLR3 widely used in the laboratory is polyinosinic-polycytidylic acid (poly(I:C)), a dsRNA analog. In physiological conditions, the dsRNA as TLR3 ligands can be derived from the replication process of ssRNA viruses or from symmetrical transcription in DNA viruses (Akira, Uematsu, and Takeuchi 2006). Both TLR7 and TLR8 can recognize ssRNA from RNA viruses. They are phylogenetically close to each other and appear to have different functions in different species (Kawai and Akira 2010). TLR7 is highly expressed in pDCs and can produce a large amount of type-I interferons in response to infection of HIV and influenza viruses (Diebold et al. 2004, Heil et al. 2004).

TLR8 is less studied than TLR7. Human TLR8 can also mediate the recognition of viral ssRNA but in mice, TLR8 deficient mice can still normally respond to ssRNA agonists (Kawai and Akira 2010). Different from human genomic DNA, in which CpG dinucleotides are of low frequency and are methylated, DNA from bacteria has a large amount of unmethylated CpG dinucleotides thus has a very strong stimulatory effect on the mammalian immune system (Yamamoto, Yamamoto, and Tokunaga 2000, Sparwasser et al. 1998, Jakob et al. 1998). By specifically binding with non-methylated CpG dinucleotides, TLR9 is used by vertebrate immune systems to distinguish bacterial DNA from self-DNA (Hemmi et al. 2000). More recently, TLR13 has been identified to be the sensor for 23S ribosomal RNA from bacteria (Li and Chen 2012, Oldenburg et al. 2012).

Interestingly, TLRs that recognized nucleic acids are also found to be involved in the pathogenesis of autoimmune diseases. In patients with systemic lupus erythematosus (SLE), a systemic autoimmune disease with production of autoantibodies (Groom et al. 2007), their serum contains self RNAs and DNAs in the form of protein complexes that can activate TLR7, TLR8, and TLR9 (Lafyatis and York 2009). TLR3 has been reported to be activated by RNA released from synovial fluid cells of patients with rheumatoid arthritis (RA) (Brentano et al. 2005). Since the activation of TLRs has been linked with the progression of autoimmune diseases, there are drugs targeting those receptors as treatment for diseases, including IRS 661 that block TLR7 signaling and inhibit the production of IFN- α in human plasmacytoid dendritic cells (pDC) (Barrat and Coffman 2008), and Chloroquine as antagonist for TLR7 and TLR9 (Sun et al. 2007).

Nucleic acid sensing in the cytosol

In addition to the TLRs on the membrane organelles, cells can also be alarmed of invading microbes by cytosolic nucleic acid sensors. One advantage of cytosolic nucleic acid sensors is that unlike TLRs, most of which are specifically expressed in immune cells like macrophages and dendritic cells, cytosolic DNA/RNA receptors are broadly expressed in different types of cells, including epithelial cells and fibroblasts, which are usually the frontlines of infections.

The major group of sensors for cytosolic RNA is the retinoic acid-inducible gene I-like receptor (RIG-I-like receptor, RLR) family, as was first identified in 2004 (Yoneyama et al. 2004). There are three RLRs identified so far, RIG-I, Melanoma Differentiation-Associated protein 5 (MDA5), and Laboratory of Genetics and Physiology 2 (LGP2) (Yoneyama and Fujita 2007). Both RIG-I and MDA5 contain two tandem caspase activation and recruitment domains (CARDs) in the N terminus that are essential for mediating the activation signals to downstream adaptor proteins, mitochondrial antiviral-signaling protein (MAVS) (Jiang et al. 2012, Goubau, Deddouche, and Reis e Sousa 2013). LGP2, however, lacks the card domain(s) and was previously regarded as a negative regulatory factor to virus-induced type-I interferon induction (Yoneyama et al. 2005, Komuro and Horvath 2006). But there are also studies indicating that LGP2 also plays a positive role in MDA5-mediated immune response (Satoh et al. 2010). RIG-I can specifically recognize single-stranded RNA with 5'-triphosphate, a marker of non-self RNA (Hornung et al. 2006). Though primary transcripts transcribed in the nucleus also have 5'-triphosphate, these RNAs are subjected to various processing and modification processes thus cannot be detected by RIG-I. Besides, Both RIG-

I and MDA5 can bind with double-stranded RNA, but MDA5 has a preference for longer RNA molecules. According to loss of function research, RIG-I is essential for the interferon production in response to the infection of Sendai virus, NDV, vesicular stomatitis virus (VSV), influenza A virus, and Japanese encephalitis virus (JEV) while MDA5 is important for detecting cytokine production by encephalomyocarditis virus (EMCV), Tyler's virus and Mengo virus, all Picornaviruses (genus cardiovirus) (Yoneyama and Fujita 2007).

DNA sensing in the cytosol has long been an interest of research and significant progress has been made in recent years. Before the discovery of cGAS as the general cytosolic DNA sensor, a number of proteins had been proposed to have the function of DNA sensing in the cytoplasm. DNA-dependent activator of IRFs (DAI) was first discovered in 2007 as the DNA sensor that elicits type-I interferon production (Takaoka et al. 2007). Though the researchers proved that DAI had DNA binding activity and can associate with TBK1 and IRF3 to promote the transcription of interferon mRNAs, later knockout studies suggest that in cells deficient in DAI has normal interferon response to DNA stimulation (Ishii et al. 2008).

Gamma-interferon-inducible protein Ifi-16 (IFI-16) has been identified as a DNA sensor that can respond to DNA in both cytosol and nucleus (Orzalli, DeLuca, and Knipe 2012, Unterholzner et al. 2010). And latest publication also shows that IFI-16 works together with cGAS in the activation of STING during DNA sensing in human keratinocytes (Almine et al. 2017). However, there are also studies showing that some cells with IFI-16 knocked down exhibit normal interferon response to cytosolic delivered DNA, suggesting that IFI-16 might not be the general DNA cytosol DNA sensor (Brunette et al. 2012, Abe et al. 2013). The stimulator of interferon genes (STING, also known as transmembrane protein 173,

TMEM173), which will be discussed more in the following part, was also proposed to be a direct DNA sensor and can bind with dsDNA through its C terminus domain (Abe et al. 2013). However, the binding affinity of STING with dsDNA is very low and cell lines with STING only (without cGAS) can only respond to cyclic di-nucleotide but not dsDNA (Burdette et al. 2011, Wu et al. 2013), suggesting STING is more of an adaptor protein in DNA sensing pathway. Other less characterized proteins proposed as cytosol DNA sensor are probable ATP-dependent RNA helicase DDX41 (Zhang, Yuan, et al. 2011), LRR Binding FLII Interacting Protein 1 (LRRFIP1) (Yang et al. 2010), DExD/H-box helicase 9 (DHX9) (Kim et al. 2010), and Ku70 (Zhang, Brann, et al. 2011).

An important, well-characterized DNA sensor in the cytosol is absent in melanoma 2 (AIM2). Instead of inducing the production of type-I interferons and proinflammatory cytokines, AIM2 activates the inflammasome pathways, represented by the activation of the proteolytic enzyme caspase-1 and the maturation of IL-1 β (Muruve et al. 2008, Fernandes-Alnemri et al. 2009, Hornung et al. 2009, Burckstummer et al. 2009, Roberts et al. 2009). AIM2 binds DNA with its HIN200 domain and its pyrin domain can interact with apoptosis-associated speck-like protein containing a caspase activation and recruitment domain (ASC) molecule to activate both NF- κ B and caspase-1 (Hornung et al. 2009).

Cytosolic DNA sensing by cGAS/STING pathway

Before cyclic GMP-AMP synthase (cGAS) was identified as the essential and general cytosolic DNA sensor, it was known that stimulator of IFN genes (STING, also known as MITA and TMEM173) is an essential adaptor protein for the induction of type-I interferons (Ishikawa and Barber 2008, Zhong et al. 2008, Sun et al. 2009). Later in 2013, the discovery

of mammalian cyclic dinucleotides, cGAMP (Wu et al. 2013), and cGAS (Sun et al. 2013) put all pieces in general DNA sensing pathway together.

When cells are transfected with DNA or infected by DNA viruses, cytosolic DNA binds and activate cGAS to form dimeric 2:2 cGAS-DNA complexes (Zhang, Wu, et al. 2014, Li, Shu, et al. 2013), which synthesizes 2'3'-cGAMP from ATP and GTP. cGAMP then acts as a second messenger and binds to the adaptor protein, STING, with a very high affinity (Wu et al. 2013). 2'3'-cGAMP binding and activation induce significant conformational changes of STING protein (Gao, Ascano, Zillinger, et al. 2013, Zhang et al. 2013). Specifically, cGAMP binding induced the two STING molecules in the dimeric complex to undergo a ~20 Å inward rotation, resulting in a deeper pocket for cGAMP binding along with the formation of a β sheet lid that covered the cGAMP binding site (Cai, Chiu, and Chen 2014). The activated STING dimer then translocate from ER to the ER-Golgi intermediate compartments (ERGIC) (Dobbs et al. 2015), during which kinases including TBK1 and probably IKK2 are recruited and activated. Then within the STING-kinase complexes, transcription factors including IRF3 and NF-κB are recruited and activated. After activation, the transcription factors translocate into the nucleus to elicit the production of type-I interferons and proinflammatory cytokines. Meanwhile, STING protein is also phosphorylated and degraded (Konno, Konno, and Barber 2013, Dobbs et al. 2015), probably as a shut-down mechanism for DNA-sensing pathway.

Since the discovery of cGAS/cGAMP pathway, it has been proven that many pathological processes that involve self or non-self-DNA sensing are mediated by cGAS. It has already been established that cGAS is the essential sensor for DNA viruses like Herpes viruses (Sun

et al. 2013), Kaposi's sarcoma-associated herpesvirus (KSHV) (Ma et al. 2015), Vaccinia virus (VACV), and Murine Gammaherpesvirus 68 (MHV-68) (Ablasser, Goldeck, et al. 2013, Schoggins et al. 2014). Importantly, cGAS is also the innate immune sensor for human immunodeficiency virus (HIV) and Mycobacterium tuberculosis (MTB). cGAS can be activated by the reverse-transcribed DNA from HIV infection and knockout or knockdown of cGAS in mouse or human cell lines blocked cytokine induction by HIV, murine leukemia virus, and simian immunodeficiency virus. (Gao, Wu, et al. 2013). Activation of the DNA-dependent cGAS/STING pathway in response to MTB infection stimulates autophagy and the production of proinflammatory cytokines thus plays essential roles in host defense against MTB (Collins et al. 2015, Wassermann et al. 2015). So far, it has also been proven that multiple bacteria including Listeria monocytogenes (Hansen et al. 2014), Francisella (Storek et al. 2015), Chlamydia trachomatis (Zhang, Yeruva, et al. 2014), Neisseria gonorrhoeae (Andrade, Agarwal, et al. 2016), and Group B streptococcus (Andrade, Firon, et al. 2016). Very interestingly, though cGAS/cGAMP and STING are majorly directly involved in cytosolic DNA sensing, it has also been reports indicating that they may also contribute to the immune response to some RNA viruses. cGAS knockout mice show more susceptibility to West Nile virus (WNV) infection, which is a positive sense single-stranded RNA virus (Schoggins et al. 2014). Researchers have also observed that Sting knockout animals infected with VSV are also significantly sensitive to lethal infection compared to controls (Ishikawa, Ma, and Barber 2009). These discoveries suggest that cGAS/STING pathway may also play a role to regulating RNA sensing pathways or contribute to the basal innate immune response.

cGAMP as an endogenous secondary messenger

The cyclic GMP-AMP (cGAMP) synthase cGAS has been defined as the major and key sensor of cytosolic DNA. Upon binding of double-stranded DNA, cGAS catalyzes the production of cGAMP from ATP and GTP. cGAMP in turn functions as an endogenous second messenger to bind and activate STING to induce type I interferons (Sun et al. 2013). Cyclic dinucleotides (CDNs) that contain uniform 3'-5' linkage, are known to be produced and involved in multiple processes in bacteria and Dictyostelium(Romling, Galperin, and Gomelsky 2013). And these CDNs are proposed to activate STING to trigger innate immune response(Burdette et al. 2011). cGAMP is generated by cGAS is the first CDN found in metazoan. Biophysical, structural and cell-based analyses have shown that cGAMP contains two unique phosphodiester bonds: one between the 2' OH of GMP and the 5' phosphate of AMP and the other between 3' OH of AMP and 5' phosphate of GMP, referred to as 2'3'-cGAMP, which makes it unique from other previously known CDNs (Ablasser, Goldeck, et al. 2013, Diner et al. 2013, Gao, Ascano, Wu, et al. 2013, Zhang et al. 2013).

Upon its discovery, cGAMP, as a key molecule in cGAS DNA sensing pathway, has been proven to be an essential small molecule in many biological processes. Besides its function in sensing microbe DNAs, cGAMP also mediated other important physiological and pathological processes. Aberrant activation of DNA sensing pathway, usually caused by the recognition of self-DNA by cGAS, can cause autoimmune diseases, which also depend on the binding and activation of STING by cGAMP (Gao et al. 2015). It was well known that point mutations in 3' repair exonuclease 1 (Trex1; also known as DNase III), which is an

important 3' DNA exonuclease, are related to autoimmune diseases like Aicardi-Goutières syndrome (Crow et al. 2006). When the Trex1 deficient mice, which display inflammatory myocarditis (Morita et al. 2004) and accumulation of cytosolic DNA (Yang, Lindahl, and Barnes 2007), were crossed with mice with STING deletion, the double knockout mice were rescued from the autoimmune disease phenotypes (Gall et al. 2012). Similarly, mice deficient in DNase II, a lysosomal endonuclease, are embryonic lethal, due to the large amount of type-I interferon produced by macrophages due to cytosolic DNA accumulation (Yoshida et al. 2005). This phenotype can only be rescued by further knocking out the adaptor protein in the cytosolic DNA sensing pathway, STING (Ahn et al. 2012), but not the endosomal DNA sensor, TLR9 (Okabe et al. 2005), suggesting that cytosolic DNA sensing by cGAS is crucial in the progress of mutation induced autoimmune diseases.

Also, researchers have shown that cGAMP can serve as an effective adjuvant to boost immune response. They showed that 2'3'cGAMP is very effective in boosting the production of antigen-specific antibodies and T cell responses in mice and this effect is dependent on the presence of STING and type-I interferon receptor (Li, Wu, et al. 2013).

Since the rapid division and frequent loss of DNA repair machinery in tumors often cause the accumulation of DNA fragments in the cytoplasm, there is a chance for cGAS to sense the abnormal presence of cytosolic DNA in tumor cells and initiate an immune response to clear these cells. Previous publications have shown that STING is essential for the host immunity to respond to cancer cells (Ho et al. 2016, Woo et al. 2014). The DNA in the cancer cells that is sensed by cGAS could be from micronuclei generated from DNA damage, chromosome missegregation (Santaguida et al. 2017), or cell cycle arrest. Researchers

observed rapid cGAS accumulation in the micronuclei (Mackenzie et al. 2017), indicating that cGAS could be activated by DNA present in micronuclei. Recently, it has also been reported that cGAMP is also an effective anti-tumor molecule via STING-TBK1-IRF3 mediated innate immune response (Li et al. 2016, Corrales et al. 2015). The combination treatment of cGAMP, which activates dendritic cells and enhanced cross-presentation of tumor-associated antigens to CD8 T cells, and PD-L1 antibody showed a synergistic effect in terms of tumor control (Wang, Hu, et al. 2017), suggesting that cGAMP could be a very promising small molecule for cancer immunotherapy.

Furthermore, as a second messenger, cGAMP can also function non-autonomously by spreading among cells through gap junctions, which represent a novel immune strategy that allows the host to rapidly convey antiviral immune response in a horizontal manner. (Ablasser, Schmid-Burgk, et al. 2013) or by incorporating into newly formed viral particles, which might be utilized to generate cGAMP loaded viral particles for future vaccine development (Bridgeman et al. 2015, Gentili et al. 2015). This current knowledge about cGAMP has set the stage for its potential therapeutic applications.

Host regulation of cGAS/STING pathway

Post-translational modifications (PTMs), including phosphorylation, glutamylation, glycosylation, ubiquitination, and lipidation, are very import ways to regulate protein activity in cells, especially in cell signaling. It has been reported that the protein kinase, Akt, can phosphorylate the catalytic domain on cGAS protein at Serine 305 site (human cGAS, Serine 291 at mouse cGAS) and plays a negative role in cGAS-STING mediated antiviral immune

response (Seo et al. 2015), suggesting that Akt might serve as a checkpoint to fine-tune the activity of cGAS. Another inhibitory modification on cGAS are the poly-glutamylation by TTLL6, which abolishes its DNA binding activity, or mono-glutamylation by TTLL4, which blocked its catalytic activity (Xia et al. 2016). Conversely, CCP6 and CCP5 can remove the poly-glutamylation and mono-glutamylation, respectively, on cGAS and thus activate cGAS. When cells are infected by HSV, an interaction between an ER ubiquitin ligase, RNF185, and cGAS was observed (Wang, Huang, et al. 2017). After binding, RNF185 specifically modifies cGAS with K27-linked poly-ubiquitination, which enhanced its catalytic activity in cGAMP production. More interestingly, elevated mRNA level of RNF185 has been found in patient samples with Systemic Lupus Erythematosus, suggesting that unexpected cGAS activity due to hyperactivity of RNF185 could be the direct cause of the disease. cGAS has also been reported to be SUMOylated. One research group showed that sentrin/SUMO-specific protease 7 (SENP7) can reverse the conjugation of SUMO (small ubiquitin-like modifier) to cGAS at lysine 335, 372 and 382, which abolishes the DNA binding activity of cGAS, and thus promote the activation of cGAS (Cui et al. 2017). Interestingly, another group found that the SUMOylation of cGAS by the ubiquitin ligase Trim38 actually prevents cGAS from being ubiquitinated and degraded, thus stabilize cGAS and promote the downstream signaling (Hu et al. 2016). It is interesting but reasonable that SUMOylation by different enzymes on different sites of cGAS lead to different regulation effects. Besides PTM, Polyglutamine-binding protein 1 (PQBP1) emerged from a targeted RNAi screening has been proved to bind with HIV-1 derived double-stranded DNA as well as bind to cGAS to facilitate the activation of cytosolic DNA sensing (Yoh et al. 2015).

As the key adaptor protein that after cGAMP binding, activates downstream kinases including TBK1 and IKK, STING is also intensively regulated by PTMs. After TBK1 recruitment to STING, TBK1 phosphorylate STING at Serine 366, which is essential for STING to further recruit and activate IRF3 (Liu et al. 2015). Moreover, there is also evidence showing that the phosphorylation of STING at Serine 366 is crucial for its subsequent degradation (Konno, Konno, and Barber 2013), which might be the shutdown mechanism for the pathway. After translocating from ER to Golgi, palmitoylation of STING by Golgi factors is required for downstream events, since treatment with palmitoylation inhibitor 2-bromopalmitate (2-BP), which abolishes STING palmitoylation, would also block type-I interferon production (Mukai et al. 2016). Furthermore, multiple ubiquitin E3 ligases have been identified to regulate STING activity. The expression of tripartite motif protein 30 α (TRIM30 α) is induced by the activation of cytosolic DNA sensing pathway in dendritic cells, which in turn interacts with STING to promote the degradation of STING via K48-linked ubiquitination on its lysine 275 site, acting as a negative regulator of cGAS-STING pathway (Wang et al. 2015). Similarly, the E3 ubiquitin ligase RNF5 also targets STING at K48-linked ubiquitination on its lysine 150 site for degradation in a signal-dependent manner, resulting in inhibited IRF3 dimerization and type-I interferon production in response to viral infection (Zhong et al. 2009). On the other hand, TRIM32 ubiquitinates STING with K63-linkage at lysine 20, 150, 224, and 236, which would enhance its interaction with TBK1 and dramatically increase the downstream signaling and interferon production (Zhang et al. 2012). TRIM 56 is also reported to have similar effects on STING. It also targets STING with K63-linked ubiquitination at lysine 150, which is essential for its dimerization and

interaction with TBK1 and IRF3 (Tsuchida et al. 2010). Besides, upon cGAMP binding with STING, Autocrine Motility Factor Receptor (AMFR) on the ER is recruited to STING dimer in an insulin-induced gene 1 (INSIG1)-dependent manner, which would form a E3 ubiquitin ligase complex and ubiquitinate STING with K27-linkage and this modification is required for TBK1 recruitment as well as STING perinuclear translocation (Wang et al. 2014). So, in conclusion, the ubiquitination modification types and sites on STING determine its function to downstream events and regulate the host immune response to cytosolic DNA. In another study, STING is SUMOylated by TRIM38 during the initial stage of DNA stimulation, when STING stability and activity are enhanced. Later the SUMOylation modification is removed by Sentrin-specific protease 2 (SENP2) so that STING can be degraded to shut down the immune response (Hu et al. 2016).

One unique feature of STING activation is that it will translocate from ER to Golgi after cGAMP binding and in the process of TBK1 recruitment and activation, which can also be regulated by various factors. A small molecule inhibitor of ADP ribosylation factor (ARF) GTPase, Brefeldin A, which can block STING trafficking from ER to Golgi, can abolish the downstream signaling and interferon production, indicating that the trafficking of STING is essential for the pathway (Konno, Konno, and Barber 2013).

Regulation of cGAS/STING pathway by viral proteins

During the evolution process, microbes co-evolve with host immune system to evade the immune response and cGAS-STING pathway is thus target by various proteins from both viruses and bacteria.

ORF52, an abundant gammaherpesvirus-specific tegument protein initially found in Kaposi's sarcoma-associated herpesvirus (KSHV), can bind both cGAS and DNA and inhibit cGAS activity and downstream signaling. And the similar mechanism is also found in other gammaherpesviruses, indicating that the inhibitory mechanism is evolutionarily conserved (Wu et al. 2015). NS2B (non-structural protein 2B) encoded by dengue virus (DENV) was reported to specifically target host cGAS for lysosomal degradation and prevent cytosolic DNA sensing pathway to be activated. Interestingly, another protease complex from DENV, NS2B3 was also previously reported to specifically degrade human STING, but not mouse STING to evade host immune response (Aguirre et al. 2012). A tegument protein found in HSV-1, UL41, also known as the virion host shutoff protein, can help the virus to evade the cGAS/STING-mediated cytosolic DNA sensing response by degrading cGAS protein via its RNase activity (Su and Zheng 2017).

IpaJ, an effector protein from *Shigella flexneri* (a Gram-negative bacterial pathogen), has found to be able to potently inhibit STING signaling by inactivating ARF GTPase and thus blocking STING translocation from ER to the ER-Golgi intermediate compartment (ERGIC) (Dobbs et al. 2015). Viral IRF-1 from KSHV has also been reported to interact with STING at latency stage and this interaction would abrogate the interaction between STING and TBK1, blocking the activation of the pathway (Ma et al. 2015). Oncogenes from DNA tumor virus also target STING to subvert the host immune activity. The Leu-X-Cys-X-Glu (LXCXE) motif in E7 protein from human papillomavirus (HPV) and E1A viral protein from adenovirus can bind with STING and potently inhibit its activation, abolishing the type-I interferon production (Lau et al. 2015).

CHAPTER TWO

IKKB IS AN IRF5 KINASE THAT INSTIGATES INFLAMMATION

Results

The transcription factor interferon regulatory factor 5 (IRF5) is essential for the induction of inflammatory cytokines, but the mechanism by which IRF5 is activated is not well understood. Here we present evidence that the kinase IKK β phosphorylates and activates IRF5 in response to stimulation in several inflammatory pathways, including those emanated from Toll-like receptors and retinoic acid-inducible gene I-like receptors. IKK β phosphorylates mouse IRF5 at specific residues, including serine 445 (S446 in human IRF5 isoform 1), as evidenced by mass spectrometry analysis and detection with a phosphospecific antibody. Recombinant IKK β phosphorylated IRF5 at Ser-445 in vitro, and a point mutation of this serine abolished IRF5 activation and cytokine production. Depletion or pharmacologic inhibition of IKK β prevented IRF5 phosphorylation. These results indicate that IKK β is an IRF5 kinase that instigates inflammation.

IRF5 forms a dimer and is essential for cytokine induction by multiple innate immunity pathways.

To investigate the function and active form of IRF5, we depleted endogenous IRF5 in THP-1 cells by shRNA and reconstituted with mouse or human IRF5 (Figure 1-1A). Then we measured cytokine induction by LPS in these cells. The expression of CXCL10 and IL-12 was

largely abolished when IRF5 was knocked down but strongly induced when either human or mouse IRF5 was ectopically expressed (Figure 1-1B); the higher induction levels in the IRF5 reconstituted cells were likely due to the higher levels of IRF5 (Figure 1-1A). Similarly, LPS induction of IFN- β and several interferon-stimulated genes (ISGs), including IFIT3, RSAD2 and ISG15, was inhibited in the absence of IRF5 but restored when IRF5 was expressed (Figure 1-1C).

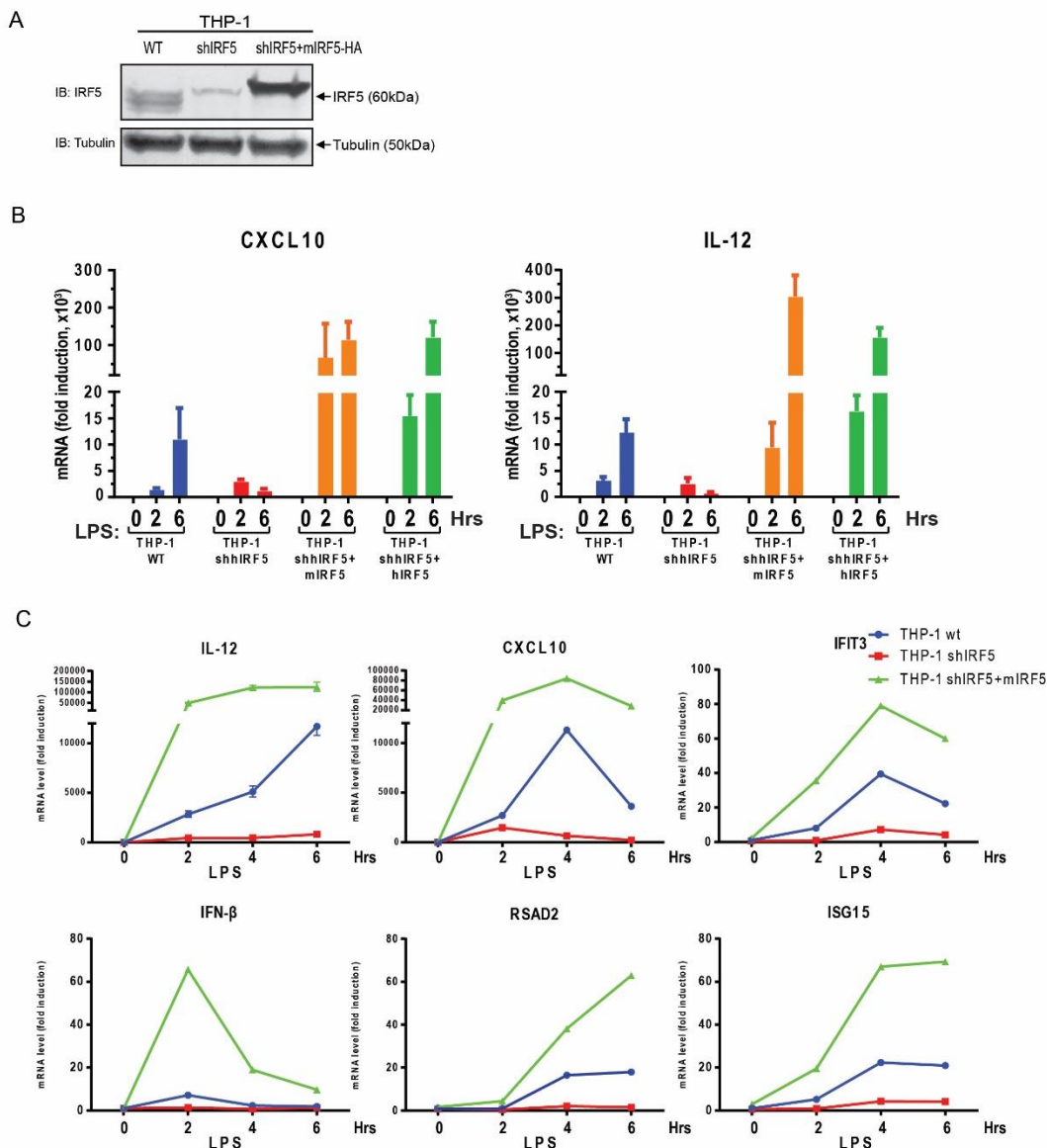


Figure 1-1. IRF5 is essential for cytokine induction by multiple innate immunity pathways.

(A) Efficiency of IRF5 knockdown and rescue in THP-1 cells. Cell extracts from WT THP1 (lane 1) and the cells stably expressing an shRNA against IRF5 with (lane 3) or without (lane 1) reconstitution with mIRF5-HA were immunoblotted with an IRF5 antibody.

(B) Depletion of IRF5 abolishes LPS-induced cytokine production in THP-1 cells. Cells used in this experiment include: Wild-type (THP-1 WT), IRF5 knockdown (THP-1 shIRF5), IRF5 knockdown and rescued with mouse IRF5 (THP-1 shIRF5+Flag-mIRF5-HA, labeled as THP-1 shIRF5+mIRF5) and IRF5 knockdown and rescued with human IRF5 (THP-1 shIRF5+HA-hIRF5, labeled as THP-1 shIRF5+hIRF5). These cells were stimulated with 5 μ g/mL LPS for the indicated time before total RNA was isolated. CXCL10 and IL-12 (p40 subunit) mRNA levels were analyzed by q-RT-PCR. Unless indicated otherwise, error bars represent standard deviations of triplicate assays.

(C) IRF5 is essential for LPS-induced expression of cytokines and interferon-stimulated genes (ISGs). THP-1 cell lines as described in (A) were stimulated with LPS (5 μ g/mL) for the indicated time. Total RNA was isolated to measure the expression of the indicated genes by q-RT-PCR.

To test whether activated IRF5 forms a dimer, we stimulated THP1 cells stably expressing HA-tagged IRF5 with LPS as well as other stimuli, including poly(dA:dT) and herring testis DNA (HT-DNA), both of which are known to activate the cGAS cytosolic DNA sensing pathway(Sun et al. 2013, Wu et al. 2013). Poly(dA:dT) also activates the RIG-I pathway through RNA polymerase III(Ablasser et al. 2009, Chiu, Macmillan, and Chen 2009). We also transfected the cells with the double-stranded RNA analog poly(I:C), which is known to stimulate the RIG-I and MDA5 pathways (Yoneyama et al. 2004). In each case, analyses by native polyacrylamide gel electrophoresis (PAGE) followed by immunoblotting showed that stimulation of the cells led to the formation of a slower migrating band that likely represents an IRF5 dimer, much like IRF3 dimerization following virus infection (Figure 1-2A). We have not been able to detect dimerization of endogenous IRF5 in THP1 cells, because the commercially available IRF5 antibody detected a strong non-specific band at the expected IRF5 dimer position on the native gel. Thus, for the remainder of this project, we measured

IRF5 activation using IRF5 dimerization assay in THP1-HA-IRF5 stable cells or by immunoblotting with a phospho-IRF5 specific antibody (see below).

To further investigate the role of IRF5 activation in inflammatory cytokine induction, we stably expressed IRF5 in HEK293T cells, which do not have detectable expression of endogenous IRF5, and then stimulated the cells by poly(I:C) transfection or infection with Sendai virus, an RNA virus known to activate the RIG-I – MAVS pathway. In both cases, the induction of TNF- α and IFN- β was strongly enhanced in 293T-IRF5 cells when compared to the parental cells. Sendai virus infection was capable of inducing IFN- β in the parental 293T cells because these cells express IRF3. Thus TNF- α induction by cytosolic RNA or RNA viruses is critically dependent on IRF5, whereas IFN- β induction was largely dependent on IRF3 but can be further enhanced by IRF5. These results suggest that the RIG-I pathway can activate both IRF3 and IRF5. Indeed, overexpression of MAVS led to the induction of both TNF- α and IFN- β (Figure 1-2B, right panels), as well as the dimerization of IRF5 (Figure 1-2C).

Interestingly, overexpression of IKK β strongly induced TNF- α expression and IRF5 dimerization but only weakly induced IFN- β (Figure 1-2B and 1-2C). The weak induction of IFN- β by IKK β overexpression can be explained by the fact that IRF3 is phosphorylated by TBK1 and IKK ϵ but not IKK β (Fitzgerald et al. 2003, Sharma et al. 2003). These results raise the interesting possibility that IKK β may play an important role in IRF5 activation.

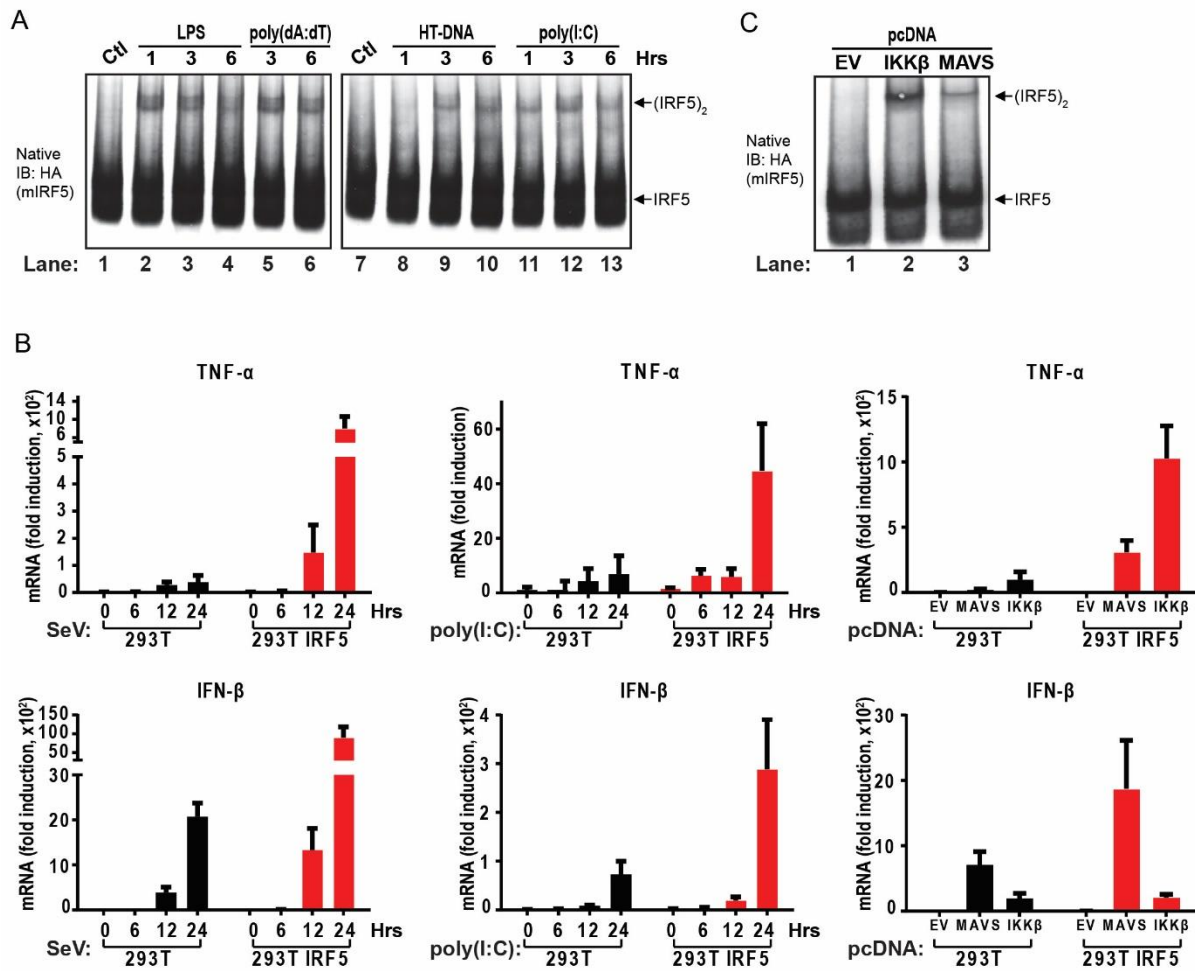


Figure 1-2. IRF5 forms a dimer in response to innate immune stimulus

(A) IRF5 forms dimer upon activation. THP-1 shIRF5+Flag-mIRF5-HA cell line as described in (1-1B) was left untreated (Control, Ctl) or stimulated by incubation with LPS (5 μ g/mL) or transfection with poly(dA:dT) (2 μ g/mL), HT-DNA (2 μ g/mL) or poly(I:C) (2 μ g/mL) for the indicated time. The formation of IRF5 dimer was analyzed by native gel electrophoresis, followed by immunoblotting with the HA antibody.

(B) IRF5 promotes cytokine induction in 293T cells. Wild-type 293T cells and those stably expressing Flag-mIRF5-HA were stimulated with Sendai virus (SeV) or poly(I:C) (2 μ g/mL) for the indicated time followed by measurement of TNF- α and IFN- β RNA levels by q-RT-PCR. Right panels: the cells were transfected with empty pcDNA vector, pcDNA-Flag-MAVS (MAVS) or pcDNA-Flag-IKK β (IKK β) for 24 hr before total RNA was isolated for analyses by q-RT-PCR.

(C) Over-expression of IKK β or MAVS activates IRF5 in cells. 293T Flag-mIRF5-HA cell line as described in (C) was transiently transfected with empty pcDNA vector or the vector

containing Flag-MAVS or Flag-IKK β for 24 hr. Dimerization of IRF5 was analyzed by native PAGE followed by immunoblotting with the HA antibody.

IKK β activates IRF5 in vitro and is important for IRF5 activation in cells

To obtain further biochemical evidence for the role of IKK β in IRF5 activation, we prepared cytosolic extracts from HEK293T cells stably expressing Flag-mIRF5-HA and incubated the extracts with recombinant IKK β or TBK1 protein together with ATP. Native PAGE analyses of the reaction mixtures revealed that IKK β caused the dimerization of IRF5 but not endogenous IRF3, whereas TBK1 had the opposite effects (Figure 1-3A). We also incubated *in vitro* translated, 35 S-labelled IRF5 with IKK β and observed IRF5 dimerization (Figure 1-3B).

To test which kinase is important for IRF5 activation in cells, we treated THP1 cells stably expressing Flag-mIRF5-HA with the IKK β inhibitor TPCA-1 or TBK1 inhibitor BX-795 and then stimulated the cells with LPS. TPCA1 but not BX-795 inhibited IRF5 dimerization, suggesting that IKK β was responsible for LPS-induced dimerization of IRF5 (Figure 1-3C). At the same time, we transiently overexpressed IKK2, TBK1, MAVS and TRIF protein to activate IKK2 and tested IRF5 activation in presence or absence of TPCA-1 and BX-795 (Figure 1-3D and E). These results proved that IKK2 was the exclusive kinase for IRF5. Surprisingly, IKK2 alone could activate IRF3 and this activation was independent of TBK1 kinase activity (Figure 1-3D, lane 3). Similarly, MAVS mediated IRF3 activation could not be blocked by TBK1 inhibitor alone while in TRIF mediated activation of IRF3, the kinase activity of TBK1 was essential, further indicating that IKK2 may also play some role in the activation of IRF3 in certain pathways.

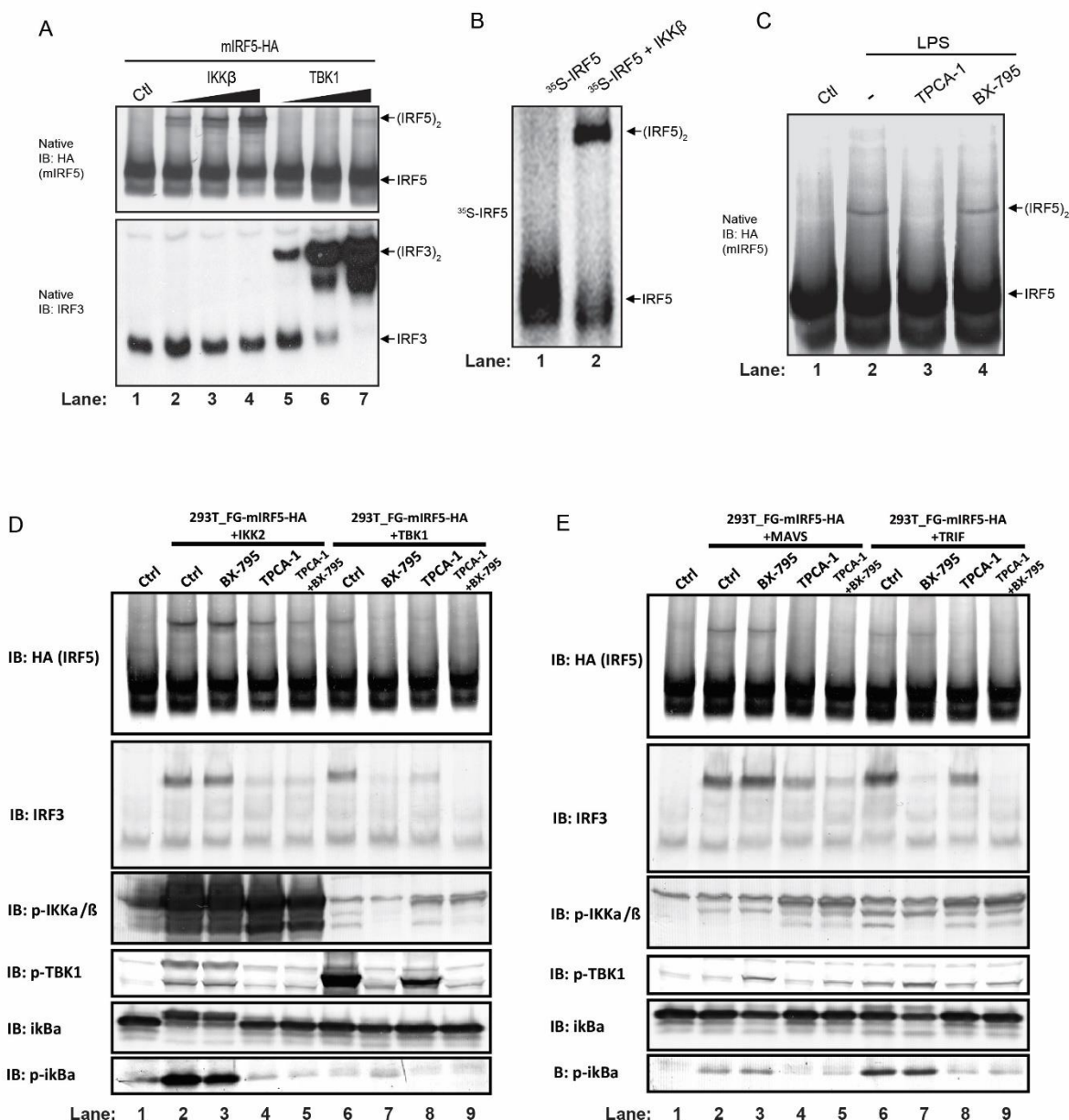


Figure 1-3. IKK β activates IRF5 in vitro and is important for IRF5 activation in cells

(A-B) IKK β activates IRF5 in vitro. (A) Cytosolic fraction (S20) from 293T Flag-mIRF5-HA cell line was incubated with purified IKK β or TBK1 protein in the presence of ATP. Dimerization of IRF5 or IRF3 was analyzed by native PAGE followed by immunoblotting. (B) In vitro translated 35 S-IRF5 or 35 S-IRF3 protein was incubated with BSA, IKK β or TBK1 in the presence of ATP. Dimerization of IRF5 or IRF3 was analyzed by native PAGE followed by autoradiography. Ctrl: control cytosolic fraction without kinase.

(C) IKK β inhibitor blocks IRF5 activation by LPS. THP-1 shIRF5 cells stably reconstituted with Flag-mIRF5-HA were treated with IKK β inhibitor (TPCA-1, 20 μ M) or TBK1 inhibitor (BX-795, 10 μ M) for 2 hr before stimulation with LPS (5 μ g/mL) for 2 hr. IRF5 activation was analyzed by native PAGE and immunoblotting. Ctl: DMSO control.

(D-E) 293T Flag-mIRF5-HA cells were first treated with TPCA-1 or BX-795 as described in (C), at the same time, the cells were also transfected with pcDNA-Flag- IKK β , pcDNA-Flag-TBK1, pcDNA-Flag-MAVS or pcDNA-Flag-TRIF as indicated for 24 hours. IRF5 and IRF3 activation were analyzed by native PAGE and immunoblotting. p-IKK, p-TBK1 and p-ikBa were also blotted.

To further examine the role of IKKs and other signaling molecules in IRF5 activation, we used shRNA to stably knock down the expression of IKK α , IKK β , TRAF6 or NEMO in HEK293T cells stably expressing Flag-mIRF5-HA. These cells were transfected with IKK β or MAVS, followed by analysis of IRF5 dimerization by native PAGE. The results showed that IKK β , TRAF6 and NEMO, but not IKK α , were required for IRF5 dimerization induced by MAVS (Figure 1-4A). And the requirement for TRAF6 in IRF5 activation was validated by the dimerization of IRF5 after overexpressing TRAF6 in TRAF6 knockdown cells (Figure 1-4B). IKK β knockdown partially inhibited IRF5 dimerization induced by IKK β overexpression, presumably because the shRNA only partially reduced the IKK β level. Knocking down other proteins, including IKK α , TRAF6 and NEMO, had little effects on IRF5 activation by IKK β . One more interesting observation was that though TNF-a treatment could potently activate IKK2, the treatment could not activate IRF5 (Figure 1-4C), suggesting that certain adapter protein, such as MAVS, TRIF, etc. might be needed in the activation process. Together, these results suggest that TRAF6, NEMO and IKK β mediate IRF5 activation by MAVS.

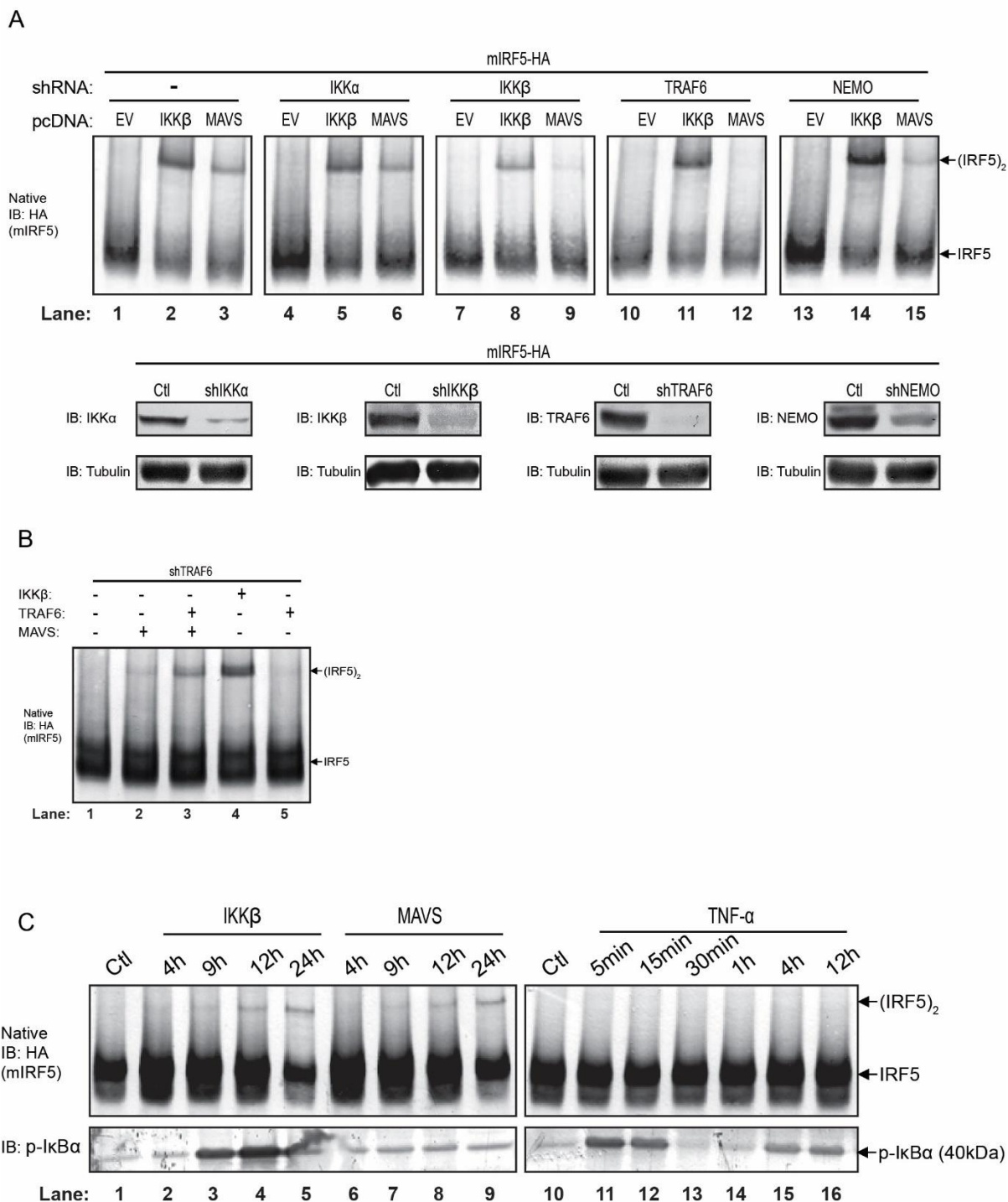


Figure 1-4. TRAF6, NEMO and IKK β mediate IRF5 activation by MAVS

(A) Knockdown of IKK β or TRAF6 abolishes IRF5 activation by MAVS. IKK α , IKK β , TRAF6 or NEMO was stably knockdown in 293T Flag-mIRF5-HA cells using lentiviral shRNA as

indicated. These cells were transfected with empty pcDNA vector, pcDNA-Flag-MAVS or pcDNA-Flag-IKK β for 24 hr. Activation of IRF5 was analyzed by native PAGE and immunoblotting. Lower panel: the knockdown efficiency for each gene was analyzed by immunoblotting.

(B) In 293T Flag-mIRF5-HA with TRAF6 knocked down cells, pcDNA-IKK β , pcDNA-MAVS, or (and) pcDNA-TRAF6 were transfected for 24 hours. IRF5 activation was analyzed by native PAGE and immunoblotting.

(c) 293T Flag-mIRF5-HA cells were transfected with pcDNA-Flag-IKK β (IKK β) or pcDNA-Flag-MAVS (MAVS) or treated with recombinant TNF- α protein (TNF- α) for the indicated time. Activation of IRF5 was analyzed by native PAGE followed by immunoblotting with an IRF5 antibody. Activation of IKK β was monitored by immunoblotting with a phospho-I κ B α antibody.

Phosphorylation of IRF5 at Ser-445 by IKK β is important for cytokine induction

To map the phosphorylation site(s) of IRF5, we incubated Flag-mIRF5-HA, which was partially purified from HEK293T cells stably expressing the protein, with IKK β or with BSA (as a control) in the presence of ATP and Mg $^{2+}$ at 30°C for 1 hour. IKK \square but not BSA caused IRF5 dimerization in this reaction (Figure 1-5A). The IRF5 protein from these reaction mixtures was further purified and analyzed by mass spectrometry, which revealed that peptides containing phosphorylated Ser-445 and Ser-434 of mIRF5 were greatly enriched in the reactions that contained IKK β , whereas the total counts of mIRF5 peptides were similar in both reactions (Table 1-1 and 1-2, Figure 1-5 B, C, and D). In addition, we also detected mIRF5 peptides containing phosphorylation at Ser-430 and 436 (Table 1-1).

Peptide	Condition	Non-phosphorylated peptide	Phosphorylated peptide
R.LQIpS445NPDLK.D	BSA	7	0
	IKK2	6	2
R.LQIpS445NPDLKDHMVEQFK.E	BSA	35	5
	IKK2	29	18
R.LLLEMFSGELpS434WSADSIR.L	BSA	55	0
	IKK2	51	12
R.LLLEMFpS430GELSWSADSIR.L	BSA	55	0
	IKK2	62	1
R.LLLEMFSGELSWpS436ADSIR.L	BSA	55	0
	IKK2	58	5

Table 1-1. IRF5 in reaction mixtures described in (1-5A) was purified with a Flag antibody and then analyzed by tandem mass spectrometry. The sequences of the peptides and number of non-phosphorylated and phosphorylated peptides in each condition are shown.

	Condition 1 (IRF5+BSA)	Condition 2 (IRF5+IKK2)
Coverage	96%	96%
Score	25151	25420
Matches	588	691
Sequences	44	46

Table 1-2. Summary of mass spectrometry data indicating the coverage of the IRF5 protein and the total numbers of peptide sequences in the experiment described in Figure 1-5A. The data were analyzed by MASCOT (MATRIX SCIENCE).

To further confirm the phosphorylation sites identified, we incubated the partially purified Flag-mIRF5-HA as mentioned above with BSA or recombinant MAVS protein (in the same condition as above). Similarly, MAVS but not BSA activated and dimerize IRF5 (Figure 1-5E). The subsequent IP-Mass spectrometry analysis detected exclusive phosphorylation modification on Serine 445 site and about 10% of the peptide detected were phosphorylated (Table 1-3).

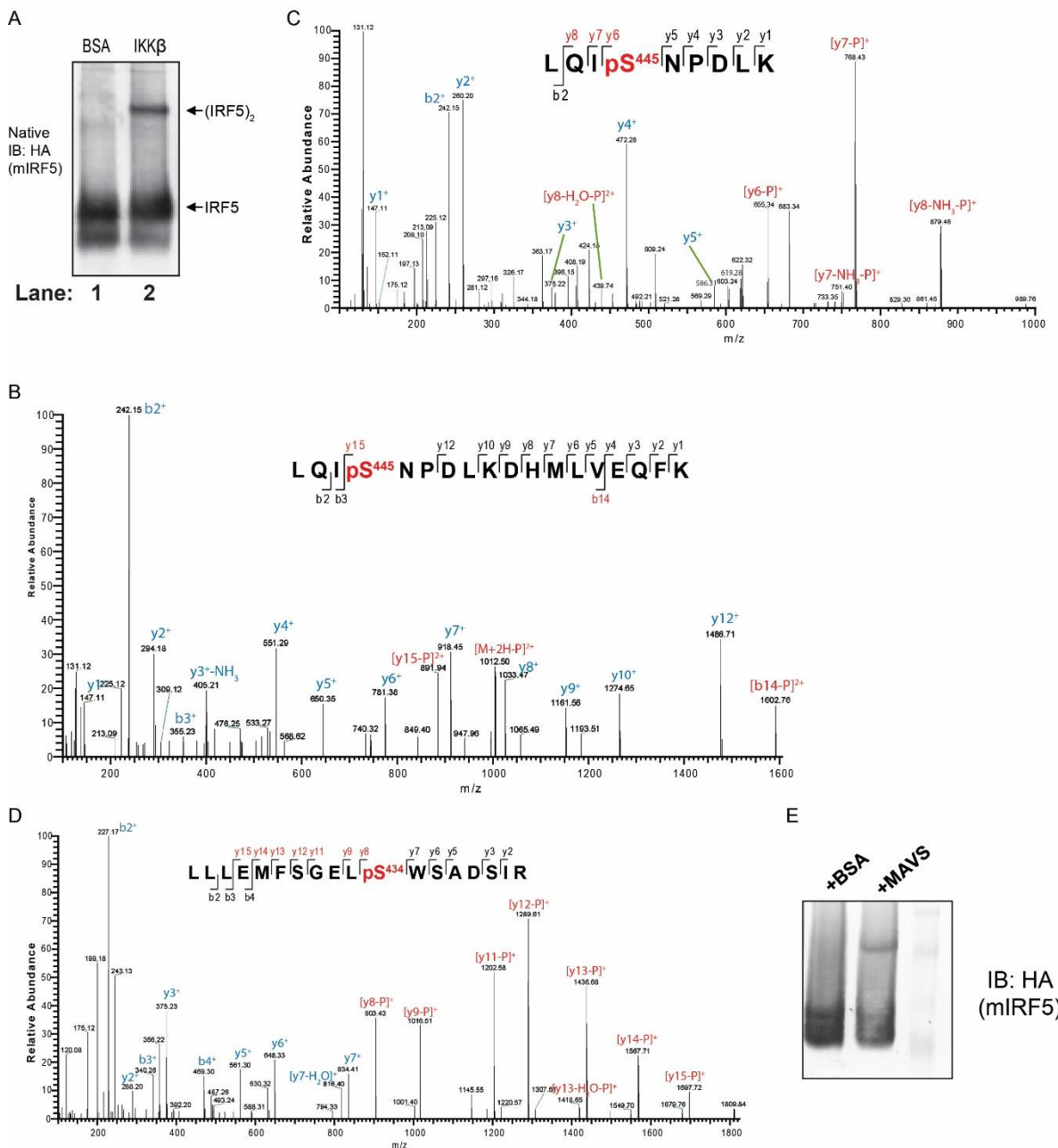


Figure 1-5. IKK β Phosphorylates IRF5 at Ser-445

(A) IKK β activates IRF5 in vitro. IRF5 partially purified from 293T Flag-mIRF5-HA cells was incubated with IKK β or BSA in the presence of ATP. Activation of IRF5 was analyzed by native PAGE and immunoblotting.

(C) A representative tandem mass (MS2) spectrum after HCD fragmentation of the ion with $m/z = 1061.50$ ($z = 2^+$) indicates phosphorylation at S445. “b” and “y” ions with or without neutral loss are labeled in blue. Diagnostic ions for phosphorylation are highlighted in red.

- (C) Tandem mass (MS2) spectrum after HCD fragmentation of the ion with $m/z = 554.28$ ($z = 2^+$), indicating S445 phosphorylation.
- (D) Tandem mass (MS2) spectrum after HCD fragmentation of the ion with $m/z = 1067.50$ ($z = 2^+$), indicating S434 phosphorylation.
- (E) *In vitro* activation of IRF5 similar to (A), but recombinant MAVS protein instead of IKK β was used.

To test which serine residues are important for IRF5 activation by IKK β , we mutated each serine residue identified above to alanine, *in vitro* translated the mutant proteins in the presence of ^{35}S -methionine, and used the proteins in reactions that contained IKK β or BSA (Figure 1-6A). Among the mutants tested, the S445A mutation completely inhibited, and S434A mutation partially inhibited, IRF5 dimerization, whereas the other mutations had little inhibitory effect. Interestingly, Ser-434 and Ser-445 are the most conserved residues among IRF5 proteins from different species and they are homologs to Ser-385 and Ser-396, respectively, of human IRF3 (Figure 1-6B), which are known to be critical phosphorylation sites essential for type-I interferon induction(Hiscott et al. 2006).

	Score	Matches	Squences	emPAI	Coverage	pS445	pS430_434_436_439
Control	38731	977	46	5415.2	88%	1/69	0/106
+MAVS	32020	856	44	5415.2	78%	7/67	0/9

Table 1-3. Summary of mass spectrometry data indicating the coverage of the IRF5 protein and the total numbers of peptide sequences in the experiment described in Figure 1-5E. The data were analyzed by MASCOT (MATRIX SCIENCE).

A previous study showed that a S480A mutation in human IRF5 (equivalent to S439A of mouse IRF5) impaired its ability to induce IFN- α (Barnes et al. 2002). When this serine was mutated to aspartic acid, (S380D in the version of human IRF5 used in the study), IRF5 formed a dimer whose crystal structure was solved (Chen et al. 2008). We therefore mutated this

residue (S439A in mouse IRF5) as well as other serine residues (S430A and S445A) and transfected them into HEK293T cells together with IKK β or MAVS. IRF5-S445A failed to dimerize in response to stimulation by IKK β or MAVS, whereas the S430A and S439A mutations had no effect (Figure 1-6C). Immunoblot analysis showed that the IRF5 serine to alanine mutants were expressed at similar levels to that of WT IRF5 (Figure 1-6C, Lower).

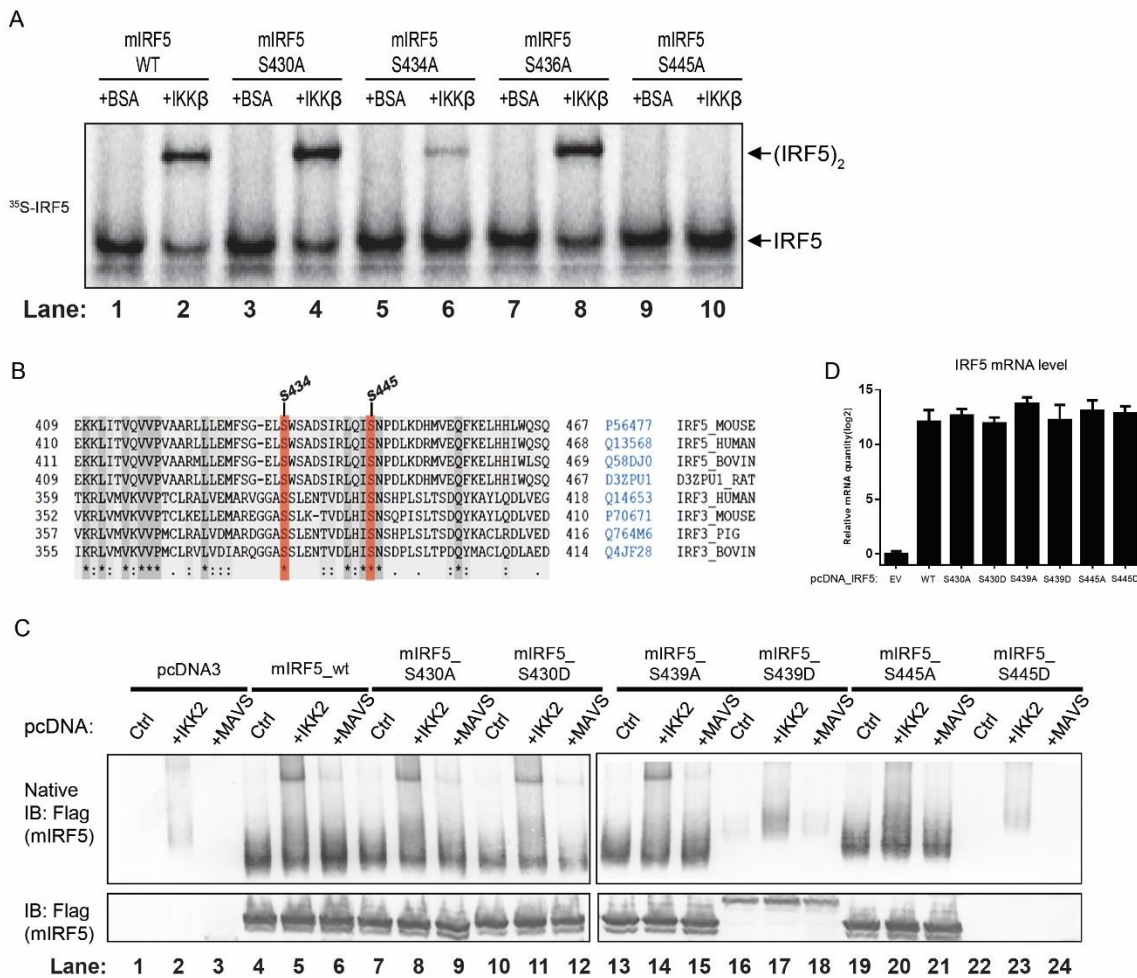


Figure 1-6. Phosphorylation of IRF5 at Ser-445 is essential for its dimerization

(A) Serine 445 is essential for IRF5 activation by IKK β *in vitro*. Wild-type or mutant 35 S-IRF5 proteins were translated *in vitro* and incubated with IKK β or BSA in the presence of ATP. Dimerization of IRF5 was analyzed by native gel electrophoresis, followed by autoradiography.

- (B) Sequence alignment of the C-termini of IRF5 and IRF3 from different species as indicated. Conserved serine residues in IRF5 and IRF3, including S434 and S445 of mouse IRF5, are highlighted.
- (C) S445A mutation of IRF5 prevented its activation by IKK β and MAVS in cells. 293T cells were transfected with the expression vectors for WT or mutant Flag-mIRF5 as indicated for 12 hr before another transfection with the expression vector encoding IKK β or MAVS for 24 hr. IRF5 dimerization (top) and expression (bottom) were analyzed by immunoblotting after native- and SDS-PAGE, respectively.
- (D) Total RNA from cells used in (C) were isolated for the measurement of IRF5 mRNA levels by q-RT-PCR.

Importantly, the S445A mutation abrogated the ability of IRF5 to stimulate the induction of TNF- α in response to IKK β , MAVS or Sendai virus infection (Figure 1-7A), whereas mutations at other serine residues did not have significant inhibitory effects (Figure 1-7C). The S445A mutation also partially inhibited IFN- β induction by MAVS but did not significantly affect IFN- β induction by Sendai virus (Figure 1-7B), presumably because IRF3 plays a dominant role in IFN- β induction in response to Sendai virus infections.

We also tested the IRF5 S445D mutant and found that this mutation largely inhibited IRF5 dimerization (Figure 1-7D) and abrogated the ability of IRF5 to boost TNF- α induction by IKK β (Figure 1-7E). Thus, the S445D mutation does not appear to mimic the effect of phosphorylation. And also, S445D mutant protein was not stable in cells. As shown in Figure 1-6C, lane 22 to 25, the protein was almost undetectable in SDS-PAGE analysis while its mRNA level was comparable to other mutants (Figure 1-6D).

As shown previously, IKK β only weakly induced IFN- β in a manner independent of IRF5, again consistent with a dominant role of IRF3 in IFN- β induction (Figure 1-7B). To determine the role of IRF5 phosphorylation in TLR signaling, we established a THP-1 stable cell line depleted of endogenous IRF5 and reconstituted with WT IRF5 or the S445A mutant.

The S445A mutation largely abrogated the ability of IRF5 to induce IL-12 in response to LPS stimulation (Figure 1-7F). Taken together, these results suggest that IKK β phosphorylates mIRF5 at Ser-445, and that this phosphorylation is important for inflammatory cytokine induction.

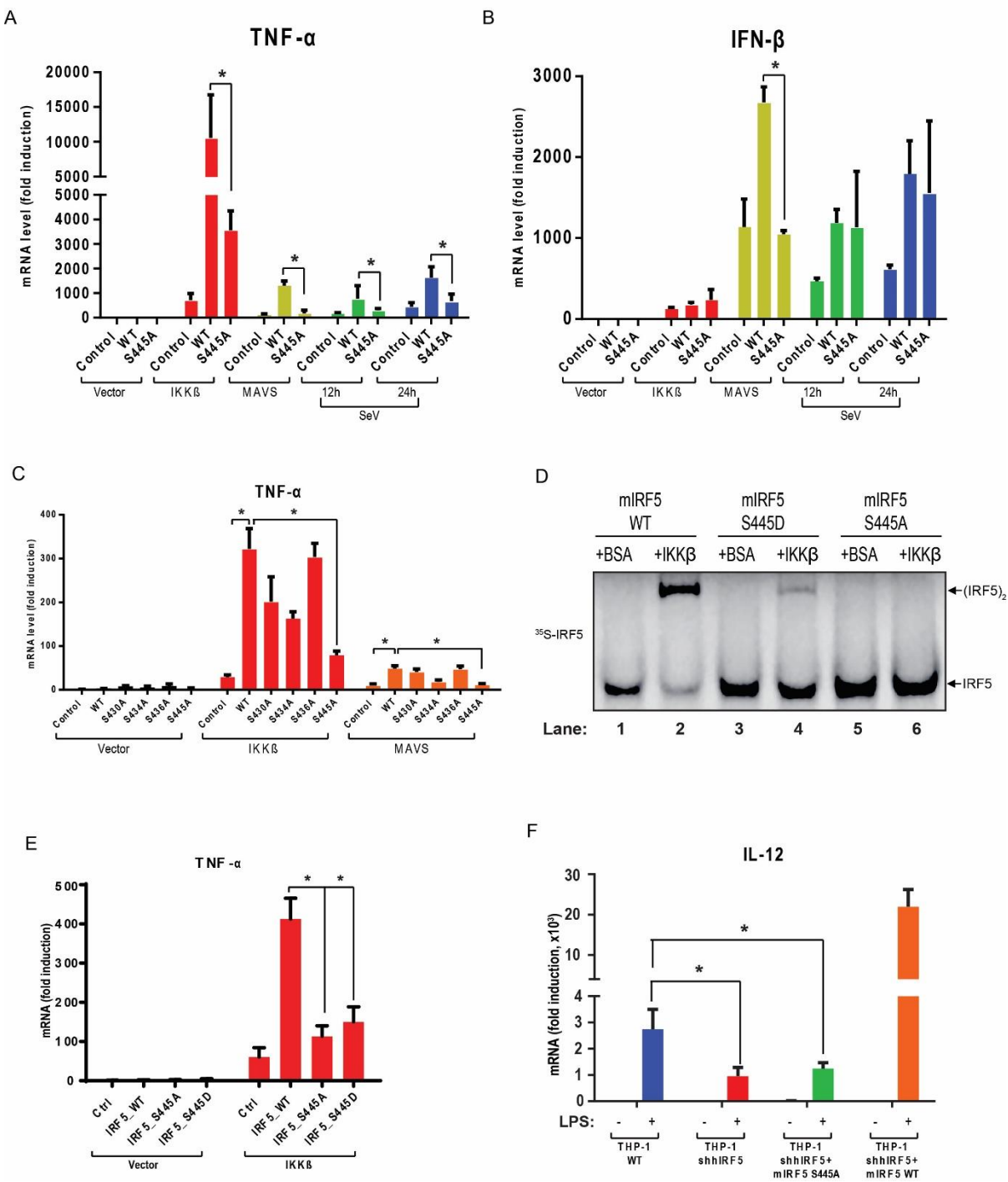


Figure 1-7. Phosphorylation of IRF5 at Ser-445 is important for cytokine induction

(A-B)293T cell lines stably expressing WT or S445A IRF5 were transfected with expression vectors for IKK β or MAVS for 24 hr, or infected with Sendai virus for the indicated time. Total RNA was isolated for the measurement of TNF- α and IFN β RNA levels by q-RT-PCR.

- (C) S445A mutation of IRF5 significantly inhibited TNF- α induction. Total RNA was isolated from cells described in (A) to measure TNF- α levels by q-RT-PCR.
- (D) S445D mutation also inhibited IRF5 dimerization. Wild-type and mutant 35 S-IRF5 (S445D and S445A) proteins were translated *in vitro* and incubated with IKK β or BSA in the presence of ATP. Dimerization of IRF5 was analyzed by native gel electrophoresis, followed by autoradiography.
- (E) S445D mutation of IRF5 inhibited TNF- α induction. Similar to (B) except that TNF- α RNA was measured by q-RT-PCR.
- (F) Wild-type (THP-1 WT), IRF5 knockdown (THP-1 shIRF5), IRF5 knockdown and rescued with wild-type or S445A mouse IRF5 (THP-1 shIRF5+mIRF5 WT or THP-1 shIRF5+mIRF5 S445A) THP-1 cell lines were stimulated with 5 μ g/mL LPS for 6 hr before total RNA was isolated. IL-12 p40 mRNA levels were analyzed by q-RT-PCR. *, P < 0.05, statistically significant difference.

Detection of IRF5 phosphorylation at Ser-445 with a phospho-specific antibody

To further investigate IRF5 phosphorylation in cells, we developed an antibody that recognizes IRF5 phosphorylated at Ser-445 by immunizing rabbits with a synthetic phosphopeptide (IRLQIP S^{445} NPDLC) corresponding to amino acids 440-450 of mouse IRF5 (441-451 of human IRF5). To test the specificity of this antibody, 293T cells stably expressing WT or S445A mutant of Flag-mIRF5-HA were transfected with an expression vector encoding IKK β or MAVS, both of which stimulated dimerization of WT but not S445A IRF5. Immunoprecipitation with the HA antibody followed by immunoblotting with the pIRF5 antibody showed that the antibody selectively detected WT but not S445A IRF5 after stimulation (Figure 1-8A), confirming that this antibody is specific for IRF5 phosphorylated at Ser-445.

To determine if IRF5 is phosphorylated at Ser-445 in response to physiological stimuli, we infected 293T cells stably expressing WT or S445A Flag-mIRF5-HA with Sendai virus. Immunoblotting with the p-IRF5 antibody confirmed that WT but not S445A IRF5 was

phosphorylated in the virus-infected cells and that this phosphorylation was abolished by the IKK inhibitor TPCA1 (Figure 1-8B, top panel). Sendai virus-induced dimerization of endogenous IRF3 was not affected by overexpression of WT or S445A IRF5 and was only partially inhibited by TPCA1 (Figure 1-8B, bottom). LPS stimulation of the macrophage cell line Raw264.7 stably expressing Flag-mIRF5-HA also led to IKK-dependent phosphorylation of IRF5 at Ser-445 (Figure 1-8C).

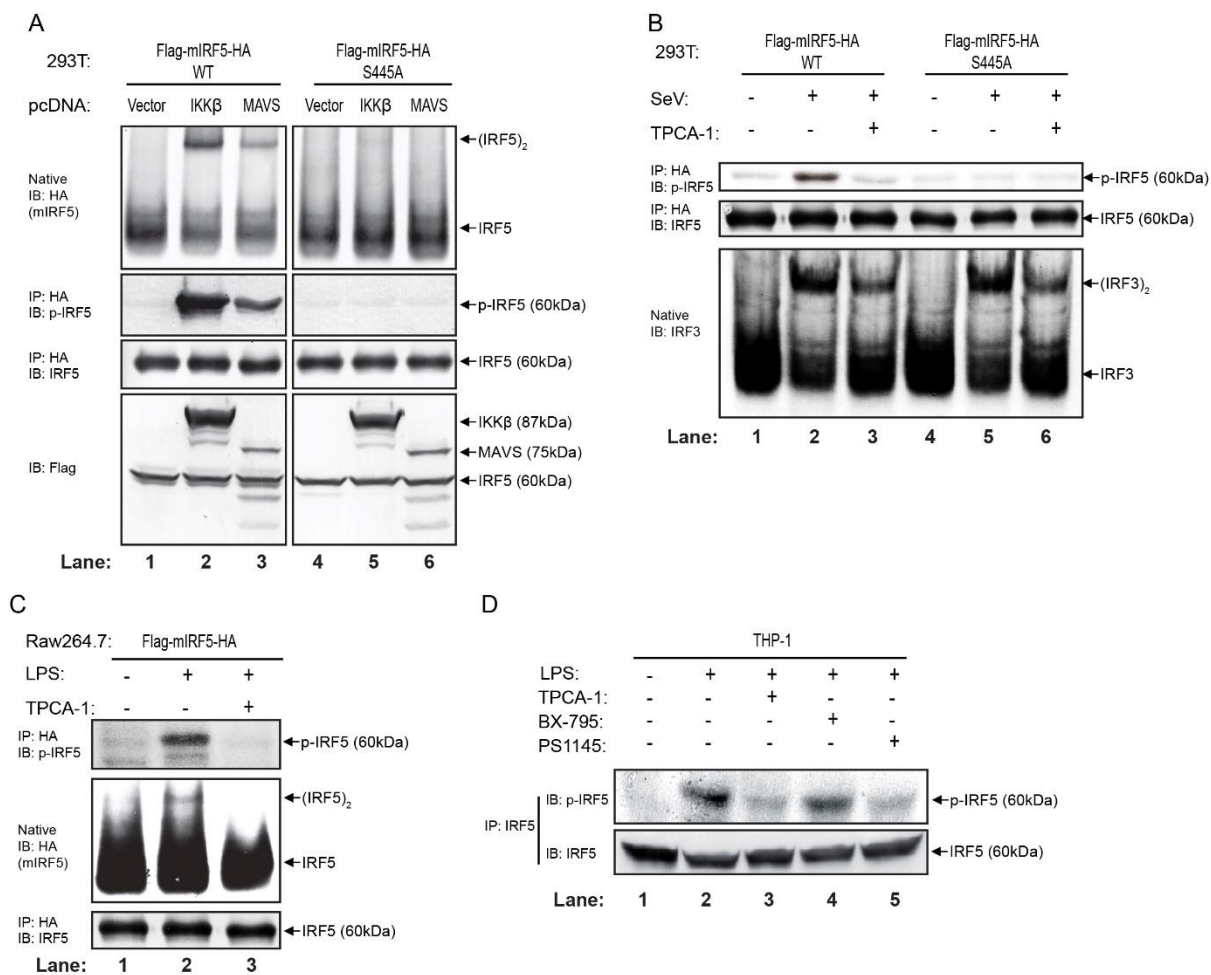


Figure 1-8. Detection of IRF5 phosphorylation at Ser-445 with a phospho-specific antibody
(A) 293T cells stably expressing WT or S445A Flag-mIRF5-HA were transfected with expression vectors for IKK β or MAVS for 24 hr. Aliquots of the cell extracts were analyzed for IRF5 dimerization by native PAGE, whereas other aliquots were immunoprecipitated

with the HA antibody followed by immunoblotting with an antibody against IRF5 or phosphorylated IRF5 at Ser-445. Expression of IKK β and MAVS was examined by immunoblotting with the Flag antibody (bottom).

(B) 293T cell lines as described above were treated with or without 20 μ M TPCA-1 for 2 hr before infected with Sendai virus for 24 hr. IRF5 was immunoprecipitated with an HA antibody followed by immunoblotting with an antibody against IRF5 or phosphorylated IRF5. Dimerization of IRF3 was detected by native PAGE and immunoblotting (bottom).

(C) Raw 264.7 cell stably expressing Flag-mIRF5-HA was treated with or without TPCA-1 (20 μ M) for 2 hr before stimulated with LPS (5 μ g/mL) for 2 hr.; IRF5 was immunoprecipitated with an HA antibody followed by immunoblotting with an antibody against IRF5 or phosphorylated IRF5. Dimerization of IRF5 was detected by immunoblotting of cytosolic extracts.

(D) THP-1 cell was treated with or without the IKK β inhibitors (TPCA-1 and PS1145) or TBK1 inhibitor (BX-795) for 2 hr before stimulation with LPS (5 μ g/mL) for 2 hr. Phosphorylated IRF5 was immunoprecipitated with an IRF5 antibody followed by immunoblotting with the same antibody or the phospho-IRF5 (S445) antibody

Finally, to determine if endogenous IRF5 is phosphorylated at Ser-445, we stimulated THP1 cells with LPS and then immunoprecipitated IRF5 with the p-IRF5 antibody followed by immunoblotting with the same antibody (Figure 1-8D). We also tested the effect of several kinase inhibitors on IRF5 phosphorylation and found that only IKK β inhibitors (TPCA-1 and PS1145), and not TBK1 inhibitor (BX-795), could inhibit the phosphorylation of IRF5 at Ser-445 in response to LPS (Figure 1-8D). Finally, we performed immunofluorescence analyses in THP1 cells using IRF5 and p-IRF5 antibodies. Consistent with previous reports (27), IRF5 translocated into the nucleus in response to LPS stimulation (Figure 1-9A). Importantly, the p-IRF5 signal was barely detectable in the absence of stimulation, and LPS stimulation led to the accumulation of p-IRF5 in the nucleus (Figure 1-9B). These experiments demonstrate that LPS stimulates the phosphorylation of endogenous IRF5 at Ser-445 and its subsequent translocation to the nucleus.

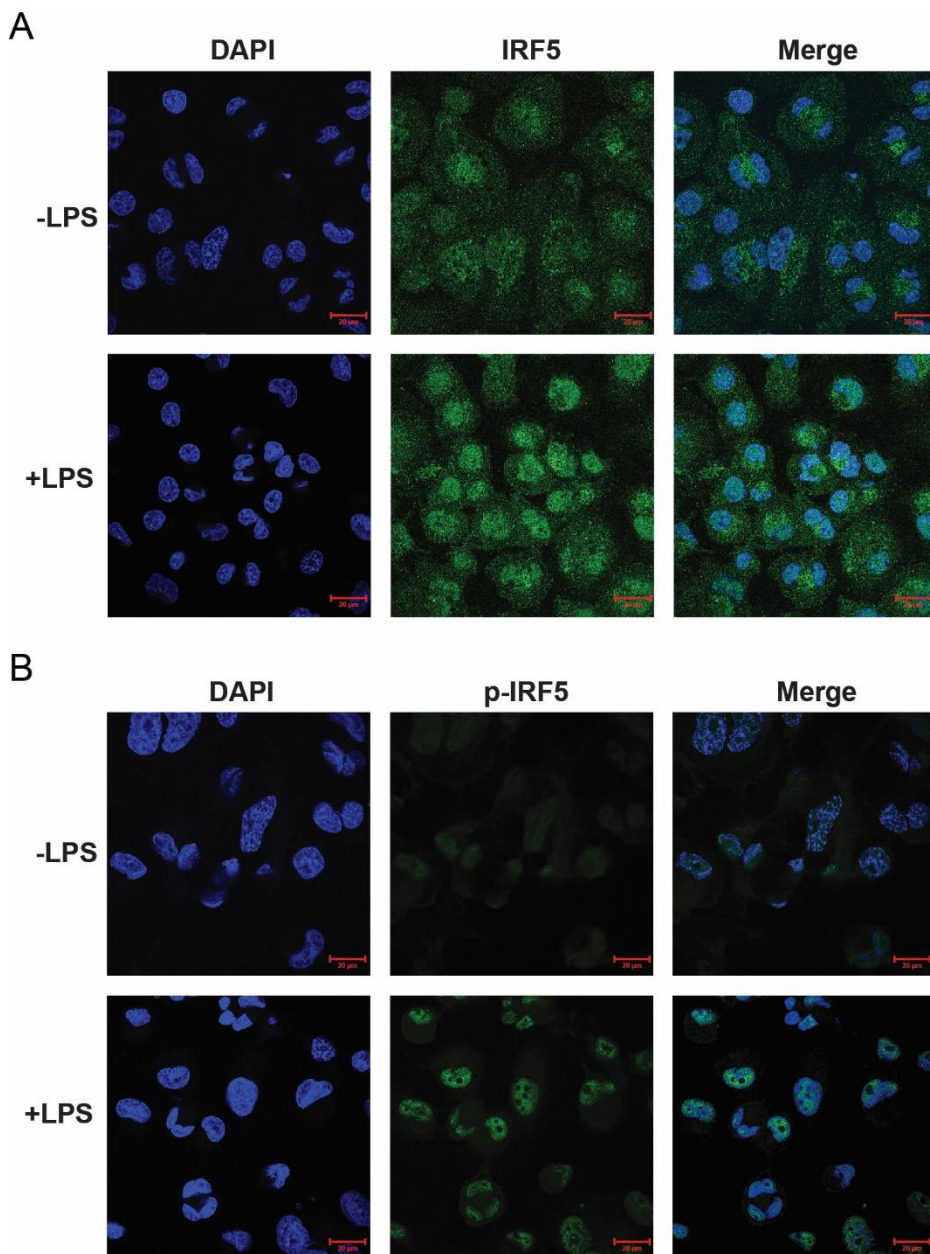


Figure 1-9. Immunofluorescence study shows that IRF5 translocates into the nucleus after phosphorylation

(A-B) Phosphorylated IRF5 accumulates in the nucleus. Differentiated THP-1 cells were stimulated with LPS for 2 hr. Nuclear translocation and phosphorylation of IRF5 were monitored by confocal immunofluorescence using antibodies against IRF5 (A) or p-IRF5 (B)

Conclusions and discussion

In this part, we presented evidence that IKK β is an IRF5 kinase and we identified Ser-445 of mouse IRF5 (Ser-446 of human IRF5) as a critical phosphorylation site that is essential for IRF5 to induce cytokines. We also developed an antibody specific for IRF5 phosphorylated at Ser-445 and we used this antibody to demonstrate that IRF5 is phosphorylated at Ser-445 in an IKK β -dependent manner in response to LPS stimulation or Sendai virus infection. Our results suggest that IKK β plays a crucial role in activating both NF- κ B and IRF5, two master regulators of pro-inflammatory cytokines.

IKK β is activated by a variety of stimulatory agents, including inflammatory cytokines and microbial pathogens that activate different pattern recognition receptors (Israel 2010, Liu et al. 2012). Consistent with the pleiotropic functions of IKK β , we found that IRF5 is activated by multiple pathways including those that engage TLRs and cytosolic DNA and RNA sensors. However, not all stimuli that activate IKK β are capable of activating IRF5. For example, we found that TNF- α , which is known to strongly stimulate IKK β , could not activate IRF5 (data not shown). Thus, IRF5 activation requires additional signals in addition to IKK β . A similar scenario has recently been reported in the cytosolic DNA sensing pathway, which employs the adaptor protein STING to not only activate TBK1 but also recruit IRF3, thereby specifying the phosphorylation of IRF3 by TBK1 (Tanaka and Chen 2012). It is possible that similar adaptor proteins may be engaged by TLR and other pathways to recruit IRF5 for phosphorylation by IKK β .

Through mass spectrometry, we identified several serine residues on mIRF5 that are phosphorylated by IKK β , and these include Ser-430, 434, 436 and 445. Our functional analyses showed that Ser-445, and to a lesser extent Ser-434, is required for IRF5 dimerization, whereas mutations of other serine residues had no effect. These results are different from those of a previous report which showed that Ser-436 and Ser-439 (equivalent to Ser-477 and Ser-480 in the human IRF5 used in the study) were important for IFN- α induction (Barnes et al. 2002). Importantly, Ser-434 and 445 of mIRF5 are homologous to Ser-385 and 396 of human IRF3 and they reside in a highly conserved region containing a cLxISN motif (Hiscott et al. 2006). The p-IRF5 antibody that we have developed clearly detected the phosphorylation of IRF5 at Ser-445 in cells stimulated with LPS or infected with Sendai virus, consistent with the phosphorylation of IRF3 at Ser-396 in response to RNA virus infection. Collectively, our results demonstrate that Ser-445 is phosphorylated by IKK β in cells in response to stimulation and that this phosphorylation is critical for IRF5 activation.

It is interesting that despite homologous domain structures and considerable sequence similarities between IRF5 and IRF3, these proteins are phosphorylated by distinct but homologous kinases, which are IKK β and TBK1, respectively. It has also been reported that IKK α is responsible for the phosphorylation of IRF7 in response to stimulation of endosomal TLRs such as TLR7 and TLR9 (Hoshino et al. 2006). Thus, IKK β and IKK-like kinases may be largely responsible for the activation of IRFs, and further work is needed to identify the kinase specific for each IRF. Future work should also delineate the biochemical basis for the specificity of IRF phosphorylation by a cognate IKK or IKK-like kinase. In the case of IRF5, which is essential for the production of inflammatory cytokines and has been closely linked

to human autoimmune diseases(Lazzari and Jefferies 2014), the work reported here, which includes the discovery of IKK β as an IRF5 kinase, the identification of Ser-445 of mIRF5 (Ser-446 of human IRF5) as a critical phosphorylation site, and the development of antibody that recognizes phosphorylated IRF5 at Ser-445, should facilitate further research on the mechanism of IRF5 activation and its role in human diseases.

Material and methods

Antibodies and Other Reagents

The antibodies used in this study and their sources are listed as follows: Santa Cruz Biotech: IRF3, IKK α , TRAF6 and NEMO; Cell Signaling: phospho-IKK α/β , phospho-TBK1, I \square B α and phospho-IkB α ; Sigma-Aldrich: Flag antibody (M2), Tubulin, M2-conjugated agarose and anti-HA-conjugated agarose; Thermo Scientific: HA; Abcam: IRF5. The antibody against phosphor-Ser⁴⁴⁵ IRF5 was generated by immunizing rabbits with a synthetic peptide (IRLQIpS⁴⁴⁵NPDLC). LPS, HT-DNA, poly(dA:dT), and poly(I:C) were from Sigma. Plasmid and DNA or RNA ligands were transfected into cells using lipofectamine 2000 (Life Technologies). The kinase inhibitors were dissolved in DMSO and used at the following final concentrations: TBK1 inhibitor (BX795, Selleckchem), 10 μ M; IKK β inhibitor (TPCA-1, Sigma), 20 μ M. GST-IKK β and GST-TBK1 recombinant proteins were expressed and purified from Sf9 cells.

Expression Constructs

For expression in mammalian cells, cDNA encoding N-terminal Flag- or HA-tagged mouse IRF5 S430A, IRF5 S434A, IRF5 S436A and IRF5 S439A were cloned into pcDNA3; HA-tagged mouse IRF5 WT, IRF5 S445A, and human IRF5 WT were cloned into pcDNA3 and pTY-EF1a-GFP-IRES-hgroR lentiviral vectors. Mutants were constructed with the QuikChange Site-Directed Mutagenesis Kit (Stratagene).

Viruses, Cell culture, and Transfections

Sendai virus (Cantell strain, Charles River Laboratories) was used at a final concentration of 100 hemagglutinating unit/ml. All cells were cultured at 37°C in an atmosphere of 5% (v/v) CO₂. HEK 293T cells and Raw 264.7 cells were cultured in Dulbecco's modified Eagle's medium (DMEM) supplemented with 10% (v/v) cosmic calf serum with penicillin (100 U/ml) and streptomycin (100 µg/ml). THP-1 cells were cultured in RPMI Media 1640 supplemented with 10% (v/v) fetal bovine serum with penicillin (100 U/ml), streptomycin (100 µg/ml) and 0.05 mM 2-mercaptoethanol.

RNAi and Rescue with Transgenes

The lentiviral shRNA vector, pTY-shRNA-EF1a-puroR-2a-GFP-Flag, was provided by Dr. Yi Zhang (Harvard Medical School). The original vector was modified to pTY- shRNA-EF1a-GFP-IRES-puroR and pTY- shRNA-EF1a-GFP-IRES-hgroR by replacing the 2A peptide sequence with IRES sequence and also by replacing puromycin resistant gene with the hygromycin-resistant gene. The shRNA sequences were cloned into the vectors with the U6 promoter. RNAi-resistant cDNA sequences were cloned into the vectors to replace GFP.

Lentiviral infection and establishment of stable cell lines were described previously (Tanaka and Chen 2012). The shRNA sequences are as follows (only the sense strand is shown): human IRF5, 5'-GAGGAAGAGCTGCAGAGGAT-3'; mouse IRF5, 5'-GCAGAGAATAACCCTGATTAA-3'; human IKK β , 5'-GGGAGAACGAAGTGAAACT-3'; human IKK α , 5'-GTACCAGCATCGGGAACTT-3'; human NEMO, 5'-GGACAAGGCCTCTGTGAAA-3'; human TRAF6, 5'-GGAGAACCTGTTGTGATT-3'.

Quantitative RT-PCR

Total cellular RNA was isolated using TRIzol. 0.1-1 μ g total RNA was used for reverse transcription (RT) using iScript Kit (Bio-Rad). The resulting cDNA served as the template for Quantitative-PCR analysis using iTaq Universal SYBR Green Supermix (Bio-Rad) and ViiTM7 Real-Time PCR System (ABIApplied Biosystems Inc., Foster City, CA). Primers for specific genes are listed as follows: human CXCL10, 5'-GTGGCATTCAAGGAGTACCTC-3' and 5'-TGATGGCCTTCGATTCTGGATT-3'; human TNF- α , 5'-CCTCTCTCTAATCAGCCCTCTG-3' and 5'-GAGGACCTGGAGTAGATGAG-3'; human IFN- β , 5'-ACTGCAACCTTCGAAGCCTT-3' and 5'-TGGAGAACACAGGAGAGC-3'; human GAPDH, 5'-ATGACATCAAGAAGGTGGTG-3' and 5'-CATACCAGGAAATGAGCTTG-3'.

Partial Purification of IRF5 for in vitro Reaction

As IRF5 would spontaneously form dimer when the protein was affinity purified with a purification tag (e.g, Flag or GST), we attempted to partially purified IRF5 from the 293T

FG-mIRF5-HA stable cell line. Cytosolic extracts from these cells were first fractionated using HiTrap Heparin HP column (GE Healthcare). Fractions containing IRF5, as judged by immunoblotting, were concentrated and buffer exchanged for 3 times with hypotonic buffer (20 mM Tris-HCl, pH 7.4; 10 mM NaCl; 3 mM MgCl₂) using Amicon Ultra-0.5mL centrifugal filters (Millipore). The partially purified IRF5 was used for in vitro assays.

Purification of IRF5 for Mapping Phosphorylation Site(s)

To determine the phosphorylation site(s) induced by IKK β , reaction mixture (60 μ L) containing 20 mM HEPES-KOH (pH 7.0), 2 mM ATP, 5 mM MgCl₂, 40 μ L of partially purified Flag-mIRF5 from 293T stable cell line and 2 μ g Flag-IKK β or BSA was incubated at 30°C for 1 hr followed by incubation with M2-conjugated agarose at 4°C for 4 hr. The beads were washed 3 times with lysis buffer containing 150mM NaCl and 1% Triton X100. Bound proteins were then eluted by boiling in 2x Laemmli Sample Buffer before SDS-PAGE and silver staining. Gel slices from each lane were excised and digested with trypsin in situ. Digested samples were subjected to mass spectrometry using Q Exactive and raw data were analyzed by the search engine MASCOT (MATRIX SCIENCE).

Confocal Microscopy

THP-1 cells (4×10^5) were seeded and differentiated with 50 nM phorbol 12-myristate 13-acetate (PMA; Sigma-Aldrich) for 48 h and then cultured for another 48 h by replacing the PMA-containing media with fresh media without PMA. The differentiated cells were left unstimulated or stimulated with LPS for 2 h. The cells were immunostained with the IRF5

antibody (Abcam; ab21689) or phosphospecific IRF5 antibody. The images were acquired and processed with the Zeiss LSM 700 confocal laser scanning microscope system.

CHAPTER THREE

STING IS THE PREDOMINANT RECEPTOR FOR CGAMP

Results

Cyclic GMP-AMP (cGAMP), as the first cyclic di-nucleotide found in metazoan, was recently identified as a second messenger molecule that plays an essential role in the cytosolic DNA sensing pathway. In mammalian cells, cGAMP is produced by the DNA sensor, cyclic GMP-AMP synthase (cGAS) from ATP and GTP when it binds to cytosolic double-stranded DNA. cGAMP binds to and activates an adaptor protein, STING, which will further activate the downstream signaling cascade and trigger the production of Type-I interferons and inflammatory cytokines. cGAMP has been proven to be a very important molecule in the defense of multiple infectious diseases as well as in the development of self-immune diseases. cGAMP can also be served as an effective adjuvant that can boost antigen-specific antibody production and T cell response. So it is intriguing to investigate if there is any other receptor for cGAMP except STING in cells that may have novel functions. To do so, we make use of the next-generation sequencing techniques and check whether cGAMP will induce any gene expression profile changes when delivered into STING depleted cells. Our conclusion here is that in multiple cell types investigated, STING is the predominant receptor for cGAMP and innate immune response.

cGAS induced Type-I interferons and inflammatory cytokines in STING dependent manner in 293T reconstitution cell line.

In 293T cells, as there is a non-detectable expression of cGAS or STING protein, the cytosolic DNA sensing pathway is absent from receptor-adaptor level. However, we can reconstitute this pathway by introducing cGAS and STING protein into 293T cells. We used lentivirus to stably express STING protein in 293T cells (293T_STING cell line). In this cell line, with transfection of cGAS plasmid, the DNA sensing pathway would be activated and would further induce IRF3 dimerization (Figure 2-1A, lane 3) and IFNb1 production (Figure 2-1B). Transfection of the pcDNA3 vector with MAVS coding sequence was used to compare between cytosolic DNA sensing pathway with RNA sensing pathway. To choose a proper amount of vector for activation, we did a titration test and used IFN- β , CXCL10, and TNF- α as indicators for transcriptional activation. Interestingly, increasing amount of cGAS encoding plasmid was toxic to cells and resulted in lower production of IFN- β and CXCL10 mRNA (Figure 2-1C and D). For MAVS overexpression activated RNA sensing pathway, more MAVS would induce much higher IFN- β mRNA level, while the induced CXCL10 and TNF- α mRNA levels were comparable to those induced by cGAS overexpression (Figure 2-1D and E). For optimal cGAS-STING pathway activation, in subsequent sample preparations, we used 0.1ug/ml.

To set up better negative control, we evaluated the effect of the transfecting pcDNA3 vector with mouse cGAS catalytic domain mutant coding sequence (G198A, S199A, cGAS_mt) versus pcDNA3 empty vector (pcDNA3_EV). As expected, the catalytic domain dead mutant

was null functional and the protein did not alter any significant gene expression, comparing with pcDNA3_EV transfection (Figure 2-1F).

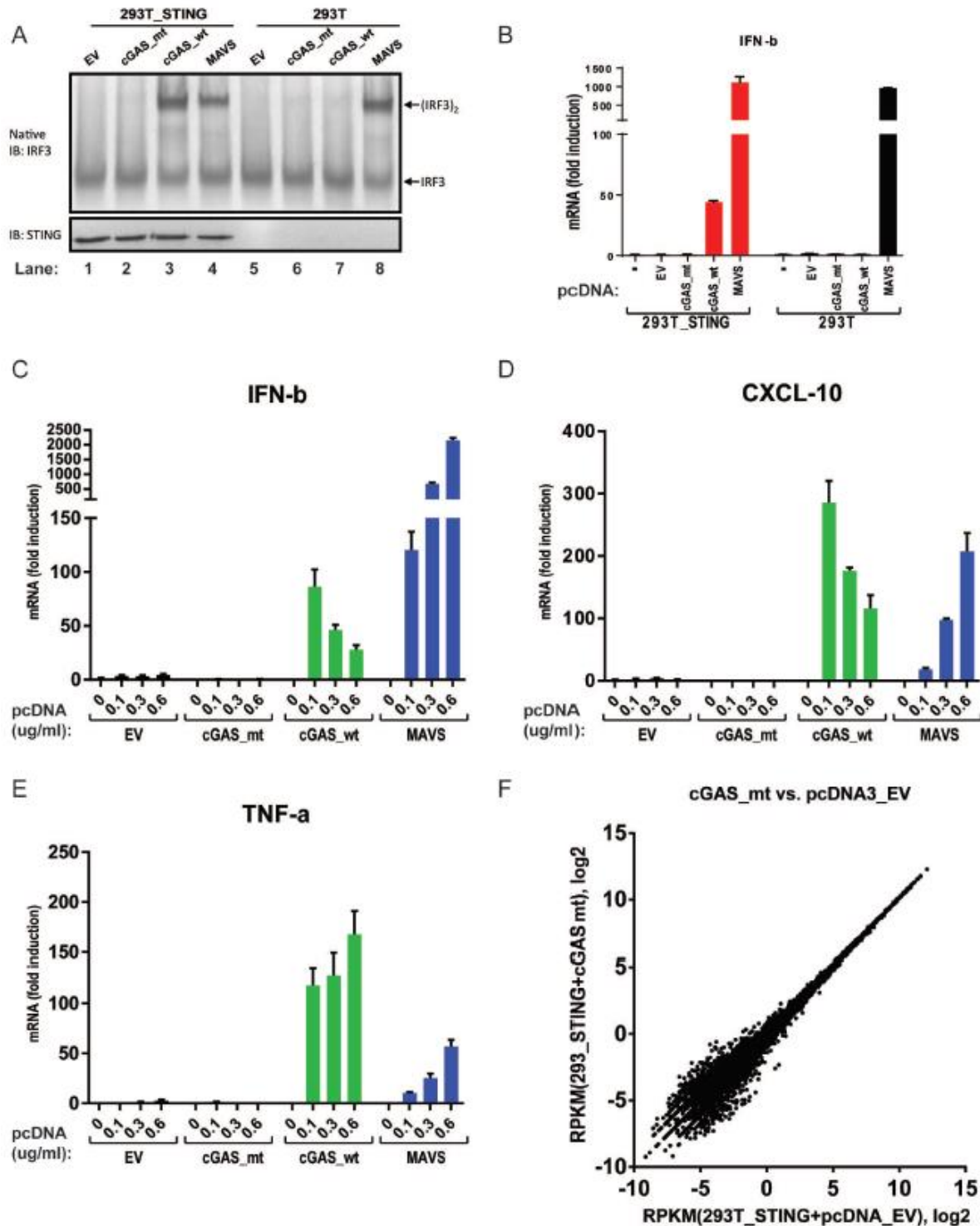


Figure 2-1. Establishment of 293T cell lines and condition tests for optimal stimulation.

- (A) 293T_STING cells respond to cGAS transfection and activate downstream signaling. 293T cells stably expressing STING (293T_STING) and 293T parental cells were transfected with 0.5ug/mL empty pcDNA vector (EV), pcDNA-cGAS (cGAS_wt), pcDNA-cGAS with G198A and S199A mutations (cGAS_mt), or pcDNA-MAVS (MAVS) for 24 hr. Activation of IRF3 was analyzed by native PAGE and immunoblotting.
- (B) 293T_STING cells produce IFN- β with cGAS transfection. Similar to (A), the cells were transfected with the indicated DNA vector for 24 hours before total RNA was isolated. IFN- β mRNA level was analyzed by q-RT-PCR. Unless indicated otherwise, error bars represent standard deviations of triplicate assays.
- (C-E) Titration test of DNA concentration for optimal activation. 293T cells were transfected with the indicated amount of DNA vectors for 24 hours. Total RNA was isolated and IFN- β , CXCL-10 and TNF-a mRNA levels were analyzed by q-RT-PCR.
- (F) cGAS catalytic dead mutation is null functional. 293T_STING cells were transfected with 0.1ug/mL pcDNA_EV or pcDNA_cGAS_mt for 24 hours. Total RNA was isolated and further processed for mRNA-sequencing. Sequencing data was mapped to 33615 genes and the result was plotted. X and Y axis represent the log base 2 transformed RPKM (Reads per kilobase per million mapped reads) values of the indicated experiment samples.

In 293T_STING cell line, we evaluated the gene expression changes after cGAS activation (by cGAS plasmid transfection). From Figure 2-2A, we can see that a number of genes were induced by cGAS transfection. 263 genes were induced by cGAS activation with induction ratio larger than or equal to 2.0 and induced expression RPKM larger than or equal to 1.0. Among them, 115 genes were induced with ratio larger than 4.0. From ontology analysis of the genes induced, we can see that genes induced by cGAS activation included genes related to cellular responses to virus and bacterium (Type-I interferons and inflammatory cytokines) (Table 2-1). Meanwhile, genes involved in myeloid cell differentiation were also induced (including ZFP36, MAFB, JUN, CSF1 etc.). Furthermore, we also noticed the induction of genes regulating cell apoptosis, which was consistent with the observation that cells underwent obvious cell cycle arrest and cell death after cGAS expression plasmid transfection.

Term	Genes	List Total	Count	%	PValue	FDR
GO:0009615~response to virus	IFIH1, TNF, BST2, ZC3HAV1, IL29, RSAD2, IFI44, CCL5, STAT1, CCL4, IFI35, ISG20, DDX58, IRF9, PLSCR1, ISG15, IFNB1, IRF7, EIF2AK2, FOSL1	188.00	20.00	1.05	0.00	0.00
GO:0006334~nucleosome assembly	HIST1H2AC, HIST2H2AA3, HIST2H2AA4, HIST1H4K, HIST1H2AG, HIST2H4A, HIST2H4B, HIST1H2BO, HIST2H2AB, HIST1H2BN, HIST1H2BK, HIST1H2BL, HIST2H2AC, HIST1H2BJ, HIST1H4E, HIST3H2A, HIST3H2BB, HIST2H3A, HIST1H2BD, HIST1H1C, HIST2H3C, HIST2H3D, HIST2H2BE, HIST2H2BF, HIST1H2AI, HIST1H3B, HIST1H2AK, HIST1H2AM, HIST1H3H	188.00	18.00	0.95	0.00	0.00
GO:0006952~defense response	CXCL1, IFIH1, CCL3, NMI, TNF, CXCL3, CXCL2, RSAD2, NFKB1, IL32, ANKRD1, C1S, CCL5, CCL4, CXCL10, TAPBP, FOS, CD44, CCL20, HIST1H2BK, TAP1, HIST1H2BJ, PTX3, FOSL1, DHX58, NFKBIZ, BCL10, IL29, IL8, APOL2, DDX58, P2RY11, IFNB1, HIST2H2BE, IRF7, PLA2G4C	188.00	36.00	1.90	0.00	0.00
GO:0006955~immune response	CXCL1, IFIH1, CCL3, TNF, IFITM3, CXCL3, CXCL2, OAS3, RSAD2, CD70, OAS1, IFI44L, IL32, NFKB2, C1S, CCL5, CCL4, IFI35, CXCL10, B2M, TAPBP, CCL20, TAP1, PTX3, DHX58, BCL10, BST2, IL29, IL8, RELB, GEM, HLA-E, TNFSF9, PSMB9, DDX58, OASL, IFI6	188.00	37.00	1.95	0.00	0.00
GO:0009617~response to bacterium	BCL10, TNF, PTGS2, SOCS3, SOCS1, NFKBIA, CCL5, STAT1, TRIB1, B2M, FOS, ADM, HIST1H2BK, CCL20, IFNB1, HIST2H2BE, JUN, HIST1H2BJ	188.00	18.00	0.95	0.00	0.00
GO:0006954~inflammatory response	CXCL1, NFKBIZ, CCL3, TNF, NMI, IL8, CXCL3, CXCL2, NFKB1, C1S, CCL5, CCL4, CXCL10, APOL2, FOS, CD44, CCL20, IRF7, PLA2G4C, PTX3	188.00	20.00	1.05	0.00	0.00
GO:0034097~response to cytokine stimulus	FOS, PTGS2, SOCS3, JUN, SOCS1, PML, STAT1, CCL5, FOSL1, JUNB	188.00	10.00	0.53	0.00	0.00
GO:0006915~apoptosis	IER3, TNF, NUAK2, TNFRSF12A, PML, NFKBIA, NFKB1, PMAIP1, ZC3H12A, BCL10, SGK1, STAT1, BIRC3, TNFSF9, BBC3, IFNB1, CSRNP1, JUN, GADD45G,	188.00	25.00	1.32	0.00	0.00

	TNFAIP3, EIF2AK2, GADD45B, PPP1R15A, GADD45A, IFI6					
GO:0045637~regulation of myeloid cell differentiation	ZFP36, TNF, HIST1H4K, MAFB, JUN, CSF1, HIST1H4E, NFKBIA, RUNX1, HIST2H4A, CCL5, HIST2H4B	188.00	9.00	0.47	0.00	0.01

Table 2-1. GO analysis of induced genes

Unexpectedly, a massive induction of histone mRNA also showed up in the list (Table 2-1), of which the mechanism and physiological significance still remains to be further explored.

To identify the potential set of genes induced by cGAMP independent of STING, we stimulated 293T wild-type cells (293T_WT) with cGAS plasmid transfection. As the result shown in Figure 2-2B, few genes were induced by cGAS activation in 293T cells in absence of STING. In Table 2-2, we can see that only 11 genes were induced with a ratio larger than or equal to 2.0 and induced RPKM larger than or equal to 1.0, among which, 2 of them with inducing ratio larger than or equal to 4.0. However, none of the listed genes overlapped with the list of genes induced by cGAS in 293T_STING cells. And when looking into each gene in the list, not only the induction ratios were low, the expression level of these genes were low even in the stimulated cells. So we regard them as experimental variations. This result leads us to the conclusion that in 293T cells, the genes induced by cGAS activation was totally dependent on the presence of STING protein, which makes STING the predominant target for cGAMP produced by cGAS.

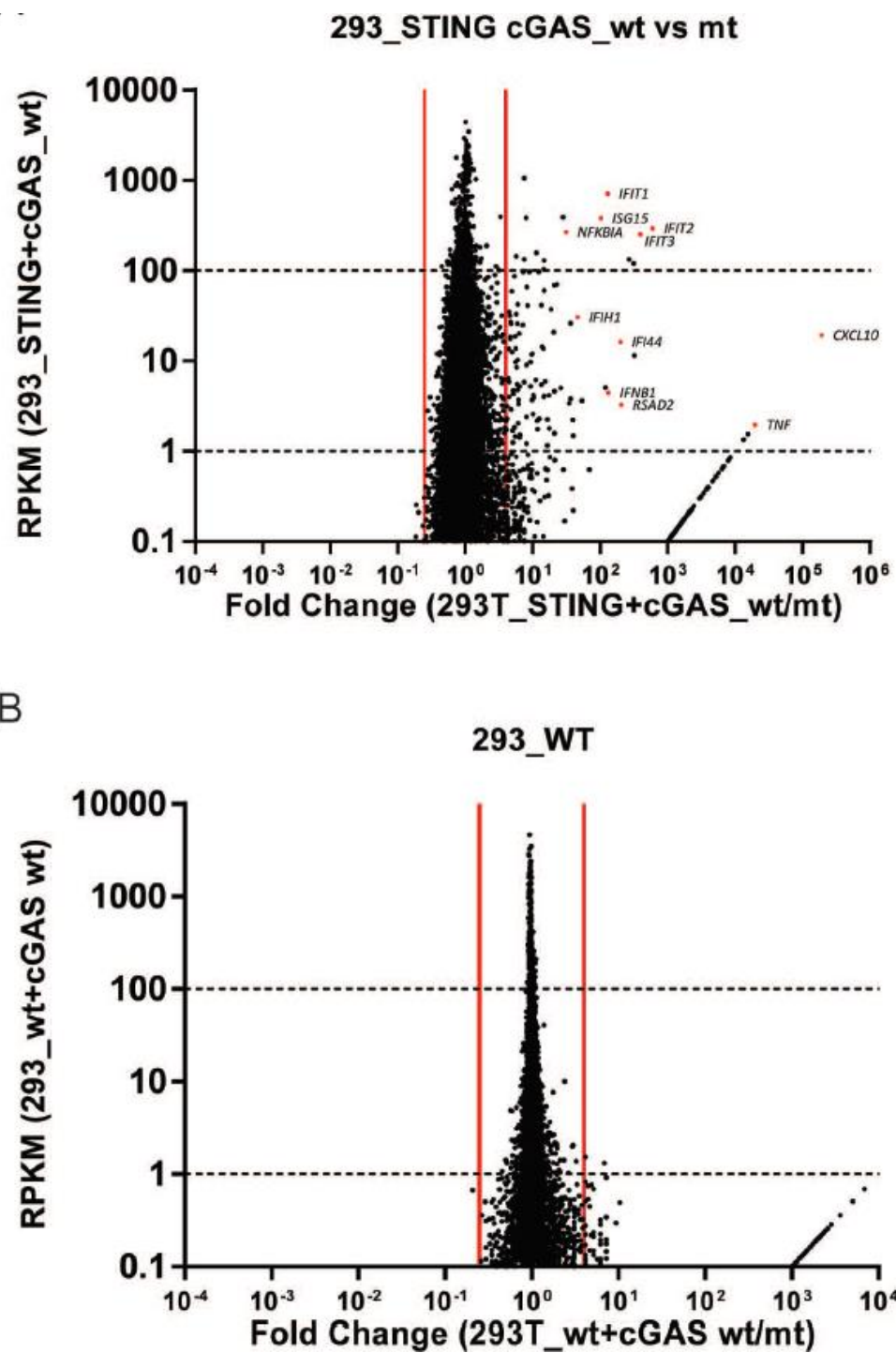


Figure 2-2. cGAS induced immune response is STING dependent in 293T cells.

(A) Wild-type cGAS plasmid transfection induces gene expression changes in 293T_STING cells. Scatter plot representation of mRNA-sequencing expression data. Each data point represents a single RefSeq gene plotted according to the fold change between cGAS_wt and

cGAS_mt transfected samples (x-axis) and the expression values (RPKM) in cGAS_wt transfected sample (y-axis). The identity of several data points is indicated for reference. Vertical red lines indicate the 4-fold differential expression cutoff to define the cGAMP activated genes. Genes were further sorted according to their mean cGAMP activated expression into high, intermediate, and low expression categories. (We used a mean cGAMP activated RPKM cutoff of 0.1 to ensure genes in lists were sufficiently expressed.) (B) In 293T cells, transient expression of cGAS_wt does not alter gene expression changes. Similar scatter plot as (A), but 293T parental cells were used.

ID	293T_WT+cGAS	293T_WT+cGAS_mt	293T_WT+cGAS/cGAS_mt
LOC100287232	1.310956069	0.189530176	6.916872528
GAFA3	1.537292074	0.3704208	4.150123517
MGC16385	1.377507887	0.421485374	3.268222269
NPB	2.061923496	0.687924343	2.997311429
LOC100289647	1.981963335	0.676553693	2.929498953
LOC100288366	1.030734514	0.386341465	2.667936546
PPAN	10.04650894	4.207017465	2.388035949
LOC100289092	1.419624895	0.604585491	2.3480962
LOC727967	1.043420726	0.489248169	2.132702363
TBC1D3B	1.418031951	0.669701182	2.117409957
NPFF	1.114017398	0.536859876	2.075061758

Table 2-2. Genes induced by cGAS activation in 293T_WT cells RPKM>1.0 Ratio>2.0 (11 genes) (Red indicates ratio>4, 2 genes)

In this set of RNA-Sequencing experiment, we also checked the genes induced by the activation of cytosolic RNA sensing pathway. To activate RNA-sensing response, we transiently over-expressed the key adapter protein, MAVS, in 293T_STING cell line. From Figure 2-3A, we can see that 91 genes were induced, 62 of which were induced with a ratio greater than or equal to 4.0. GO analysis showed that most of the induced genes were related to immune response against virus or bacterium. By comparing the gene lists induced by cGAS and MAVS respectively (Figure 2-3B and C), we can see that cGAS induced a broader spectrum of inflammatory cytokines than MAVS did. Representing gene expression values

(RPKM) from RNA-sequencing result are shown in Figure 2-4 and part of them are validated by qPCR (Figure 2-5A). Interestingly, the induction of histone genes and apoptosis-related genes (growth and DNA damage related, GADD genes) observed by cGAS induction was absent by MAVS activation (Figure 2-5B to E). These results indicate that cGAS activation (cytosolic DNA sensing pathway activation) may trigger more intense and broader immune response than RNA sensing pathway activation does.

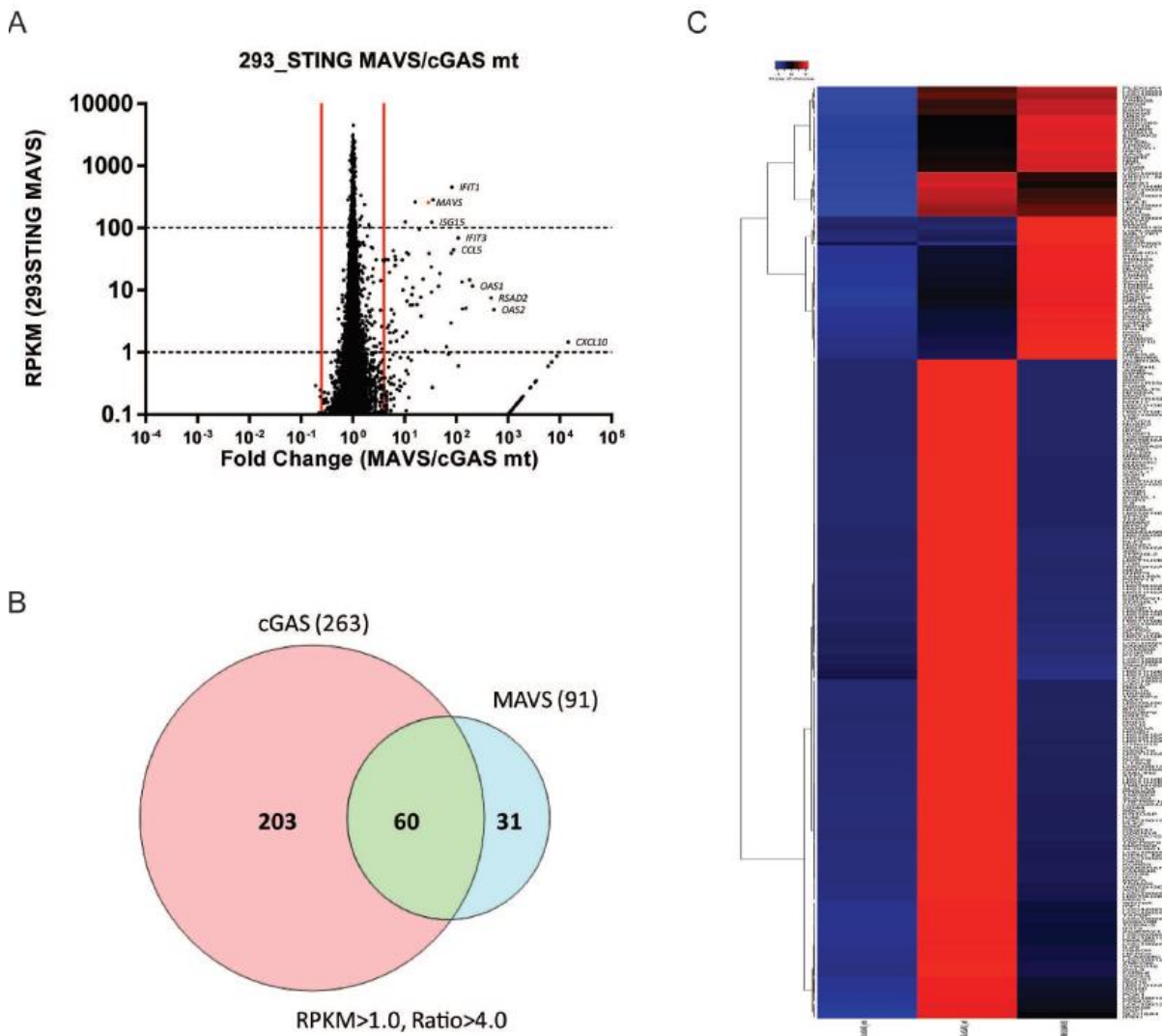


Figure 2-3. cGAS induces broader gene expression changes than MAVS.

- (A) MAVS expression in 293T_STING cells induces gene expression changes. Scatter plot representation of mRNA- sequencing expression data. X-axis represents the fold change between MAVS and cGAS_mt transfected samples. Y-axis represents the RPKM values in MAVS transfected sample.
- (B) Venn diagram comparing genes that are induced by cGAS and MAVS. With the sequencing data represented in figure 2-2A and 2-3A, a cut-off of induction fold greater than 4.0 and induced expression RPKM greater than 1.0 was applied.
- (C) Heatmap of RPKM data showing the gene expressions in 293T_STING cells transfected with pcDNA-cGAS_mt, pcDNA-cGAS_wt, or pcDNA-MAVS.

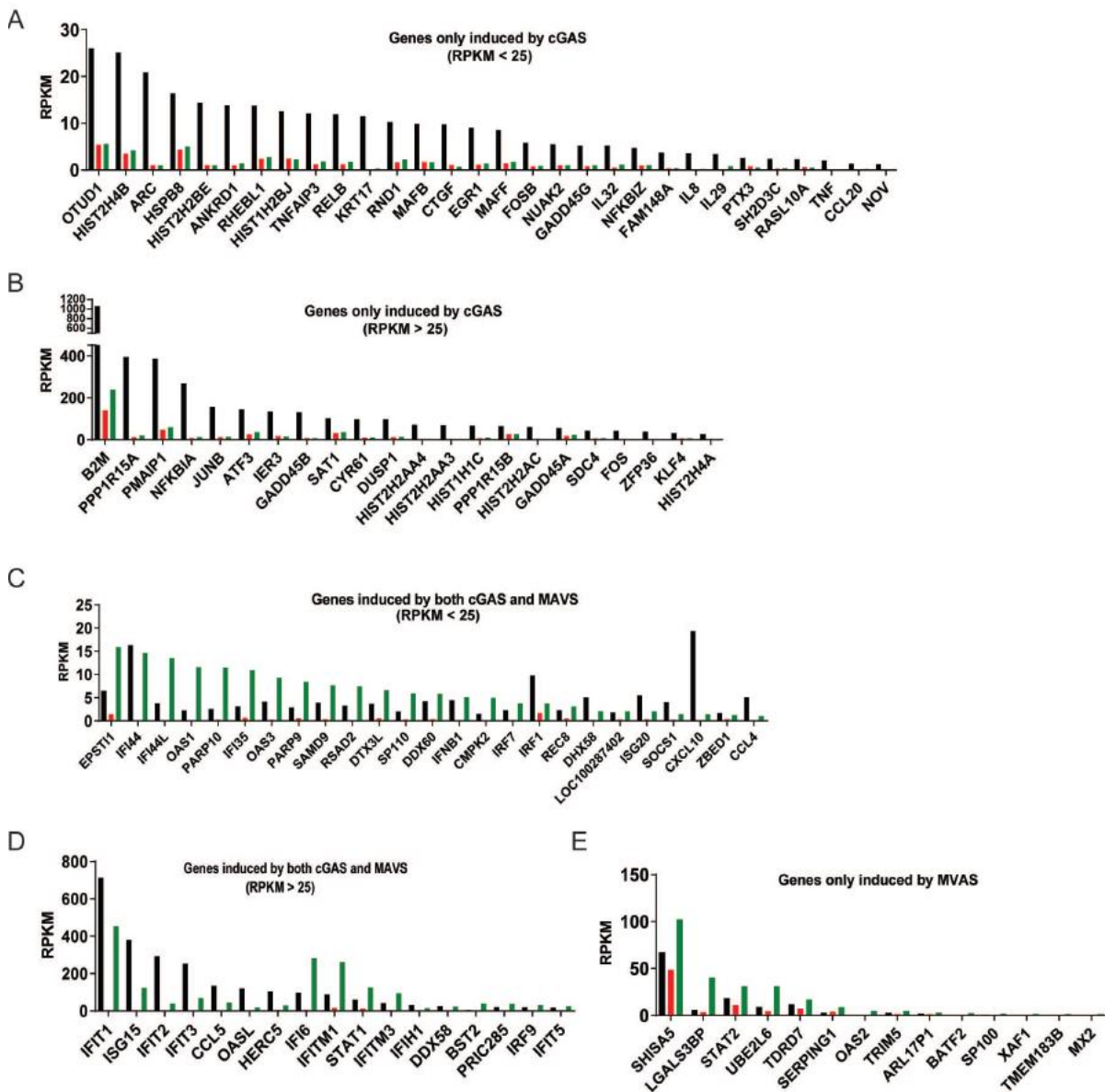


Figure 2-4. Representing lists of genes that are commonly or specifically induced by cGAS and MAVS.

(A-B) List of representing genes and their RPKM values that were only induced by pcDNA-cGAS_{wt} transfection. (A) Genes with induced RPKM value less than 25; (B) Genes with induced RPKM value larger than 25.

(C-D) List of representing genes and their RPKM values that were induced in both pcDNA-cGAS_{wt} and pcDNA-MAVS transfected samples. (C) Genes with induced RPKM value less than 25; (D) Genes with induced RPKM value larger than 25.

(E) List of representing genes and their RPKM values that were only induced by pcDNA-MAVS transfection.

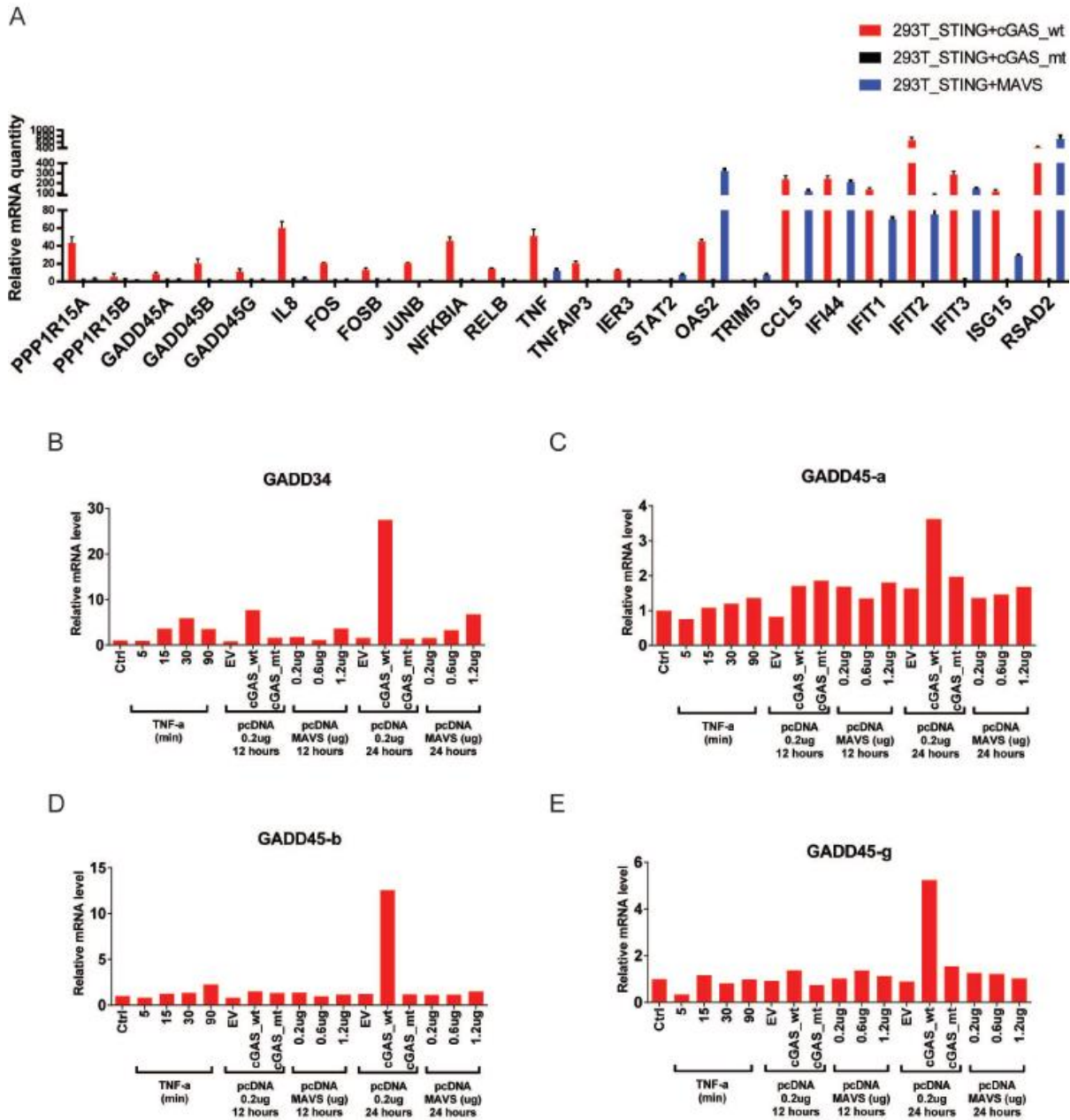


Figure 2-5. Confirmation of genes induced by cGAS and MAVS.

(A) 293T_STING cells were transfected with 0.1ug/ml pcDNA-cGAS_wt, pcDNA-cGAS_mt, or pcDNA-MAVS for 24 hours. Total RNA was isolated and mRNA levels of indicated genes were analyzed by q-RT-PCR.

(B-E) The expression of GADD family genes was induced specifically by cGAS expression. 293T_STING cells were either treated with recombinant TNF- α for the indicated time or transfected with indicated DNA vector for the indicated time. Total RNA was isolated and mRNA levels of GADD34, GADD45-a, GADD45-b, and GADD45-g were analyzed by q-RT-PCR.

cGAMP activates primary lung fibroblast and bone marrow-derived macrophages in STING dependent manner.

In order to test the function of cGAMP in presence or absence of STING under more physiological conditions, we further checked the genome-wide gene expression changes in response to cGAMP treatment in primary lung fibroblasts (LF) and bone marrow-derived macrophages (BMDM). In LF and BMDM, activation of cGAS-STING pathway by cGAS-encoding plasmid transfection was not efficient (data not shown), so we evaluated three different methods to deliver cGAMP into the cells to directly activate STING. As shown in Figure 2-6A and B, adding relatively high concentration of cGAMP into the culture medium only induced very small amount of IFN- β and CXCL-10 production. Delivery of cGAMP along with Lipofectamine 2000 increased cytokine induction but the activation was still weak. In comparison, an even very low concentration of cGAMP (0.1uM) could induce very high level of IFN- β and CXCL-10 production when it was delivered with Digitonin to partially permeabilize cell membrane. We also did a titration and time course test on cGAMP concentration for optimal activation. As shown in Figure 2-6A to D, 0.1uM of cGAMP was already saturated for maximum activation and increasing amount of cGAMP did not further elicit higher production of IFN- β . So in preparation for RNA-sequencing samples, we used digitonin to permeabilize the cells and delivered 0.1uM of cGAMP. We treated cells from wild-type and STING Goldenticket mice and compared the IFN- β and CXCL-10 mRNA induction (Figure 2-6E and F) before sending the samples for next-generation sequencing.

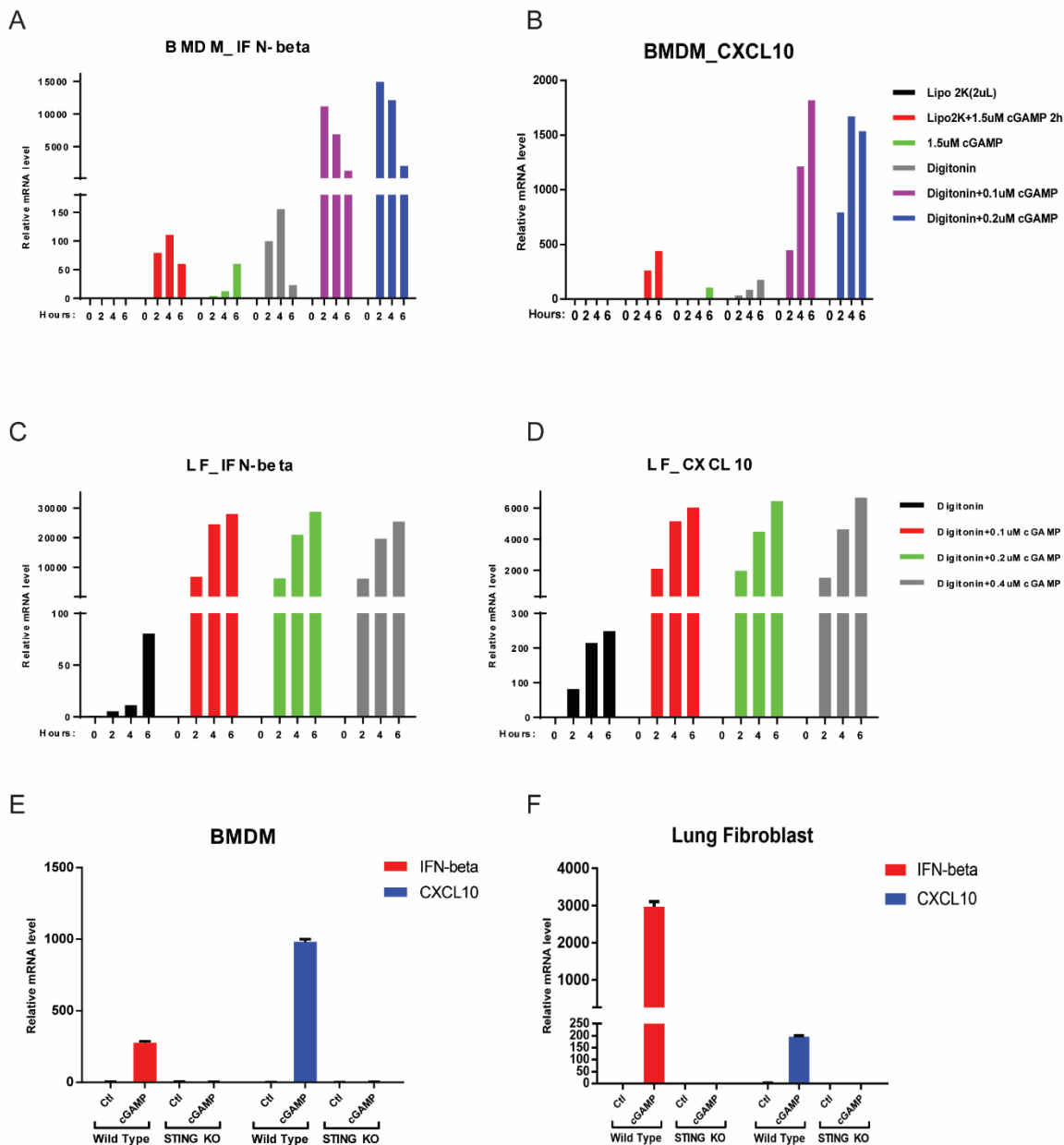


Figure 2-6. Condition tests for optimal cGAMP stimulation in BMDM and LF.

(A-B) Delivery methods test for cGAMP treatment. BMDM cells were plated 7 days after differentiation. The cells were treated by following methods for indicated time: Lipofectamine 2000 alone, Lipofectamine 2000 along with 1.5uM cGAMP, 1.5uM cGAMP alone added to culture medium, Digitonin permeabilization buffer alone, Digitonin permeabilization buffer with 0.1uM or 0.2uM cGAMP. Total RNA was isolated and mRNA levels of IFN- β (A) and CXCL-10 (B) were analyzed by q-RT-PCR.

(C-D) cGAMP dosage test for optimal cGAMP induced activation. Lung fibroblast cells were treated with Digitonin permeabilization buffer alone, or Digitonin permeabilization buffer with 0.1, 0.2, or 0.4uM cGAMP, for the indicated time. Total RNA was isolated and mRNA levels of IFN- β (A) and CXCL-10 (B) were analyzed by q-RT-PCR.

(E-F) Sample test for subsequent sequencing data collection. BMDM (E) and lung fibroblast (F) cells were treated with Digitonin permeabilization buffer (Ctl) or Digitonin permeabilization buffer with 0.1uM cGAMP (cGAMP). Total RNA was isolated and mRNA levels of IFN- β and CXCL-10 were analyzed by q-RT-PCR.

In wild-type primary lung fibroblasts (Figure 2-7A), 844 genes were sufficiently induced (induction ratio greater than or equal to 2.0 and induced RPKM greater than or equal to 1.0).

Among these induced genes, most of them are related to immune defense response, including inflammatory cytokines, chemokines, antigen processing and presentation related genes and adaptive immune response regulations. However, in lung fibroblast from STING Goldenticket mice, only 74 genes were upregulated at minor levels in response to cGAMP treatment (Figure 2-7B) and most of the genes were only expressed at very low levels. As the majority of the induced genes were unannotated genes and did not overlap with the gene list induced in wild-type cells, they were considered to be caused by experimental variations.

Similar results were also observed in primary bone marrow-derived macrophages (Figure 2-8A and B). These results indicate that in primary lung fibroblast and bone marrow-derived macrophage, STING was the predominant target for cGAMP.

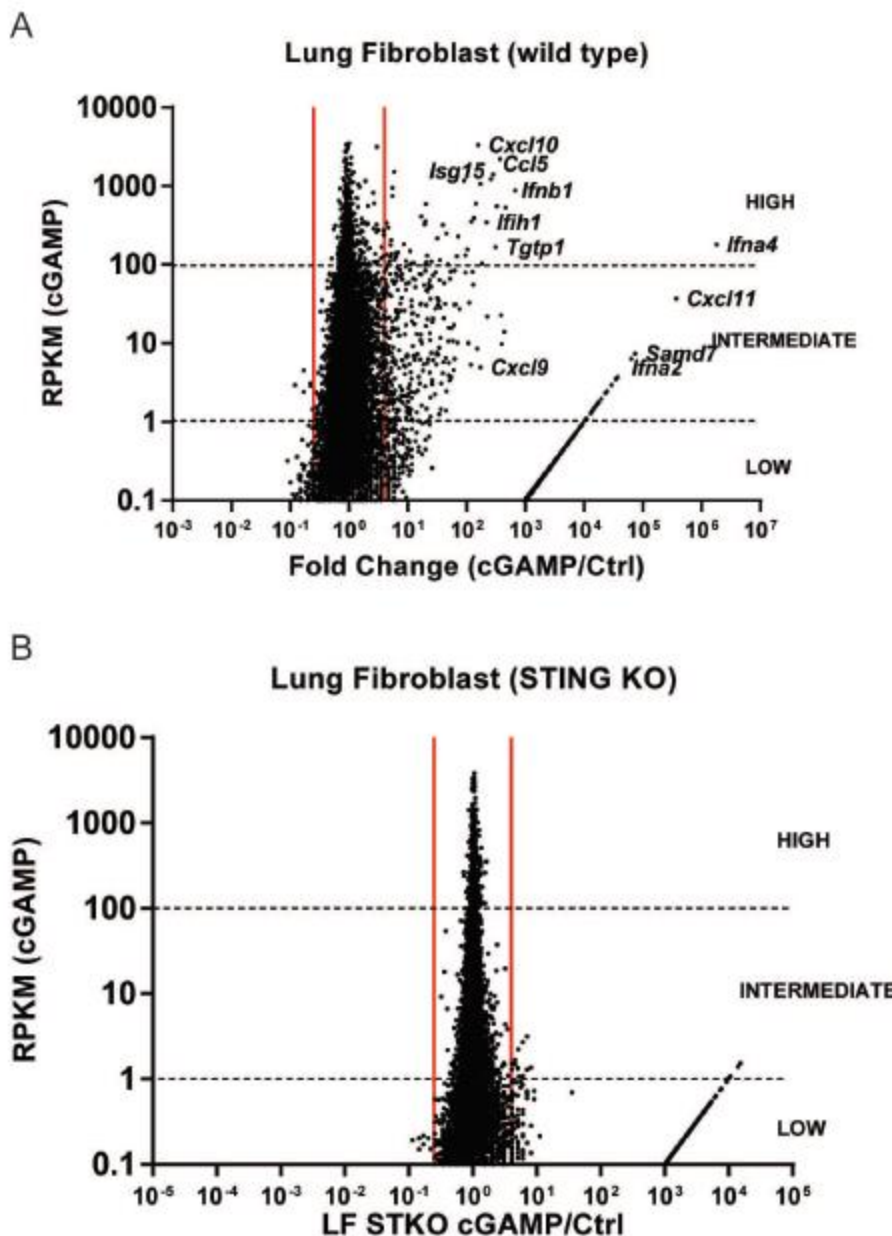


Figure 2-7. cGAMP induced immune response is STING dependent in lung fibroblast cells.

(A) cGAMP induces gene expression changes in wild-type lung fibroblast cells. Scatter plot representation of mRNA- sequencing expression data. The x-axis represents the fold change between cGAMP and Digitonin alone treated samples. Y-axis represents the RPKM values in cGAMP treated sample.

(B) In lung fibroblast from STING Goldenticket mice, cGAMP does not alter gene expression changes. Similar scatter plot as (A), but lung fibroblast from STING Goldenticket mice were used.

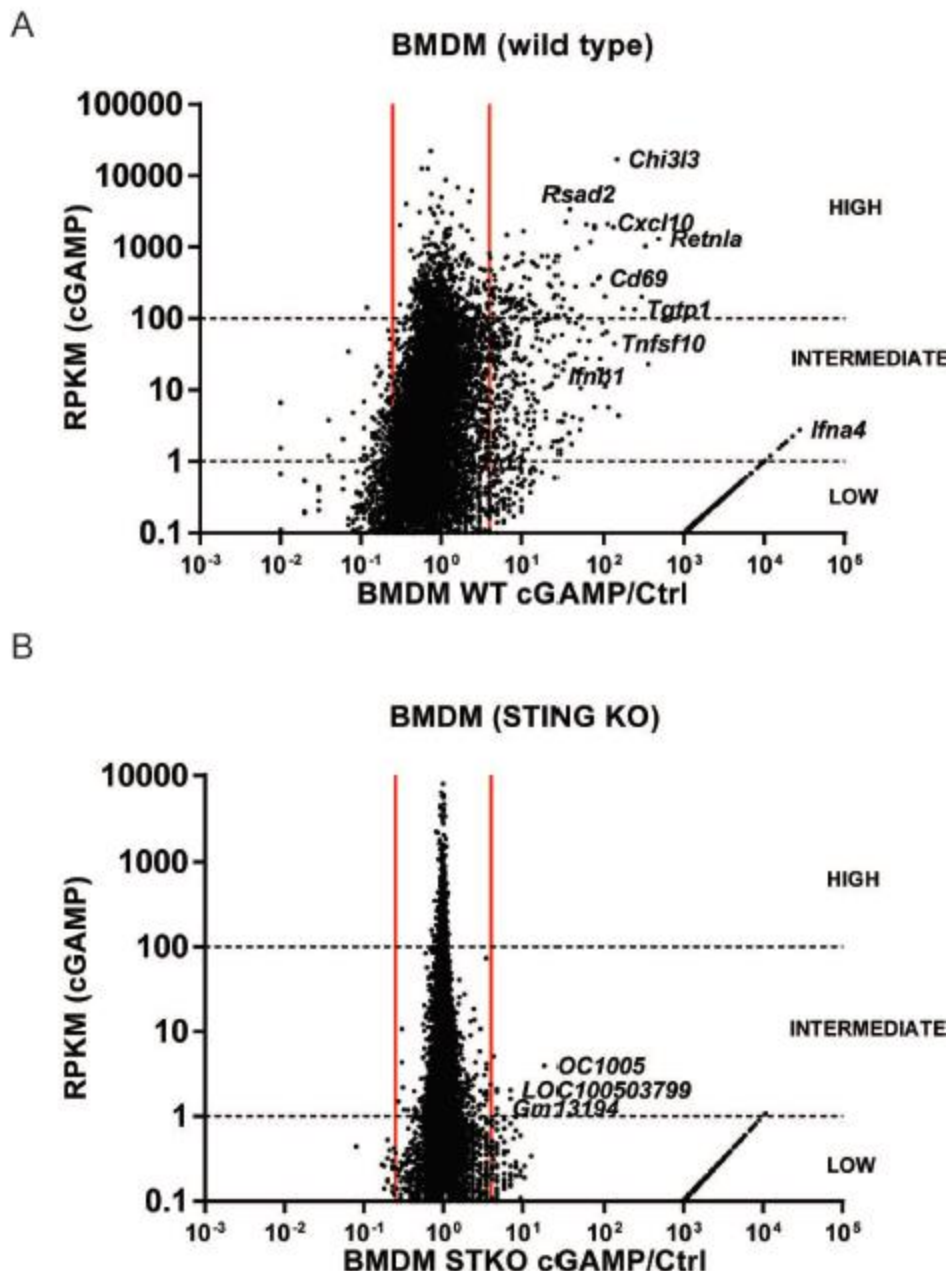


Figure 2-8. cGAMP induced immune response is STING dependent in BMDM cells.

(A) cGAMP induces gene expression changes in wild-type BMDM cells. Scatter plot representation of mRNA- sequencing expression data. The x-axis represents the fold change between cGAMP and Digitonin alone treated samples. Y-axis represents the RPKM values in cGAMP treated sample.

(B) In BMDM from STING Goldenticket mice, cGAMP does not alter gene expression changes. Similar scatter plot as (A), but BMDM from STING Goldenticket mice were used.

cGAMP activates bone marrow-derived conventional dendritic cells in STING dependent manner

Further, we tested the genes induced by cGAMP in bone marrow-derived conventional dendritic cells (cDCs). In this set of experiment, we collected and differentiated bone marrow cells into conventionally dendritic cells (cDCs). The treatment method used was similar to the method used for LF and BMDM but with a lower optimal dosage of Digitonin.

We found that after 6 or 12 hours' treatment of cGAMP, the innate immune response was sufficiently activated in wild-type cDCs (Figure 2-9A and B). While in cDCs from STING Goldenticket mice, the activation or gene induction was minimum (Figure 2-9C and D). And when comparing the induced genes in wild-type and STING deficient cells, there was little significant overlap (Table 2-3), indicating that the genes induced in STING deficient cells were probably due to experimental variations.

(6 hours treatment)	(12 hours treatment)
Gm16721	9130017N09Rik
Gm8624	Atp5l-ps1
Rps6-ps2	Cxcl11
	Cxcl9
	Gbp1
	Gbp11
	Gm10736
	Gm11216
	Gm12551
	Gm16094
	Gm17383
	Gm4613
	Gm7729
	Pou3f1 (chr4 124334049..124337899)
	Rpsa-ps10

Table 2-3. Comparison of genes induced in wild-type and STING KO cDC

Meanwhile, in this set of sequencing experiment, we also evaluated the gene induction by cGAMP treatment in interferon alpha receptor knockout (IFNAR KO) cells. As shown in Figure 2-9E and F, in IFNAR KO cDCs, only a subset of interferons and cytokines were induced (including Ifnb1, Ifnas, and certain Isgs). When comparing with genes induction in wild-type, the fact that most of the genes were uniquely induced in wild-type cells suggest that the majority of the gene induction was secondary response and was dependent on interferon signal.

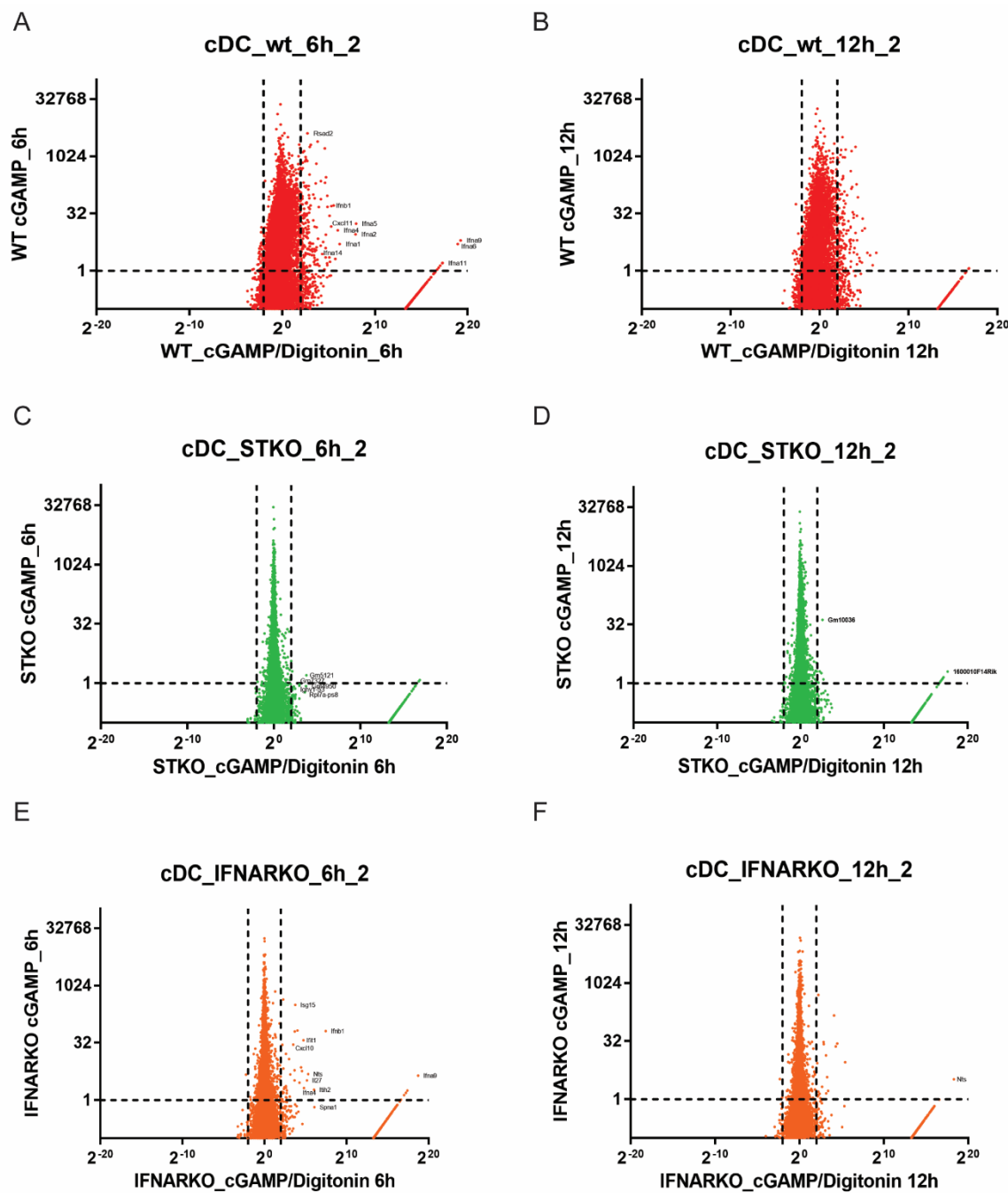


Figure 2-9. cGAMP induced immune response is STING dependent in conventional dendritic cells.

(A-B) cGAMP induces gene expression changes in wild-type cDC cells. Conventional dendritic cells were treated for 6 hours (A) or 12 hours(B). Scatter plot representation of mRNA- sequencing expression data. The x-axis represents the fold change between cGAMP

and Digitonin alone treated samples. Y-axis represents the RPKM values in cGAMP treated sample.

(C-D) Similar to A and B, but cDC cells from STING Goldenticket mice were used.

(E-F) Similar to A and B, but cDC cells from interferon alpha receptor knockout mice were used.

DNA activates bone marrow-derived conventional dendritic cells in cGAS and STING dependent manner

Since in all the types of cells tested above, STING always shows as the predominant target for cGAMP and in absence of STING protein, the function of cGAS (cGAMP) is almost totally abolished. We wanted to further test whether cGAS is the predominant receptor for double-stranded DNA.

Firstly, we derived cDC from wild-type bone marrow cells and tested different conditions for optimal stimulation condition. We used liposome (Lipofectamine 2000® Transfection Reagent from Invitrogen) to facilitate delivery of stimulatory DNA into cells. As suggested by manufacturer protocol, we used a Lipofactamine 2000 / DNA ratio of 1:3. Interestingly, we found that even at low concentration (3uL/mL), liposome alone could induce considerable amount of CXCL-10 (Figure 2-10C). And at higher concentration (12 to 24uL/mL), liposome induced significant amount of IFN- β production also (Figure 2-10A). Moreover, increasing amount of liposome was very toxic to dendritic cells, as indicated by the amount of total RNA harvested after treatment (Figure 2-10D). Taking all these factors into account, we used 2ug/mL of ISD along with 6uL/mL Lipofectamine 2000 for cDC stimulation for later experiments. To determine the optimal DNA stimulation time in cDCs, we did a time course test and found out that the IFN- β mRNA level reached a peak as soon as 3 hours and dropped dramatically between 6 and 9 hours (Figure 2-10E). Considering we were also looking for the

induction of unknown genes that may have different activation dynamics, we collected and sequenced samples that were stimulated for 3 and 6 hours. In Figure 2-10F, we confirmed our samples from wild-type, cGAS knockout and STING Goldenticket mice and verified that the induction of IFN- β by ISD (interferon stimulatory DNA) was totally abolished in cGAS or STING null cells.

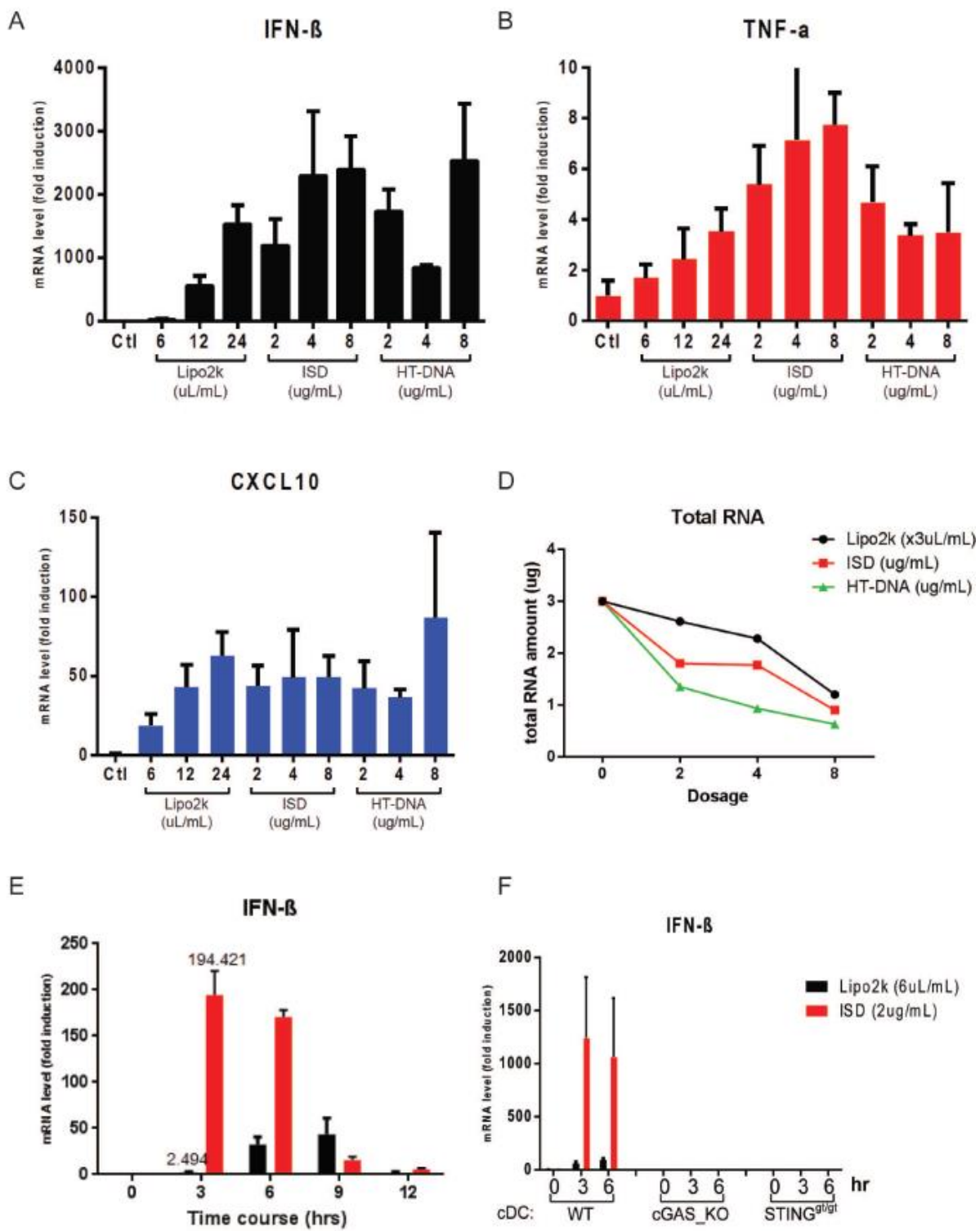


Figure 2-10. Liposome and ISD induce IFN- β and ISG expression in conventional dendritic cells.

(A-C) Liposome, ISD, and HT-DNA induce the expression of IFN- β , TNF-a and CXCL-10 in cDCs. cDC cells were plated at day 8 post-differentiation and were treated with indicated amount of liposome alone (Lipo2K), liposome with ISD, or liposome with HT-DNA for 6 hours. Total RNA was isolated and mRNA levels of IFN- β (A), TNF-a (B), and CXCL-10 (C) were analyzed by q-RT-PCR.

(D) Liposome or DNA stimulation is toxic to cells and lower total RNA yield. cDC cells were treated as in A-C, the total amount of RNA (in ug) isolated from per million cells was measured and plotted.

(E) The mRNA level of IFN- β decreases after 6 hours of DNA stimulation. cDC cells from wild-type mice were treated with either 6ul/ml Lipofectamine 2000 alone or along with 2ug/ml ISD for the indicated time before total RNA was isolated. mRNA level of IFN- β was analyzed by q-RT-PCR.

(F) Sample test for subsequent sequencing data collection. cDC cells from wild-type, cGAS knockout, and STING Goldenticket mice were treated with either 6ul/ml Lipofectamine 2000 alone or along with 2ug/ml ISD for the indicated time before total RNA was isolated. mRNA level of IFN- β was analyzed by q-RT-PCR.

In cDCs from wild-type mice, 3 hours after we transfected interferon stimulating DNA (ISD), Type-I interferons and inflammatory cytokines were highly induced (Figure 2-11A); and even more genes were with higher induction level were observed 6 hours after transfection (Figure 2-11B). In comparison, the gene induction in cells from STING Goldenticket mice or from cGAS knockout mice was much less significant (Figure 2-11C to F). These results suggest that cGAS/STING axis play dominant roles in eliciting an innate immune response to cytosolic double-stranded DNA.

When the cDC cells were treated with only Lipofectamine 2000 alone, significant gene induction was also observed in wild-type cells (Figure 2-12A and B). And when comparing the gene induction lists by ISD and liposome alone (Figure 2-12G), the significant overlap suggests that liposome may trigger the activation of DNA sensing pathway in wild-type cDC cells. Furthermore, the fact that the gene induction by liposome in cGAS or STING deficient cells was much weaker further proved this conclusion (Figure 2-12C to F). As in vitro cGAS

activity assay showed that liposome could not directly activate cGAS protein in absence of DNA, the activation of DNA sensors by liposome could be triggered by the DNA leakage caused by liposome treatment.

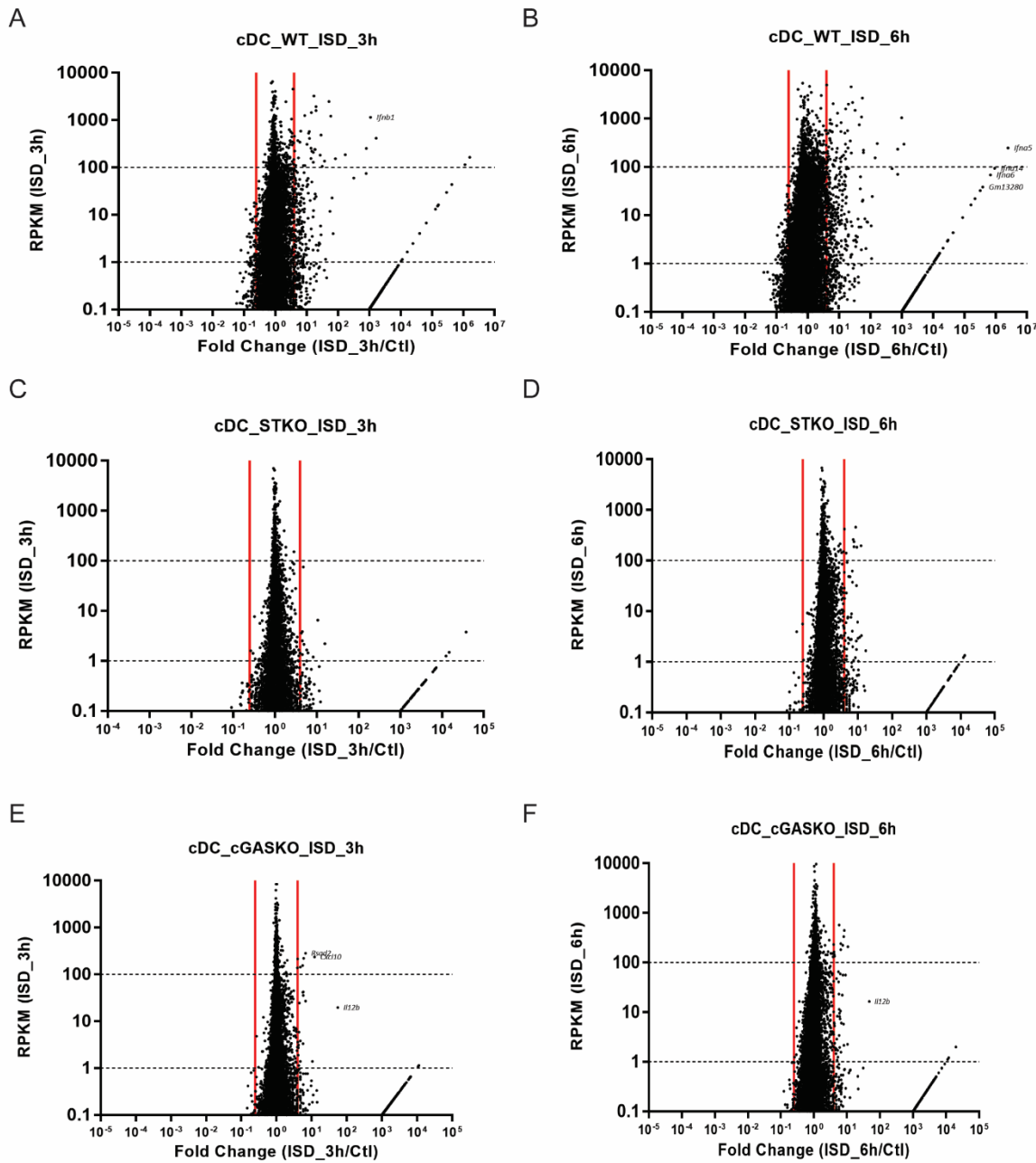


Figure 2-11. ISD induced immune response is largely cGAS and STING dependent in conventional dendritic cells.

(A-B) ISD induces gene expression changes in wild-type cDC cells. Conventional dendritic cells were treated for 3 hours (A) or 6 hours(B). Scatter plot representation of mRNA-sequencing expression data. X-axis represents the fold change between ISD treated and non-treated (Ctl) samples. Y-axis represents the RPKM values in ISD treated sample.

(C-D) Similar to A and B, but cDC cells from STING Goldenticket mice were used.

(E-F) Similar to A and B, but cDC cells from cGAS knockout mice were used.

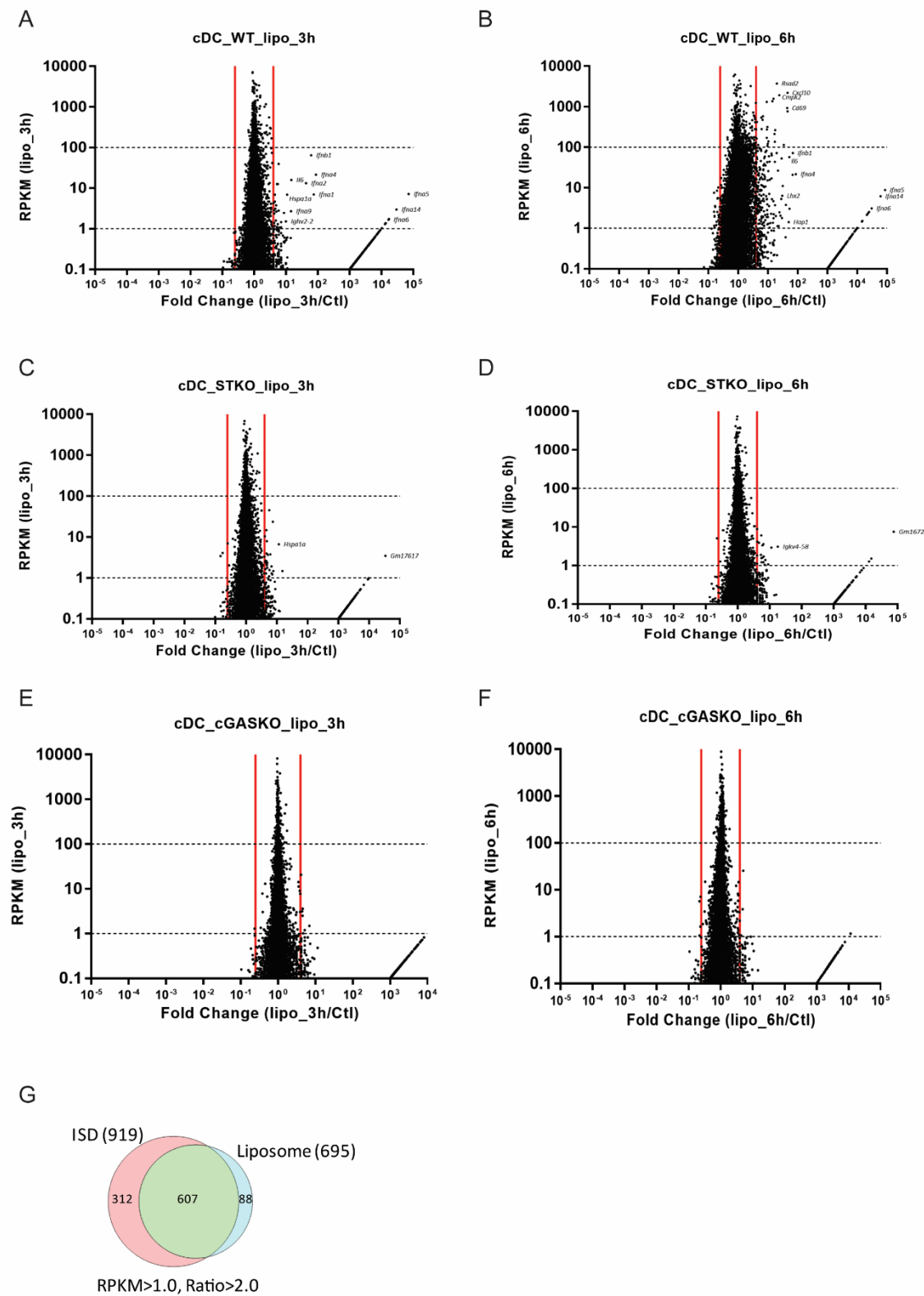


Figure 2-12. Liposome induced immune response is largely cGAS and STING dependent in conventional dendritic cells.

(A-B) Liposome induces gene expression changes in wild-type cDC cells. Conventional dendritic cells were treated for 3 hours (A) or 6 hours(B). Scatter plot representation of mRNA- sequencing expression data. The x-axis represents the fold change between liposome treated and non-treated (Ctl) samples. Y-axis represents the RPKM values in liposome treated sample.

(C-D) Similar to A and B, but cDC cells from STING Goldenticket mice were used.

(E-F) Similar to A and B, but cDC cells from cGAS knockout mice were used.

(G) Venn diagram comparing genes that are induced by 6 hours treatment of ISD and liposome alone. With the sequencing data represented in figure 2-11B and 2-12B, a cut-off of induction fold greater than 2.0 and induced expression RPKM greater than 1.0 was applied.

cGAS-STING independent gene induction by DNA stimulation in cDCs and pDCs

Though with less intensity and variety of gene induction, we still observed a considerable amount of genes whose expression increased in STING or cGAS deficient cells, especially at 6 hours after ISD transfection. When we compared gene expression changes in STING deficient and cGAS deficient cells (Figure 2-11D and F), there was a significant overlap of genes induced (including interleukins and ifit genes, representing genes are shown in Figure 2-13A and B). This result suggests that there could be other potential but weaker sensors for double-stranded DNA that contributed the gene induction in absence of cGAS or STING proteins. An interesting phenomenon was that when looking into the induced genes by ISD independent of cGAS and STING, we found that for majority of these genes, their basal expression levels were much lower in cGAS or STING knockout cDCs than in wild-type cDCs. Figure 2-13C lists the expression values of representing genes that were expressed at lower level in cGAS or STING knockout cells. Statistically, there were 127 genes that were induced by 6 hours of ISD stimulation, with induction ratio larger than or equal to 2.0 and induced expression RPKM larger than or equal to 1.0. Among these genes, 104 of them (82%) were in

the list of genes whose basal expression levels were 1.5 fold higher in wild-type cDCs than in both cGAS and STING knockout cells (Figure 2-13D).

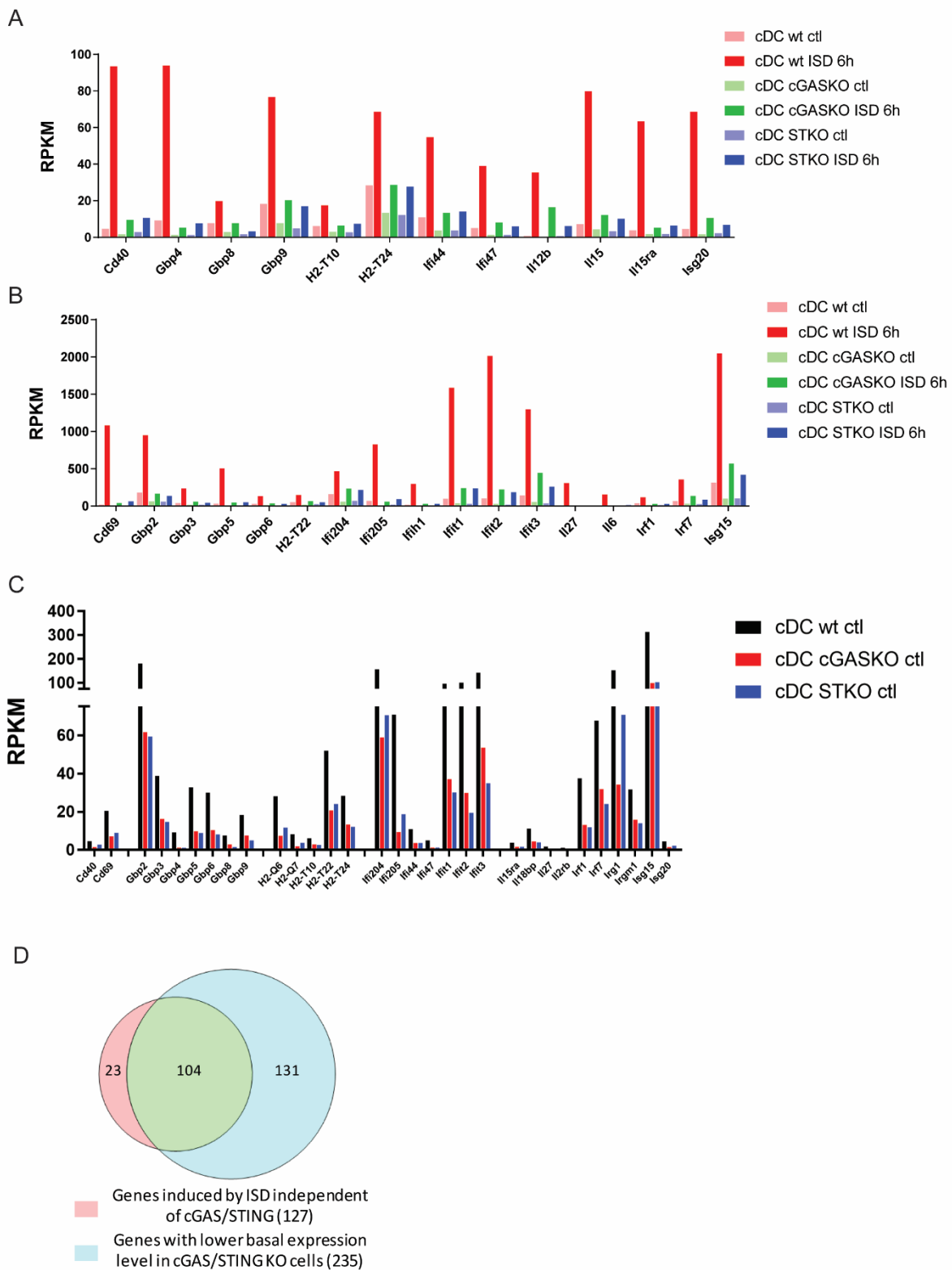


Figure 2-13. Representing genes that are induced by ISD independent of cGAS and STING

- (A-B) List of representing genes and their RPKM values that were induced by 6 hours of ISD treatment in cGAS knockout and STING Goldenticket cDC cells. (A) Genes with induced RPKM value less than 100; (B) Genes with induced RPKM value larger than 100.
- (C) List of representing genes and their RPKM values whose basal expression level is 1.5 folds lower in cGAS knockout and STING Goldenticket cDC cells than in wild-type cDC cells.
- (D) Venn diagram comparing genes that are induced by 6 hours treatment of ISD independent of cGAS/STING and genes with lower basal expression level in cGAS knockout and STING Goldenticket cDC cells.

One of the genes that was induced in cGAS or STING knockout cells, IL12b, drew our attention.

From Figure 2-14A, where we plotted the RPKM value of IL12b gene from the sequencing results, we can see that in cGAS or STING knockout cDCs, ISD induced a significant amount of IL12b expression, though, in STING knockout cell, the induction was weaker. To further confirm this, we repeated the stimulation, along with stimulation with cGAMP, HSV, and SeV and checked the mRNA level of IFN- β , IL-6, and IL-12b (Figure 2-14B to D). Consistent with previous RNA-sequencing data, cGAMP induced a high level of IFN- β and IL-6, but little IL-12b. With ISD stimulation, on the other hand, induced high level of IFN- β and lower level of IL-6, which totally depends on cGAS or STING, but it also induced IL-12b expression, which was independent of cGAS but seemed partially dependent on STING. Interestingly, though HSV infection only induced a low level of IFN- β expression, comparing with ISD stimulation, it elicited very high expression of IL-12b.

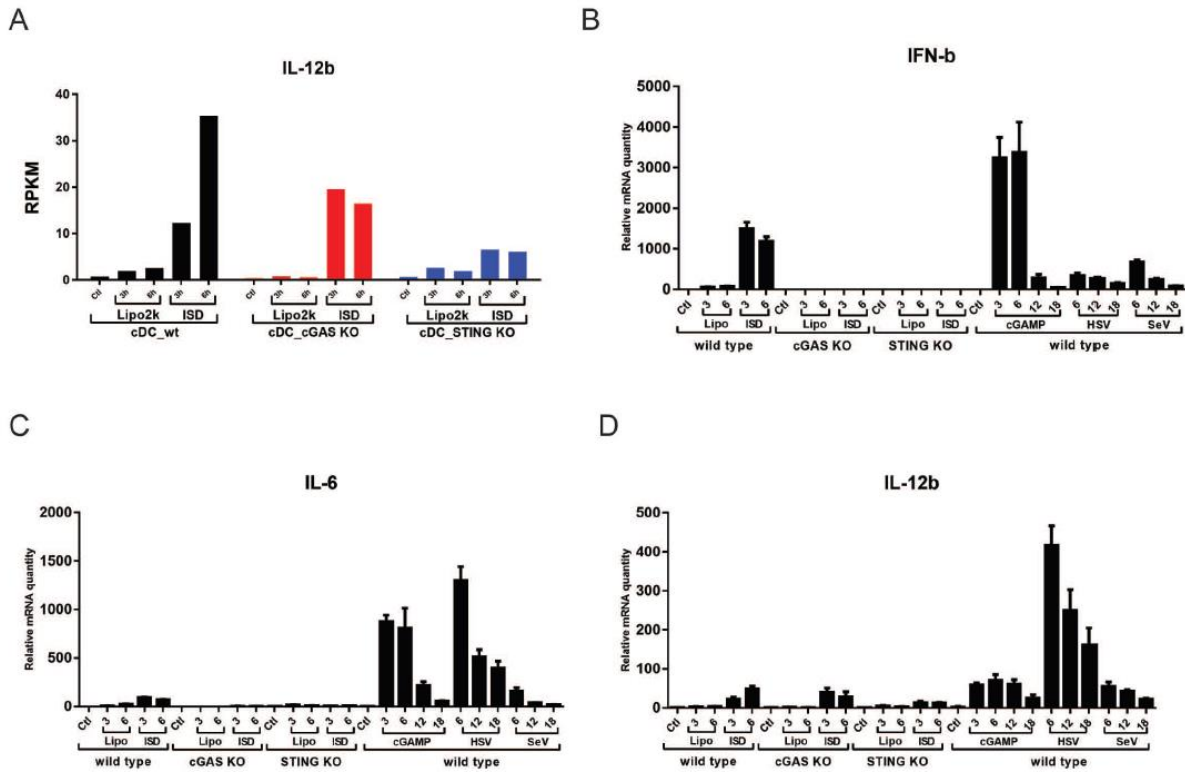


Figure 2-14. IL-12b gene expression is induced by ISD, but not cGAMP in cDCs.

(A) RPKM values of IL-12b gene in the RNA-sequencing dataset (as shown in Figure 2-11 and 12).

(B-C) The induction of IFN-b and IL-6, but not IL-12b by ISD was dependent on cGAS and STING. cDC cells from wild-type, cGAS knockout, and STING Goldenticket mice were plated and treated with liposome alone, with ISD, cGAMP, or infected with herpes simplex virus (HSV) or Sendai virus (SeV) for the indicated time. Total RNA was isolated and mRNA levels of IFN-b (B), IL-6 (C), and IL-12b (D) were analyzed by q-RT-PCR.

To further investigate if the induction of IL-12b by ISD and also to check if there is any synergistic effect between cGAS-STING pathway and TLR9 pathway, we differentiated bone marrow cells from wild-type, cGAS knockout, and TLR9 knockout mice into cDCs and plasmacytoid dendritic cells (pDCs), and then stimulated the cells with either ISD, CpG DNAs, or in combination, with or without liposome (Figure 2-15A to F). In both cDCs and pDCs, ISD could induce a high level of IFN-b and IL-6, which was totally cGAS and liposome dependent.

It also promoted the expression level of IL-12b in cDCs, which was independent of both cGAS and TLR9. CpG-A, when delivered with liposome, could activate cDCs or pDCs in cGAS dependent but TLR9 independent manner. This is probably due to that CpG-A can partially activate cGAS with its phosphodiester linkage double-stranded DNA region. With CpG-DNA along treatment, cDCs didn't express much IFN- β or IL-6 but significant amount of IL-12b, while pDCs were strongly activated and expressed a high level of IFN- β , IL-6 and IL-12b, which totally dependent on TLR9.

Interestingly, when stimulated with combination of CpG-DNAs and ISD, instead of synergistic effect, we observed that in cDCs, the expression induction of IFN- β and IL-6 by ISD was almost totally abolished after adding CpG-DNAs, especially with CpG-B and CpG-C. These results were consistent with the discovery that phosphorothioate backbone-modified single-stranded DNA can potently inhibit cGAS activity (which will also be discussed in the following chapter).

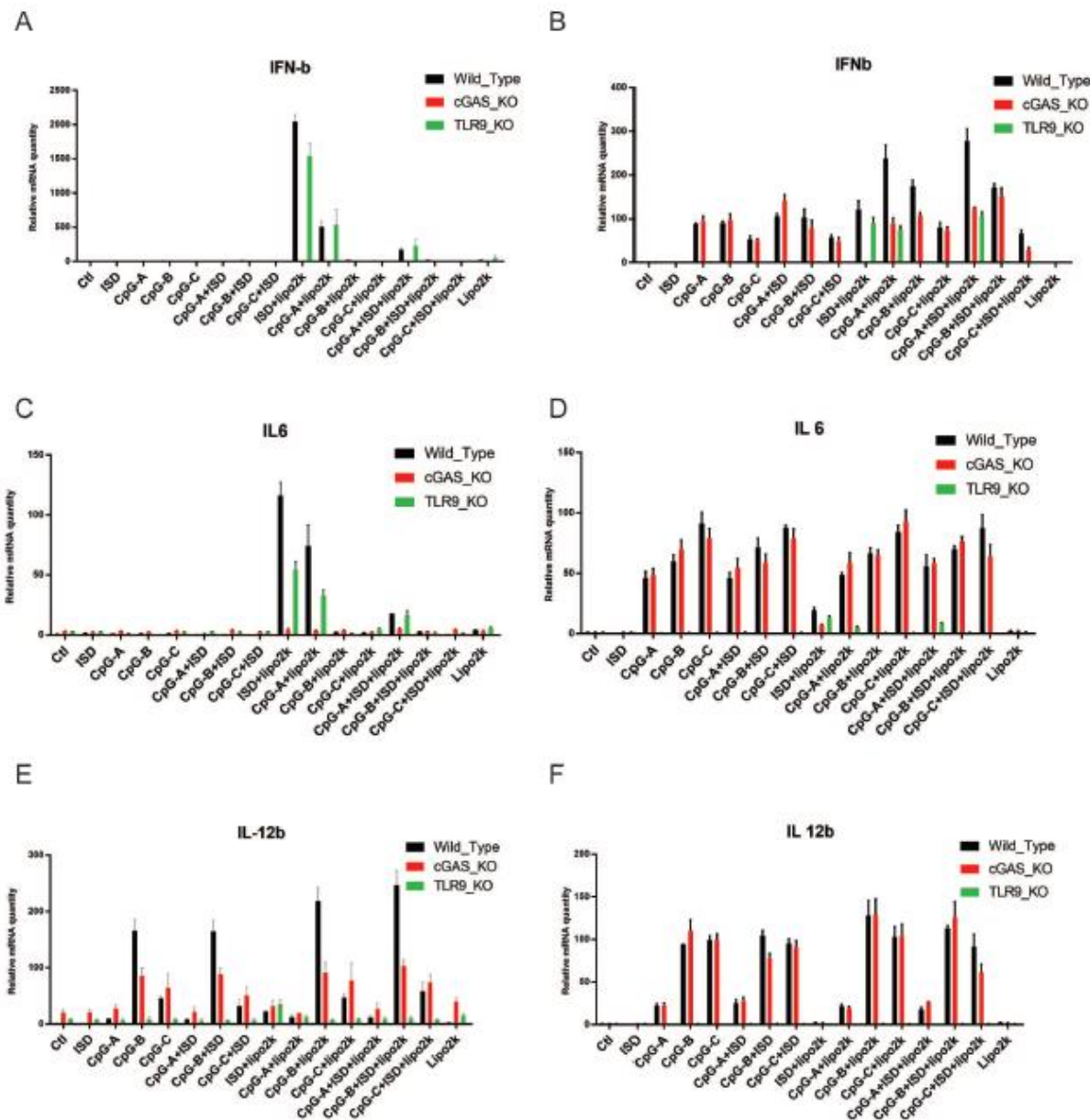


Figure 2-15. Gene expression by ISD and CpG-DNAs in pDC and cDC cells.

Plasmacytoid dendritic cells (pDCs, B, D, and F) and Conventional dendritic cells (cDCs, A, C and E) from wild-type, cGAS knockout, and TLR9 knockout mice were treated by liposome, ISD, CpG-DNAs, or in combination for 6 hours. Total RNA was isolated and mRNA levels of IFN- β (A-B), IL-6 (C-D), and IL-12b (E-F) were analyzed by q-RT-PCR.

Conclusions and discussion

In this project, we analyzed the global gene expression changes triggered by cGAS or cGAMP in different cell types, including 293T cell lines, primary mouse lung fibroblasts, bone marrow-derived macrophages, conventional dendritic cells, and plasmacytoid dendritic cells, with or without STING expression and found that in cells lacking STING protein expression, the gene expression changes induced by cGAMP were almost totally abolished. Our results confirmed that STING is the predominant receptor for cGAMP.

In response to DNA or RNA derived from infectious pathogens, different receptors and adaptor proteins are activated and lead to the activation of kinases and transcription factors, including NF-kb, IRF3, IRF7, etc. By comparing the genes induced by cGAS-STING and MAVS, we found that except from type-I interferon genes, interferon-stimulated genes and chemokines that are commonly activated by both cytosolic DNA sensing and RNA sensing pathways, cGAS-STING triggers the increased expression of much more genes, consistent with reported and our own observations that cGAS-STING pathway also involves in processes including autophagy, cell death, cell senescence, antigen cross-presentation and etc. This suggests that cGAS-STING pathway may serve as a very promising method or target for therapeutic interventions.

The invading DNAs from infectious pathogens provide the stimuli for the host to identify the infection and initiate immune response. Till the discovery of cGAS, many cytosolic DNA sensors, including DDX41(Zhang, Yuan, et al. 2011), IFI16(Unterholzner et al. 2010), and DAI(Takaoka et al. 2007), were reported to recognize intracellular double-stranded DNAs. All

these putative DNA sensors rely on STING, which does not bind to DNA, to initiate type I interferon production. The binding of STING with cyclic dinucleotides such as c-di-GMP or c-di-AMP to activate TBK1-IRF3, leading to the production of interferon added mysteries to this field (O'Connell et al. 2004). Since cGAS identified as the most important cytosolic DNA sensor, the puzzles were clearly solved. Upon binding of pathogen-derived dsDNA or self-generated DNAs, cGAS utilize ATP and GTP to produce the second messenger, cGAMP, which binds with STING to activate the downstream signaling cascade. Although cGAS plays pivotal roles in cytosolic DNA sensing, there are still other putative known or unknown DNA sensors that may also respond to the ligand. In cGAS or STING knockout dendritic cells, when stimulated with ISD, we still observed considerable genes expression changes. One example is IL-12b gene, whose mRNA expression was not induced by cGAMP treatment but was induced by ISD stimulation in cGAS independent manner. So it is possible that there are other DNA sensors contribute to add the immune response on the basis of cGAS or they may take the responsibilities in cells that lack cGAS or STING expression.

Previous research reported that either liposomes or herpesvirus derived nucleic acid-free particles could lead to the translocation of STING and thus activation of the downstream signaling (Holm et al. 2012). Here we observed similar result with Lipofectamine 2000 treatment alone without ISD and we showed that this immune response was dependent on both cGAS and STING. So it's more likely that the activation is still DNA dependent but the presence of liposome or virus-like particles makes the otherwise inaccessible DNA available to cGAS recognition. Interestingly, this activation of the cGAS-STING pathway by liposome was absent in cell types like lung fibroblasts or cell lines including 293T, BJ, Hela, etc., which

suggests that dendritic cells or macrophages may utilize additional mechanisms to access these DNA ligands.

Material and methods

Mice, Cells, and Nucleotides

cGas-/ mice were generated in our lab as previously described (Li, Wu, et al. 2013). STING Goldenticket mice were from the Jackson Laboratory (Stock No: 017537). All mice used in this study were on the C57/B6 background. The mice were bred and maintained under specific pathogen-free conditions in the animal care facility of the University of Texas Southwestern Medical Center at Dallas according to experimental protocols approved by the Institutional Animal Care and Use Committee.

To isolate primary lung fibroblasts, lung tissues from each mouse were minced and digested twice in 5 ml of DMEM with 0.1% collagenase D (Roche) and 0.2% trypsin (Sigma) at 37°C for 45-60 min. After washing with DMEM containing 10% calf serum, cells were seeded in a 10-cm dish in 12 ml DMEM containing 10% FBS in addition to 10% calf serum and antibiotics. Bone marrow cells were collected from femurs and tibiae of mice. To obtain BMDM and cDCs, about 10 million bone marrow cells were cultured in RPMI-1640 (Gibco 21870076) containing 10% FBS (Sigma), antibiotics, 1% NEAA, 1% sodium pyruvate, 1% glutamax, 50uM beta-mercaptoethanol and recombinant GM-CSF (20ug/ml, Preprotech, 315-03). After 7 days, attached cells were collected as mature macrophages and cultured in 12-well plates for experiments, and suspension cells were collected as conventional dendritic

cells. To obtain pDCs, 100ng/ml hFLT3L was used instead of GM-CSF and the culture time is 10 days. Floating and loosely adherent cells were harvested. Cultures were analyzed by FACS before use.

2'3'cGAMP was synthesized and purified as described (Zhang et al. 2013). Herring testes DNA (HT-DNA) was from Sigma (D6898). ISD was annealed from the forward and reverse DNA oligos, which were synthesized from Sigma using the following sequences: 5'-TACAGATCTACTAGTGATCTATGACTGATCTGTACATGATCTACA-3' and 5'-TGTAGATCATGTACAGATCAGTCATAGATCACTAGTAGATCTGTA-3'; CpG DNAs were synthesized from Sigma with the following sequences: CpG-C: T*C*G*T*C*G*T*T*T*C*G*G*C*G*C*G*C*G*C*G; CpG-B: T*C*C*A*T*G*A*C*G*T*T*C*C*T*G*A*C*G*T*T; CpG-A: G*G*GGTCAACGTTGAG*G*G*G*G (* indicates phosphorothioate backbone-modification).

Stimulation methods

For 293T cells, cells were transfected with indicated amount of pcDNA3 vector with sequence encoding wild-type or mutant cGAS, or MAVS for 12 hours for proper activation before proceeding to following experiments. For cGAMP treatment for lung fibroblasts, BMDM and BMDC, the cells were incubated in the following delivering buffer with or without the following buffer: 50 mM HEPES pH 7.0, 100 mM KCl, 3 mM MgCl₂, 0.1 mM DTT, 85 mM Sucrose, 0.2% BSA, 1 mM ATP, and 10 µg/mL Digitonin, for 15 minutes and then recovered in normal media for the indicated time. For ISD transfection, indicated

amount of DNA was transfected into cells using DNA (μg) to LipofectamineTM 2000 (μl) ratio of 1:3.

RNA-sequencing process and data analysis

The total RNA from the cells after stimulation was extracted with RNeasy Mini Kit from Qiagen (Cat No.: 74104). Samples are then run on the Agilent 2100 Bioanalyzer to determine the level of degradation thus ensuring only high-quality RNA is used (RIN Score 8 or higher). The samples were sent to UTSouthwestern Next Generation Sequencing Core for subsequent preparation and sequencing. The Qubit fluorometer was used to determine the concentration prior to cDNA library preparation. 4 μg of total DNase treated RNA was then prepared with the TruSeq Stranded Total RNA LT Sample Prep Kit from Illumina. Poly-A RNA was purified and fragmented before strand-specific cDNA synthesis. cDNA was then A-tailed and indexed adapters were ligated. After adapter ligation, samples were PCR amplified and purified with Ampure XP beads, then validated again on the Agilent 2100 Bioanalyzer. Samples were quantified by Qubit before being normalized and pooled, then run on the Illumina HiSeq 2500 using SBS v3 reagents. The sequencing data was processed using RNA-Seq CLC-Bio analysis for mRNA expression values, represented by Reads Per Kilobase per Million mapped reads values (RPKM).

Quantitative RT-PCR and Primers

Total cellular RNA was isolated using TRIzol. 0.1-1 μg total RNA was used for reverse transcription (RT) using iScript Kit (Bio-Rad). The resulting cDNA served as the template

for Quantitative-PCR analysis using iTaq Universal SYBR Green Supermix (Bio-Rad) and Viia™7 Real-Time PCR System (ABIApplied Biosystems Inc., Foster City, CA). The primers used are listed in Table 2-4.

Gene Name	Forward Primer	Reverse Primer
IFN- b	ATGACCAACAAGTGTCTCCTCC	GGAATCCAAGCAAGTTGTAGCTC
CXCL-10	GTGGCATTCAAGGAGTACCTC	TGATGGCCTCGATTCTGGATT
TNF-a	CCTCTCTAATCAGCCCTCTG	GAGGACCTGGGAGTAGATGAG
PPP1R15A	ATGATGGCATGTATGGTGAGC	AACCTGCAGTGTCCCTATCAG
PPP1R15B	CCTTCATCCCCTGTACTCT	AGGGTTCAGCAAATAGGATACCA
GADD45A	GAGAGCAGAAGACCGAAAGGA	CAGTGATCGTGCCTGACT
GADD45B	TACGAGTCGCCAAGTTGATG	GGATGAGCGTGAAGTGGATT
GADD45G	CAGATCCATTTACGCTGATCCA	TCCTCGAAAACAGGCTGAG
IL8	ATGACTTCAAGCTGGCGTGGCT	TCTCAGCCCTTCTAAAAACTCTC
FOS	GGGGCAAGGTGGAACAGTTAT	CCGCTTGGAGTGTATCAGTCA
JUNB	ACAAACTCCTGAAACCGAGCC	CGAGCCCTGACCAGAAAAGTA
NFKBIA	CTCCGAGACTTCGAGGAAATAC	GCCATTGTAGTTGGTAGCCTCA
RELB	CCATTGAGCGGAAGATTCACT	CTGCTGGTCCCAGATATGAGG
TNFAIP3	TCCTCAGGCTTGTATTTGAGC	TGTGTATCGGTGCATGGTTTA
IER3	CAGCCGCAGGGTTCTCTAC	GATCTGGCAGAACGATGGT
STAT2	CTGCTAGGCCGATTAACCTACCC	TCTGATGCAGGCTTTGCTG
OAS2	ACGTGACATCCTCGATAAAACTG	GAACCCATCAAGGGACTTCTG
TRIM5	AAGTCCATGCTAGACAAAGGAGA	GTTGGCTACATGCCGATTAGG
CCL5	CCAGCAGTCGCTTGTAC	CTCTGGTTGGCACACACTT
IFI44	GGTGGGCATAATACAACACTGG	CACACAGAATAACGGCAGGTA
IFIT1	AGAAGCAGGCAATCACAGAAAA	CTGAAACCGACCATAGTGGAAAT
IFIT2	GACACGGTTAAAGTGTGGAGG	TCCAGACGGTAGCTTGCTATT
IFIT3	TCAGAAGTCTAGTCACGGGG	ACACCTCGCCCTTCATTTC
ISG15	CGCAGATCACCCAGAAGATCG	TTCGTCGCAATTGTCCACCA
RSAD2	CAGCGTCAACTATCACTTCACT	AACTCTACTTGCAGAACCTCAC
IL12b	ACCCTGACCATCCAAGTCAA	TTGGCCTCGCATCTAGAAAG
IL6	ACTCACCTCTCAGAACGAATTG	CCATTTGGAGGTTCAGGTTG
GAPDH	GGAGCGAGATCCCTCCAAAAT	GGCTGTTGTCATACTTCTCATGG
ATF3	ATGATGCTCAACACCCAGG	TTTCGGCAGTTGCAGCTG

Table 2-4. List of qRT-PCR primers

CHAPTER FOUR

CHARACTERIZATION AND PURIFICATION OF CGAS INHIBITOR(S)

CERTAIN RNA AS CGAS INHIBITOR

Results

Establishment of biochemical assay for purification of cGAS activity regulator(s).

To purify and identify regulators for cGAS activity, we modified a previously established a cell-free cGAMP synthesis assay. Briefly, as shown in Figure 3-1A, when we mix cGAS activity provider, which can be either recombinant cGAS protein or L929 cell lysate (s20, the supernatant of 20,000g centrifugation), with DNA, ATP, and GTP, the reaction would synthesize cGAMP when incubated at 37 degrees. Then the synthesized cGAMP can be delivered into THP1-LuciaTM ISG cells (a cell line that expresses the secreted luciferase (Lucia) reporter gene under the control of an IRF-inducible promoter, allowing the monitoring of the IRF pathway by determining the activity of Lucia luciferase in the cell culture supernatant) at 1:10 dilution in the culture medium with PFO permeabilization (25ng/ml perfringolysin O), and the concentration of cGAMP in the reaction was evaluated by comparing the Lucia signal with cGAMP standards that were delivered into the reporter cells. Figure 3-1C shows an example of the readout for this assay. We can see that with 40ug of L929 s20, it can produce about 30nM of cGAMP in the 40ul reaction mixture. Alternatively, we incorporate [α -³²P]-ATP in the reaction and after reaction ends, the ³²P labeled product can be separated and analyzed by thin layer chromatography (TLC) assay. Figure 3-1B shows two example TLC runs. Depending on the kinds of TLC plates and running buffer, cGAMP could run either above (left panel) or below (right panel) the inorganic phosphate. With the assays

described above, we can add cell lysate or its fractions into the reaction and test its regulation to cGAS activity by measuring the concentration of cGAMP after reaction being terminated by 95 degrees heating for 5 minutes.

In cells with intact cGAS-STING DNA sensing pathway, when transfected with interferon stimulatory DNA, IRF3 dimerization and type I interferon production can be detected (data not shown). To show that cGAS is activated by DNA transfection, we transfected L929 and THP-1 cells with 2ug/mL ISD and 2 hours post-transfection, the cells were collected and lysed in hypotonic buffer. The cell lysate was heated at 95 degrees for 5 minutes and was delivered into the THP-1 reporter cells to measure the cGAMP concentration. In Figure 3-1D, we can see that in both cell lines, cGAMP was produced with DNA transfection. Interestingly, however, when we isolated the cytosol (s20) from L929 and THP-1 cells and applied them to the in vitro cGAS activity assay described above, we can only detect cGAS activity in L929 lysate (Figure 3-1E), even though there was relatively high level of cGAS protein in THP-1 cell lysate (data not shown).

To check if there were potential regulatory factor(s) in THP-1 lysate, we investigated the regulatory effect of the lysate on cGAS activity. We found that with increasing amount of THP-2 cytosol, the cGAS activity from both L929 s20 (Figure 3-1F) and from human recombinant cGAS (Figure 3-1G) were gradually inhibited. This suggests that certain components in THP-1 cell lysate can inhibit the activity of cGAS in in vitro reactions, which also explains why we were not able to detect cGAS activity in THP-1 lysate.

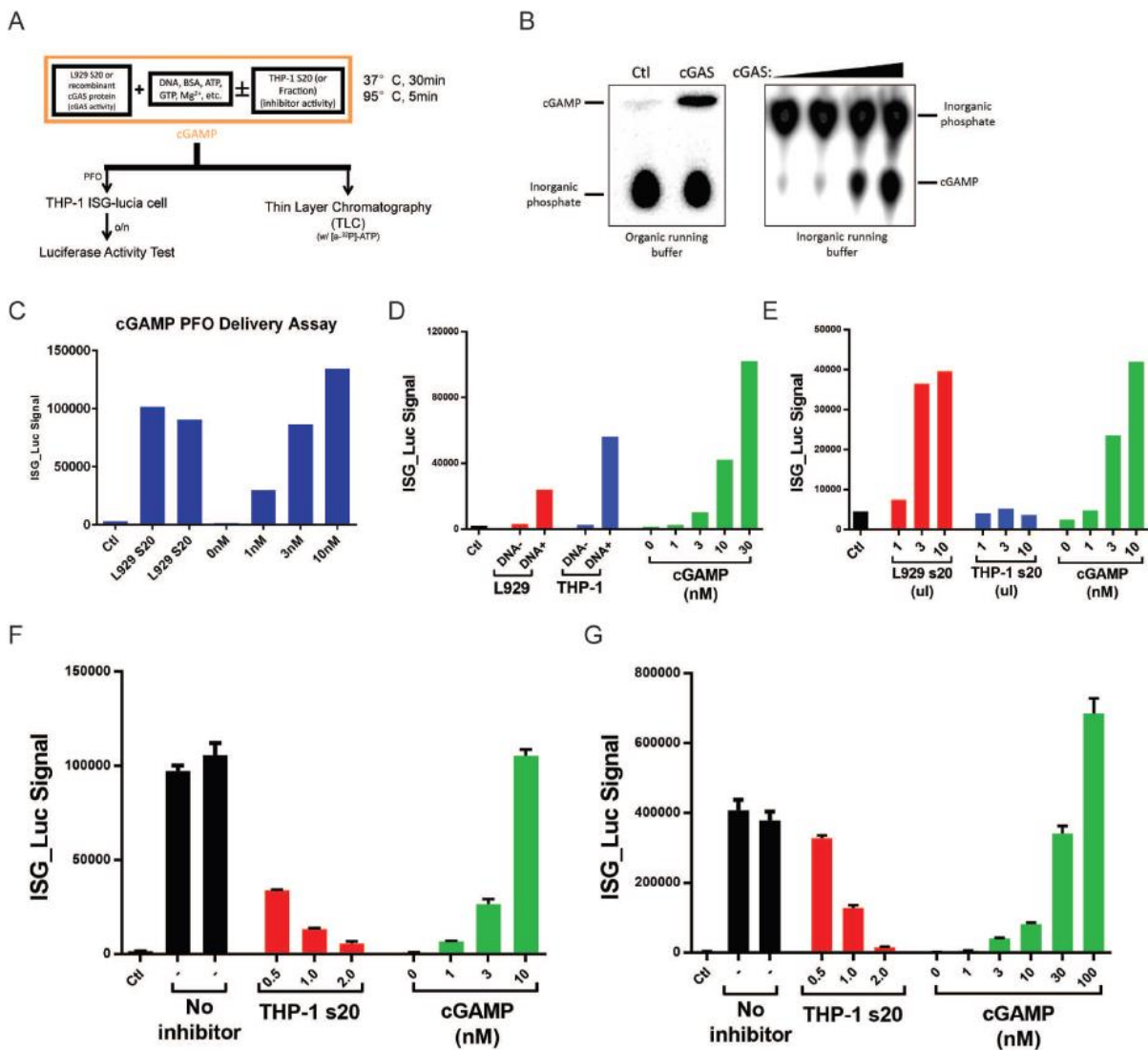


Figure 3-1. Establishment of biochemical assay for purification of cGAS activity regulator(s).

(A) Experimental design of the in vitro assay to test the activity of cGAS and its putative inhibitor(s)

(B) Representative data from thin layer chromatography analysis showing the synthesis and detection of cGAMP. Organic running buffer (left) or inorganic running buffer (right) was used to separate inorganic phosphate and cGAMP.

(C) Representative data from PFO permeabilization mediated cGAMP delivery assay.

Cytosol (S20) from L929 cells was used as cGAS activity provider in assay shown in (A), the reaction mix was boiled and delivered to THP-1 reporter cells using PFO. cGAMP standard was also delivered as controls.

- (D) L929 and THP-1 cell can produce cGAMP in response to DNA transfection. L929 and THP-1 cells are transfected with 2ug/ml HT-DNA for 3 hours. Cells are collected and lysed in hypotonic buffer. Cytosol was heat inactivated by boiling at 95 degrees for 5 minutes and the supernatant was delivered to THP-1 reporter cells with PFO permeabilization.
- (E) THP-1 cytosol (S20) shows no detectable cGAS activity. L929 and THP-1 cytosol was collected using hypotonic buffer lysis and subjected to cGAS activity test as shown in (A). The reaction mix was boiled and delivered to THP-1 reporter cells.
- (F-G) THP-1 cytosol (s20) shows cGAS inhibitory activity. L929 cytosol (F) or 3ng human recombinant cGAS (G) showed cGAS activity (No inhibitor groups). Adding THP-1 s20 into the reaction can inhibit the activity of cGAS in dosage-dependent manner.

Characterization and purification of a putative cGAS inhibitor in THP-1 cell lysate.

To test if this cGAS inhibitory activity in THP-1 was regulated in cells, we first treated THP-1 cells with HT-DNA and found more potent cGAS inhibitory effect in the cell lysate (Figure 3-2A). To investigate if this induction effect was specific to DNA stimulation, we also treated THP-1 cell with poly(I:C) or HSV before extract cytosol for inhibitory effect tests.

The result shows that all these treatments can enhance the cGAS inhibitory activity in the THP-1 cytosol, suggesting this factor could be interferon inducible. This might be a positive feedback regulation mechanism that cells utilize to shut down the immune response after the downstream signal has been properly activated.

To characterize the inhibitory factor, we did several tests to show that the inhibitory activity in the THP-1 lysate was not due to protease(s) that degrade cGAS protein (data not shown), that the factor was sensitive to heat (95 degrees for 5 minutes, Figure 3-2B), and that it did not inhibit cGAS activity through competing against cGAS-DNA binding (Figure 3-2C).

Interestingly, we found that adding more than 1mM ATP alone in the reaction inhibited cGAS activity.

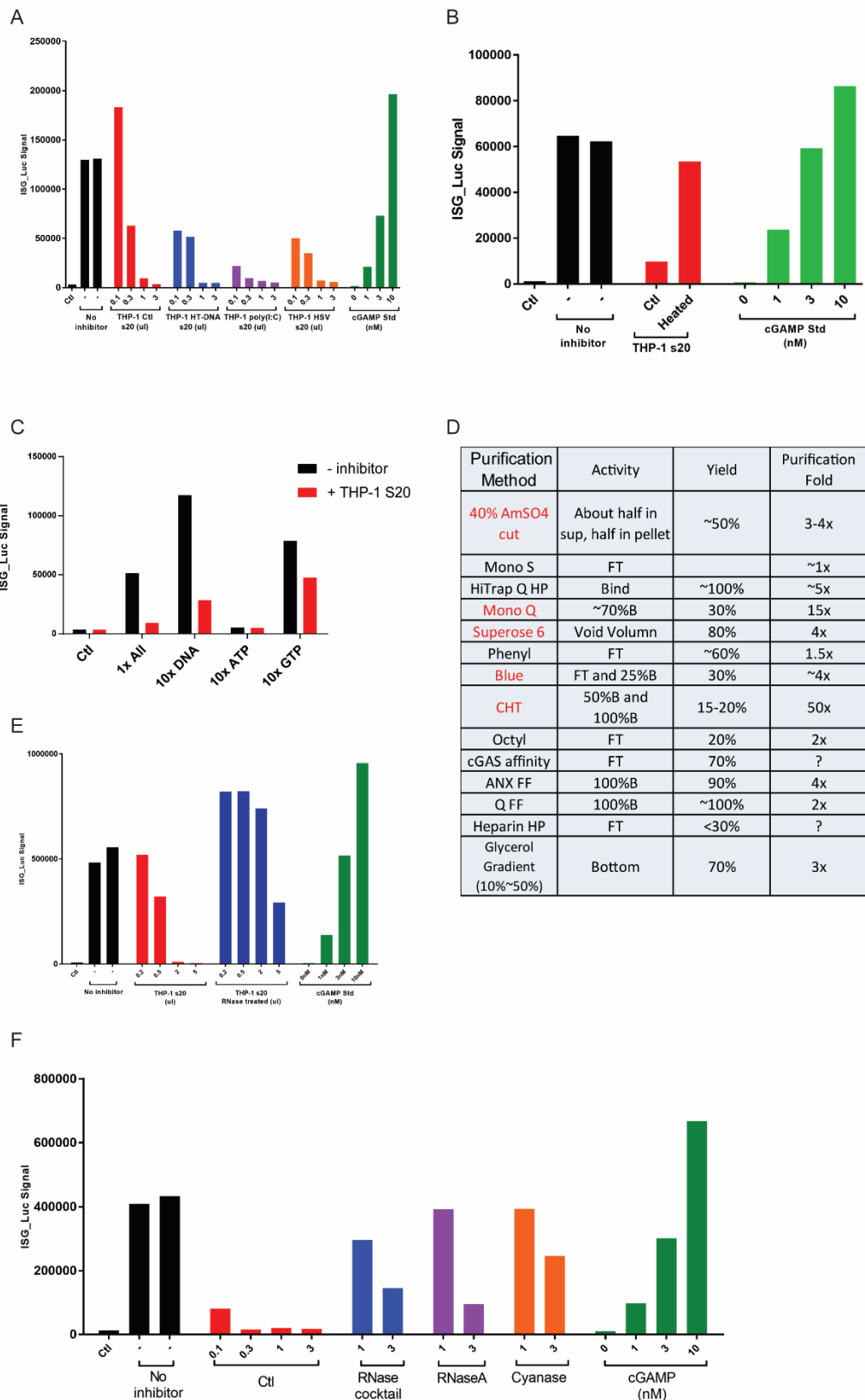


Figure 3-2. Characterization and purification of a putative cGAS inhibitor in THP-1 cell lysate.

- (A) The putative cGAS inhibitor from THP-1 cytosol is further induced by ligand stimulations. THP-1 cell were treated with HT-DNA (2ug/ml), poly(I:C) (2ug/ml), HSV (MOI=5), or left untreated before cytosol (s20) was collected. The concentration of cytosols was adjusted to 6ug/ml and indicated volume of cytosol was used for cGAS inhibitory activity test.
- (B) Putative cGAS inhibitor(s) from THP-1 cytosol is heat-sensitive. Inhibitory THP-1 cytosol was heated at 95 degrees for 5 minutes and its cGAS inhibitory activity was tested.
- (C) Effect of adding more DNA, ATP, or GTP to the cGAS reaction. In control reaction (1x All), 10ng/ul HT-DNA, 1mM ATP, and 0.5mM GTP were used. In 10x DNA reaction, 100ng/ul HT-DNA was added; in 10x ATP reaction, 10mM ATP was used; and in 10x GTP reaction, 5mM GTP was added to reaction.
- (D) Purification methods and their purification folds tested is summarized in the table. Those with good purification effects were labeled as red.
- (E) RNase can greatly reduce the inhibitory activity in THP-1 cytosol. THP-1 cytosol was left untreated or treated with RNase A and RNase T1 cocktail on ice for 1 hour. Then indicated amount of treated and untreated cytosol were tested in cGAS activity assay.
- (F) Inhibitory fraction eluted from Hitrap Q column is sensitive to RNase activity. THP-1 cytosol was loaded on Hitrap Q column and eluted with gradient concentration of NaCl. The fractions were collected and tested for cGAS inhibitory activity. The inhibitory fraction was left untreated or treated with RNase cocktail, RNase A, or Cyanase, after which the indicated amount of fraction was tested in cGAS activity assay.

We then tried to fractionize THP-1 cell lysate using different methods or with FPLC columns. Table in Figure 3-2D listed the methods and columns and labeled the ones with good purification efficiency red. The fact that the factor bound to Q and CHT columns suggested that it was negatively charged and that it was rich in phosphate group. However, we also found that the inhibitor we were looking for formed huge complex and was eluted at the void volume on SuperoseTM 6 columns (suggesting a molecular weight of heavier than 5×10^6 Dalton). And as we tested, the cGAS inhibitory complex was resistant to high salt (up to 2M NaCl), detergent (up to 1% sodium deoxycholate and 0.5% SDS) (data not shown). Surprisingly, we found that either nucleases, like Cyanase, or RNase could break the large complex (as shown on gel filtration columns, data not shown). And we can see that RNase or

Cyanase treatment could kill the cGAS inhibitory effect in THP-1 s20 (Figure 3-2E) and also in its inhibitory fraction eluted from Hitrap Q column (Figure 3-2F). These results above strongly indicated that the inhibitor we were looking for should be certain RNA species.

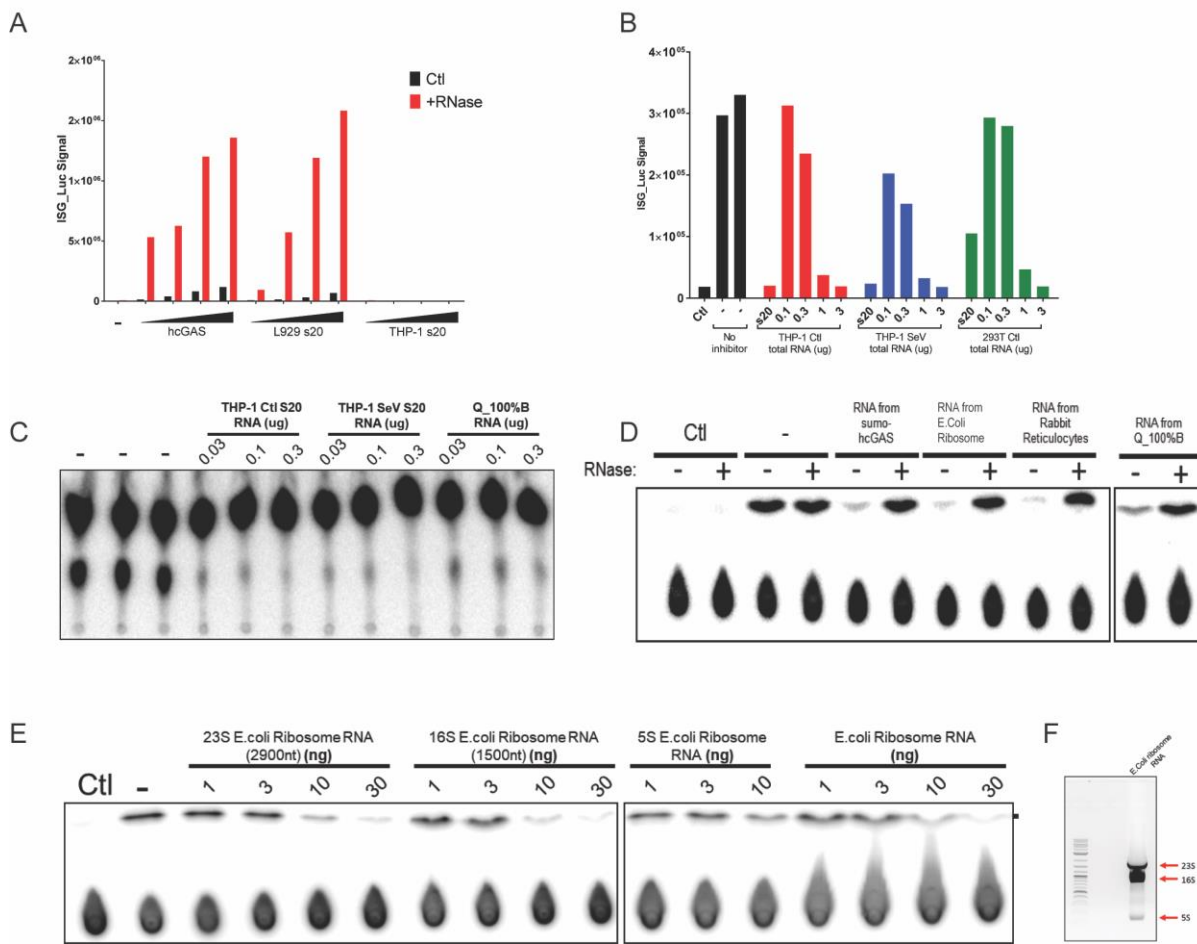


Figure 3-3. Certain RNA species can inhibit cGAS activity in vitro.

(A) RNase can greatly enhance the production of cGAMP in cGAS activity assay. Increasing amount of human recombinant cGAS, L929 cytosol (s20), or THP-1 cytosol was tested in cGAS activity assay in presence or absence of RNase cocktail.

(B-C) Total RNA extracted from THP-1 cell and 293T cell can inhibit cGAS activity in vitro. Total RNA was isolated from THP-1 cell (Ctl), Sendai virus treated THP-1 cell (SeV), 293T cell, or inhibitory fraction eluted from Hitrap Q column (Q_100% B) and tested in cGAS activity assay. The cGAS inhibitory effect was evaluated by THP-1 reporter cell assay (B) or TLC assay (C).

(D) RNA from different source can inhibit cGAS activity. RNA extracted from human recombinant sumo-cGAS, E.Coli ribosomes, rabbit reticulocytes, or inhibitory fraction eluted from Hitrap Q column (Q_100% B) was tested in cGAS activity assay in presence or absence of RNase.

(E-F) 23S and 16S ribosomal RNA from E.coli can potently inhibit cGAS activity. E.coli ribosomal RNA was separated on agarose gel (F) and bands representing different subunits were cut and extracted. The indicated amount of RNA was added to test in cGAS activity assay.

Certain RNA species can inhibit cGAS activity in vitro.

To confirm that RNA can inhibit cGAS activity in vitro, we treated THP-1 s20 with RNase, expecting to release the cGAS in the lysate from inhibition. However, the RNase treatment could not restore cGAS activity in the cytosol (Figure 3-3A), probably because RNase could not degrade all the inhibitory RNA in the lysate (since cGAS activity is very sensitive to temperature, we could only treat the sample with RNase at 4 degrees). Yet, we did find that with RNase included in the reaction mix, the activity of human recombinant cGAS or cGAS from L929 s20 increased dramatically. This was due to that the residual RNA in the purified cGAS and in the L929 lysate can inhibit the cGAS activity to some extent.

We also purified total RNA form THP-1 cells (either control cells or cells treated with Sendai virus), 293T cells or from inhibitory fraction eluted from Hitrap Q column and found that total RNA from all these cells could inhibit cGAS activity in vitro (Figure 3-3B and C). Also, we tested RNA extracted from E. coli ribosome, rabbit reticulocytes, or from purified recombinant cGAS from E. coli, all of which could inhibit cGAS activity and including RNase in the reaction fully released the inhibition (Figure 3-3D). Further, we separated E. coli ribosome RNA on agarose gel (Figure 3-3F), cut the bands for different subunits,

extracted/purified the RNA and found that both 23S and 16S showed potent inhibition to cGAS activity. The inhibition effect of 5S subunit was relatively weak.

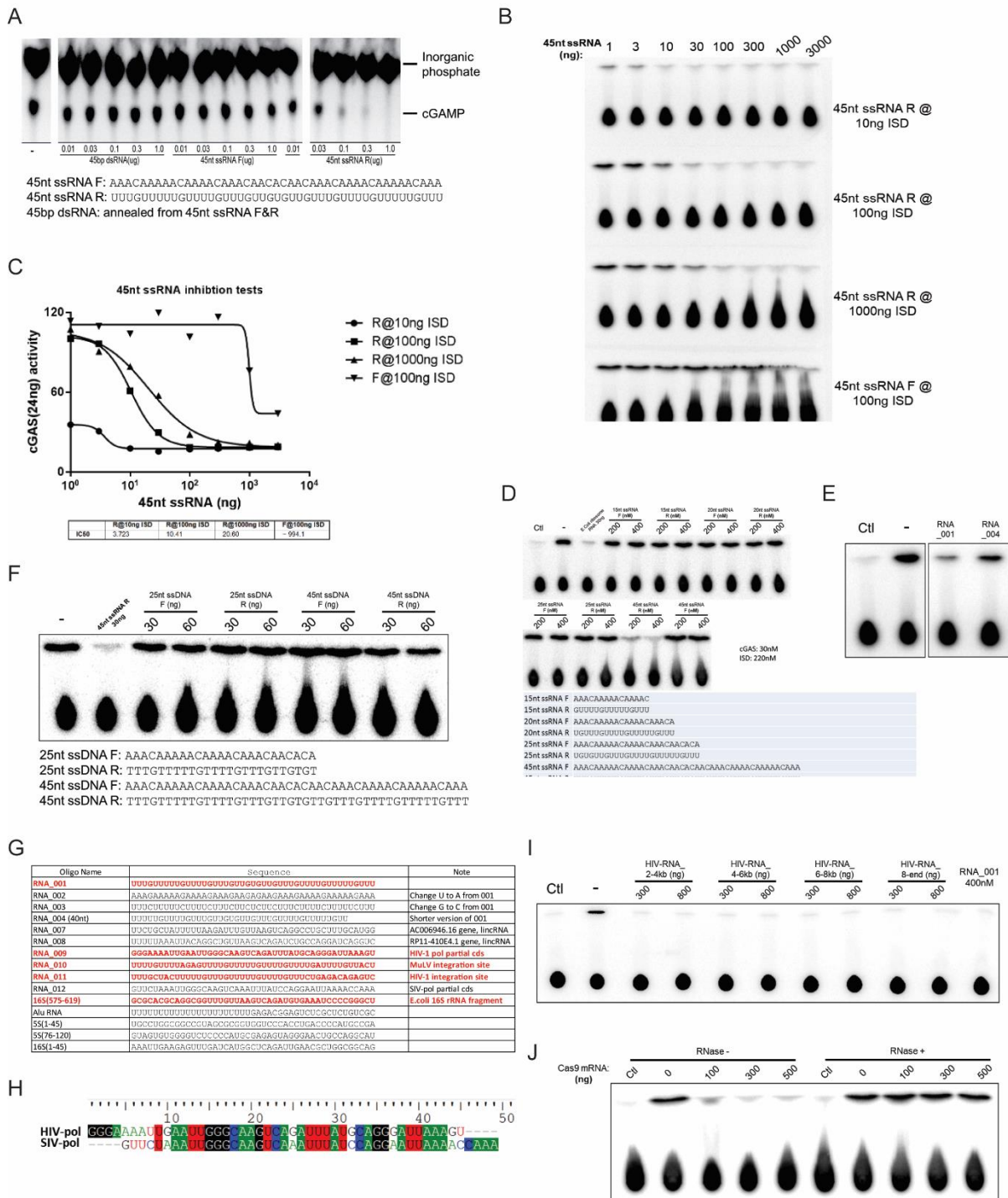
Short synthesized RNA oligos inhibit cGAS activity in sequence and length-dependent manner.

To further test the inhibition of cGAS activity by RNA, we synthesized and tested series of 45-nucleotide single-stranded RNA (ssRNA). Interestingly, one of the RNA sequences, which was consist of random A and C combination (ssRNA F), showed no inhibition effect while its complimentary reverse sequence (ssRNA F) showed very potent inhibition to cGAS activity in vitro (Figure 3-4A). Notably, the double-stranded RNA (dsRNA) annealed from the ssRNA above did not inhibit cGAS activity. In Figure 3-4B, we tested the kinetics for cGAS inhibition by RNA. We titrated the amount of both ssRNA and ISD used in the reaction and used ssRNA F as a negative control. The data was analyzed and quantified by ImageJ software (Figure 3-4C). With 24ng (20nM) cGAS and 100ng (166nM) ISD in the reaction, the IC₅₀ for the inhibitory RNA oligo was 10.41ng (30nM). And when ISD concentration increased by 10-fold, the IC₅₀ only doubled to 20.60ng (68.37nM).

To test if the inhibition of cGAS activity by RNA dependent on the length of cGAS, we truncated the original 45nt ssRNA R (also labeled as RNA_001) and tested if the RNA oligo of shorter version could inhibit cGAS activity. Surprisingly, deleting only 5 nucleotides from the original sequence largely killed the inhibitor activity (Figure 3-4E, RNA_004) and further truncation would totally abolish the inhibitory effect (Figure 3-4D). We also synthesized the DNA oligos with the same sequence as the inhibitory RNA and as expected, the single-stranded DNA oligo did not inhibit cGAS activity (Figure 3-4F).

The inhibition of cGAS by RNA seemed to be dependent on the sequence of the RNA. In order to test this, we synthesized series of RNA oligos, either found in the database that shares sequence similarity to RNA_001 or with sequence derived from RNA_001 with small changes. The sequences of oligos tested are listed in Figure 3-4G and the ones with potent inhibitory effect are labeled in red. Of the listed sequence, one striking data was that comparing RNA_009 and RNA_012, which were selected sequence from polymerase coding sequence of HIV and SIV, respectively. From the alignment in Figure 3-4H, we could see that the two RNA share very similar sequences, however, as RNA_009 had very strong cGAS inhibition activity while RNA_012 could not inhibit cGAS activity at all.

With the data above, we were interested to see if specific RNA region from virus origin can inhibit cGAS and regulate host immune response. We in vitro transcribed HIV genome RNA fragments (2 kilobases for each fragment). Surprisingly, all fragments can potently inhibit cGAS activity in vitro (Figure 3-4I). We further tested some random long mRNA sequences (Cas9 mRNA, as an example in Figure 3-4J) and found that they all had cGAS inhibition activity. This suggests that when reaching a certain length, single-stranded RNA can inhibit cGAS in a sequence-independent manner.



- (A) Synthesized dsRNA R reserve strand but not forward or annealed double-stranded RNA can inhibit cGAS activity in vitro. Forward (F) or reverse (R) RNA was synthesized with sequences shown at bottom. Indicated amount of RNAs was tested in cGAS activity assay.
- (B-C) Kinetics for cGAS inhibition by RNA oligo. Indicated amount of RNA oligos and ISD were added in the cGAS activation assay. The result (B) was quantified with ImageJ software and showed in (C)
- (D-E) Inhibition of cGAS by RNA oligo is dependent on its length. Indicated truncated RNA oligos were added in the cGAS activity assay.
- (F) Single-stranded DNA with the same sequence show no inhibitory effect on cGAS activity. DNA oligos with indicated sequences were added in the cGAS activity assay.
- (G) Summary of sequences of RNA oligos test in cGAS activity assay. Those with potent inhibitory effect were labelled as red.
- (H) Alignment of regions from HIV polymerase and SIV polymerase coding sequence.
- (I) In vitro transcribed HIV genome RNA can potently inhibit cGAS activity. The indicated fragments from HIV genome was transcribed in vitro. Indicated amount of the RNA was added to evaluate their cGAS inhibitory effect.
- (J) Caspase 9 mRNA can potently inhibit cGAS activity. Commercially purchased mRNA encoding Caspase 9 was added to cGAS activity assay in presence or absence of RNase.

Phosphorothioate bond DNA oligos inhibit cGAS activity.

Previous research reported that Synthetic oligodeoxynucleotides with phosphorothioate (PS) bond containing suppressive TTAGGG motifs could abolish DNA sensing response by inhibiting AIM2 inflammasome activation (Kaminski et al. 2013). So, we were interested in finding out if phosphorothioate bond DNA oligos would inhibit the activity of cGAS. We synthesized the PS bond and phosphodiester (PO) bond DNA oligos, and also RNA with TTAGG repeats (A151) and control sequence (C151), as described in the publication above. Interestingly, we found that both P-S bond DNA can inhibit cGAS activity but not PO bond DNA or RNA (Figure 3-5A). We did a titration of the PS bond DNA with a sequence of random A's and C's and found it had an IC₅₀ of 135nM when cGAS was 30nM in the reaction (Figure 3-5B and C).

To further test if the PS bond DNA oligo could inhibit cGAS in cells, we co-transfected ISD with CpG DNA oligos and checked the induced expression of type-I interferons and inflammatory cytokines (Figure 3-5D). As expected, ISD alone transfection in conventional dendritic cells induced high mRNA levels of IFN- β , IFN-a4, and IL-6, which dependent on the DNA sensor, cGAS. Surprisingly, adding CpG DNA oligos (either CpG-B or CpG-C) would totally abolish the induction. These results suggest that PS bond DNA can inhibit cGAS activity both in vitro and in cells.

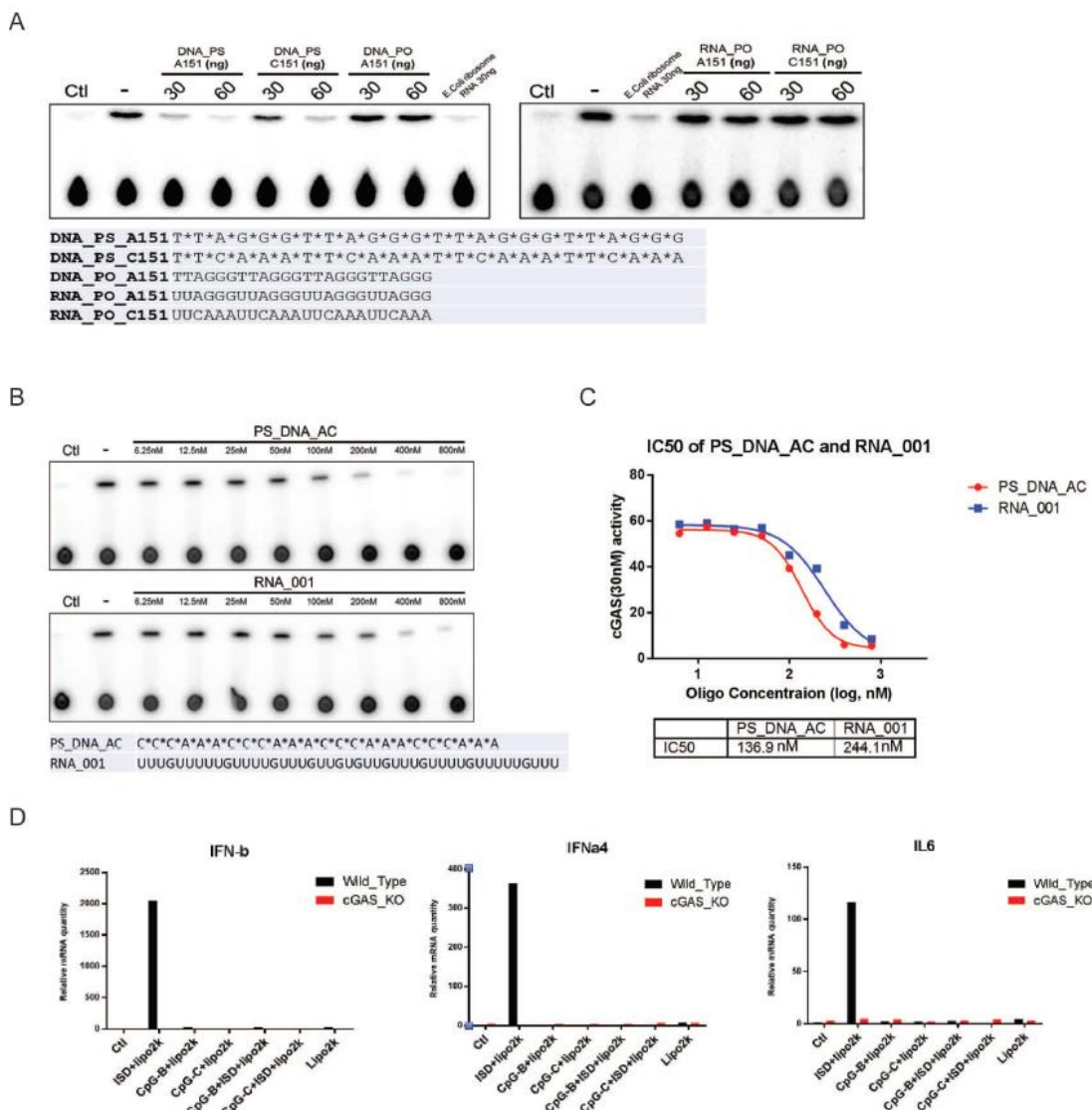


Figure 3-5. Phosphorothioate bond DNA oligos inhibit cGAS activity.

(A) DNA oligo with phosphorothioate bond but not phosphodiester bond backbone can inhibit cGAS activity in vitro. The oligos with the indicated sequences was added evaluate their cGAS inhibitory activity.

(B-C) Kinetics for cGAS inhibition by Phosphorothioate bond DNA oligo. A titration of indicated oligos were added in cGAS activity assay. The result (B) was quantified with ImageJ software and showed in (C).

(D) Phosphorothioate bond DNA oligo can inhibit cGAS activation by ISD transfection. ISD and CpG DNA oligos were transfected to bone marrow-derived dendritic cells individually or in combination as indicated, for 4 hours. RNA was isolated. IFN- β , IFN- α 4, and IL-6 mRNA levels were analyzed by q-RT-PCR.

Conclusions and discussion

In this part, we discovered that certain RNA species from selected cell lines can inhibit the activity of cGAS in vitro. This putative cGAS inhibitory RNA can be further induced by interferon, which may indicate that a regulatory feedback loop could exist in cells to control the activity of cGAS after being activated.

It's surprising that single-stranded RNA could potently inhibit cGAS. As shown in Figure 3-3E, for E.coli 16S and 23S ribosomal RNA, as little as 10ng (0.9nM and 1.7nM respectively for 23S and 16S) could almost totally abolish the activity from reaction with 30nM cGAS with 220nM ISD in the mixture. This inhibition could due to that ssRNA can bind with cGAS. Indeed, with electrophoretic mobility shift assay (data not shown), we found that ssRNA can bind with purified cGAS, with similar or a little bit higher affinity than double-stranded DNA. However, all RNA oligo observed, including inhibitory, non-inhibitory ssRNA, and dsRNA can bind to cGAS. Probably because RNAs are negatively charged while cGAS is positively

charged at physiological pH. The inhibition of cGAS by RNA dependent on the length of the oligo and the inhibition very sequence sensitive when the oligo is short. But when the RNA is long, it can inhibit cGAS activity without sequence specificity. This raises the question that why in cells, with all the ribosomal RNA and mRNAs presence in the cytosol, how cGAS can be activated by DNA. A possible explanation could be that for the majority of ribosomal and mRNAs, they are bound by RNA-binding proteins and thus kept away from cGAS.

We have not been able to purify or identify the exact RNA species that act as the physiological cGAS inhibitor in cells. There have been the following difficulties. The first is that there are no effective methods to fractionate and purify specific RNAs. We did try to pull down cGAS binding RNAs through co-immunoprecipitation with or without cross-linking. However, there were always contaminations from ribosomal and mRNAs, which were difficult to get rid of. And we also tried to understand the mechanism by which RNA inhibit cGAS by cGAS-RNA co-crystallization. However, we were not able to get crystals with good quality, probably due to that the inhibitory RNAs were too long for crystallization and we could not truncate the RNA while preserving its inhibitory activity.

CGAS INHIBITOR(S) FROM NUCLEUS

Results

cGAS is considered to be the cytosolic DNA sensor due to the fact that it was originally purified and identified in the cytoplasm. This raised the question that during the cell cycle, when nucleus membrane breaks down, why cGAS is not activated if it can bind to chromosome DNA. In the beginning, a possible explanation was that during M phase, genomic DNA is highly condensed to chromosomes and cGAS would not be able to access to chromosomal DNA. However, here we discovered that after nuclear membrane breaks down, cGAS is recruited to chromosome and resides in the nucleus after mitosis finishes and nuclear membrane re-established. This leads to a surprising phenotype that in cultured cell with active cell division, the majority of cGAS is localized in the nucleus. So, it is interesting to investigate how the activity of cGAS is regulated in the nucleus and whether nuclear cGAS has any physiological functions.

The majority of cGAS in dividing cells present in the heavy fractions and is resistant to detergent extraction.

In experiments that we separated different fractions of cell lysate using differential centrifugation, we unexpected found that instead of being in the supernatant of 20,000g centrifugation, as most cytosol proteins do, cGAS was located at very heavy fractions (data not shown). Further, we tested different methods to permeabilize or break the cells to extract cGAS, as shown in Figure 3-6A. We did the test in both THP-1 wild-type cells and also THP-1 cGAS knockout cells that were rescued with Flag-tagged cGAS. With collected cell pellet,

we used PBS, or PBS with PFO (which only permeabilize cell membrane and thus only extract cytosolic proteins to supernatant) or with NP-40 (which should extract both cytosol proteins but also proteins from membrane organelles). As expected, ikb-alpha, which is a cytosolic protein, can be isolated by both PFO and NP-40 containing PBS. MAVS, as a mitochondria protein, can only be efficiently extracted by NP-40 containing buffer. However, to our surprise, cGAS, which we considered to be a cytosolic protein, was resistant to both PFO and NP-40 extraction. Further, we used sequential extraction methods to isolate proteins from different cellular components (Figure 3-6B). We first used hypotonic buffer to break the cell membrane and extracted cytosols (s20), then with the pellet (p20) from hypotonic buffer extraction, we used Radioimmunoprecipitation assay buffer (RIPA buffer) to extract both membrane organelle proteins and nuclear proteins. Finally, we used 1M NaCl buffer to extract proteins that were in the pellets from RIPA buffer extraction. As shown in Figure 3-6B, ikb-alpha and MAVS proteins are in s20 and RIPA buffer extract respectively. While there was a small amount of cGAS protein in the cytoplasm, the majority of cGAS could only be extracted with 1M NaCl (hi-salt extract). Similarly, we also tested this on Hela cGAS knockout cells and Hela wild-type cells and cGAS showed similar pattern with extraction (Figure 3-6C). These results above suggest that cGAS is not a “simple” cytosolic protein. It could either be forms heavy, detergent resistant complex in the cytosol, or it could be localized in the nucleus.

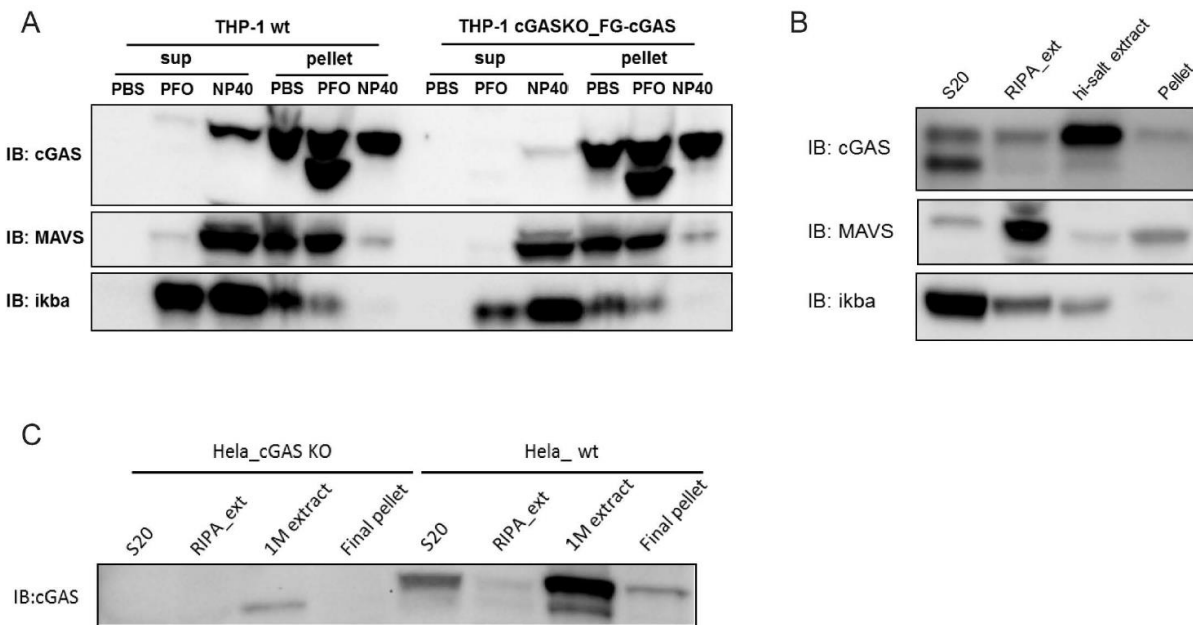


Figure 3-6. The majority of cGAS in dividing cells presence in the heavy fractions and is resistant to detergent extraction.

(A) The majority of cGAS is resistant to detergent extraction in THP-1 cells. THP-1 cell (THP-1 wt) and THP-1 cell with cGAS knocked out and rescued with Flag-tagged cGAS (THP-1 cGASKO_FG-cGAS) were collected and suspended in PBS or PBS supplemented with PFO or NP-40. After incubation, the cells were centrifuged at 20,000g for 5 minutes and the supernatant and pellet were collected for Western Blot analysis.

(B) High salt can extract cGAS from THP-1 cells. THP-1 cells were first lysed in hypotonic buffer and cytosol protein (s20) was collected. For the pellet was further extract with RIPA buffer (RIPA_ext). The pellet left from RIPA buffer extraction was extracted with hypotonic buffer supplemented with 1M NaCl (hi-salt extract). The pellet from the 1M NaCl extraction was boiled in SDS loading buffer. All fractions were processed for Western Blot analysis.

(C) High salt can extract cGAS from Hela cells. Hela cells (HeLa_wt) and Hela cGAS knockout cells (HeLa_cGAS KO) were subjected to the same sequential extraction in (B) and different fractions were analyzed with Western Blot for cGAS distribution.

cGAS is recruited to chromosomes during mitosis and is present in the nucleus in actively dividing cells.

To further study the localization of cGAS in cells, we stably expressed GFP tagged cGAS in Hela cells (Hela_GFP-cGAS cell line, and as control, we also express GFP protein in Hela

cells, Hela_GFP cell line). To our surprise, in Hela_GFP-cGAS cells, the nucleus showed very strong GFP-cGAS signal, indicating that indeed most of the protein was localized in the nucleus (Figure 3-7A, left panels). More interestingly, as outlined by rectangular boxes, in dividing cells at anaphase, the cGAS-GFP signal perfectly co-localized with the chromosomes. As control, in Hela_GFP cells, the GFP signal just showed ubiquitous distributions in both cytoplasm and nucleus (Figure 3-7A, right panels).

To confirm that cGAS-GFP would co-localize with chromosomes at metaphase, we treated both cell lines with Nocodazole to synchronize the cells at M phase. After Nocodazole treatment for 12-16 hours, the cells that were synchronized at M phase become rounded and lose most of their attachment to the substratum. And due to lack of polymerized tubulin to form spindles, instead of aligning at the mitotic plate of the cells, the chromosomes form a condensed structure that gave very strong signal with DAPI staining (Figure 3-7B). And strikingly, the cGAS-GFP signal in these M phase cells also formed the same condensed structures and exactly co-localized with the DAPI signal. And interestingly, in the cells that were not in M phase after Nocodazole treatment, the majority of cGAS-GFP signal came from the cytoplasm. The reason for this observation could be that these cells somehow escaped the Nocodazole induced cell-cycle arrest and were then arrested at G1 phase, during which the localization of cGAS should be mainly in the cytoplasm (as will also be shown below). In contrast, the GFP signal in Hela_GFP cell line was non-specifically distributed in the whole cells.

To fully understand how the localization of cGAS changes dynamically within a cell cycle, we used double-thymidine method to synchronize the cells at G1 phase, released the arrest so that

the cell enters next cycle and monitored the localization of GFP-cGAS at different stages of division (Figure 3-7C). After thymidine treatment for extensively long time (about 36 hours), we can see that the majority of GFP-cGAS was located in the cytoplasm (G1/S phase). About 10 hours after releasing, most of the cells enters M phase. During prometaphase and metaphase, almost all of the GFP-cGAS protein were recruited to and co-localized with chromosomes. In contrast, in Hela_GFP cells, during prometaphase and metaphase, GFP protein was excluded from chromosomes. When cells entered telophase (nuclear membrane reformed) and cytokinesis (nucleoli reappeared, and chromosomes unwound into chromatin), the majority of the GFP-cGAS protein still presented in the nucleus. As tested, after cytokinesis and cell division completed, if the cell cycle was not arrested, then most of the GFP-cGAS protein was still localized in the nucleus when the next cell cycle began thus leading to the phenomenon that most of the cGAS protein was detected in the nucleus. However, if we arrested the cell cycle in G1/S phase, after 24-36 hours, more and more GFP-cGAS signal appeared in the cytoplasm. This is probably due to the fact that newly translated cGAS protein could not enter the nucleus until nuclear membrane breaks down. Meanwhile the GFP-cGAS signal in the nucleus decreased which could be caused either by the exportation of nuclear cGAS or by the degradation of the cGAS in the nucleus. Overall, these data show that the cellular localization of cGAS is dynamically regulated by cell cycle and in actively dividing cells, most of the cGAS protein actually exists inside the nucleus.

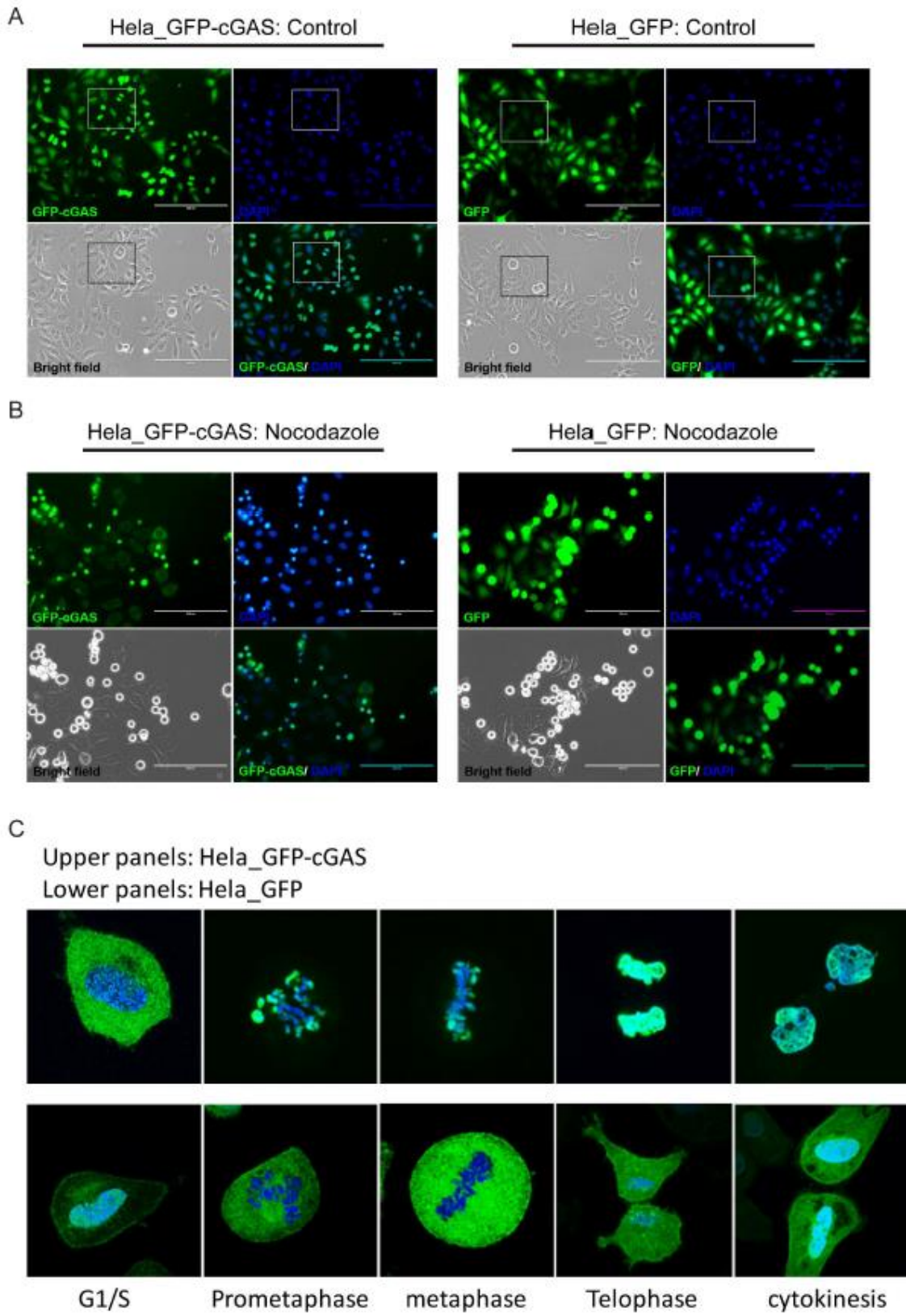


Figure 3-7. cGAS is recruited to chromosomes during mitosis and is present in the nucleus in actively dividing cells.

- (A) Strong GFP-cGAS signal detected in Hela_GFP-cGAS cell line. Hela cell stably expressing GFP (Hela_GFP) or GFP tagged cGAS (Hela_GFP-cGAS) were visualized with fluorescence microscope with DAPI nuclear staining.
- (B) GFP signal perfectly co-localize with nuclear content in Nocodazole synchronized cells. Hela_GFP and Hela_GFP-cGAS cells were first synchronized with Nocodazole for 12 hours before visualized with fluorescence microscope with DAPI nuclear staining.
- (C) Co-localization of GFP-cGAS with chromosome/chromatin at different stages of division. Hela_GFP and Hela_GFP-cGAS cells were synchronized at G1/S phase with double thymidine protocol and then release for mitosis progress. Cells at different stages were visualized with confocal microscope with DAPI nuclear staining.

Chromatin high salt extract contains putative cGAS inhibitor(s).

Since we detected that the majority of the cGAS in dividing cells is localized in the nucleus, it is intriguing to check if the nuclear cGAS can be activated by chromatin DNA and DNA from other sources. From Hela cells that stably express Flag-tagged cGAS (Hela_FG-cGAS), we used hypotonic buffer to isolate both cytosol and nucleus. Then with or without ISD in the reaction mix, we checked the activity of cGAS in these fractions. As expected, the cytosolic cGAS could be activated in ISD dependent manner (Figure 3-8A, Cytosol). Interestingly, we found that the nucleus cGAS could also be activated by ISD, but it was not activated by the chromatin already in the nucleus (Figure 3-8A, Nucleus). Furthermore, we found that though containing the majority of cGAS in the cells, we were not able to detect any cGAS activity from high salt extract from the nucleus (data not shown). Instead, the high salt extract could further inhibit the activity of recombinant cGAS (Figure 3-8B, 0.5M NaCl extract). This observation indicated that there should be certain cGAS inhibitor(s) in the 0.5M NaCl extract from the nucleus.

To further test if the putative inhibitor in the high-salt extract binds with cGAS, we isolated cell cytosol (s20) and nuclear high-salt extract (1M NaCl extract) from Hela_FG-cGAS cells. Consistent with previous results, s20 showed good cGAS activity (Figure 3-8C, s20) while the high-salt extract did not exhibit any cGAS activity (Figure 3-8C, 1M NaCl extract). For both s20 and 1M NaCl extract, we performed immunoprecipitation using agarose beads conjugated with M2 antibody at two conditions: one with 0.4M NaCl and the other with 1M NaCl in the immunoprecipitation buffer. After immunoprecipitation, we used flag peptide to elute the binding proteins from the beads. As shown in Figure 3-8C, eluates of s20 immunoprecipitation at both salt conditions showed good cGAS activity. Interestingly, though eluates of 1M NaCl extract immunoprecipitation at both salt conditions resulted in the similar amount of cGAS protein (Figure 3-8D), the eluate of immunoprecipitation with 1M NaCl in the buffer showed good cGAS activity while that with 0.4M NaCl showed none. These data suggest that in the high salt extract from the nucleus, there are both cGAS and inhibitor(s) that can suppress cGAS activity. When performing the immunoprecipitation with 1M NaCl, the putative inhibitor was disassociated from cGAS and thus remained in the flow through, and that's the reason we could detect cGAS activity. With lower ion strength (0.4M NaCl), the putative inhibitor still bound with cGAS and was co-immunoprecipitated. In this case, the inhibitor would also be eluted from the beads along with cGAS.

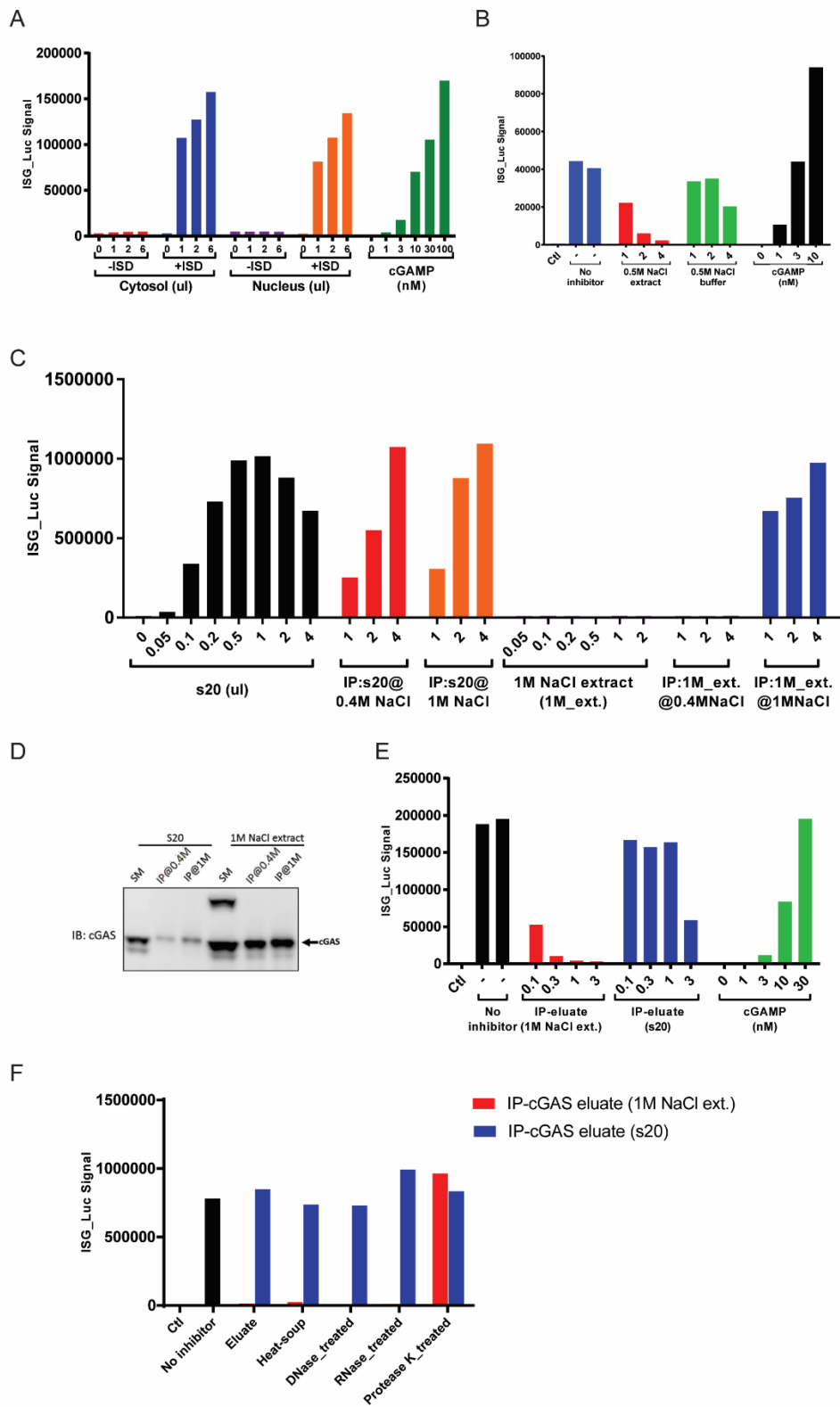


Figure 3-8. Chromatin high salt extract contains cGAS inhibitor.

(A) cGAS from both cytosol and nucleus can be activated in DNA dependent manner. Hela cell stably expressing Flag-tagged cGAS (Hela_FG-cGAS) was lysed in hypotonic buffer. The cytosol and nucleus fractions were collected and tested for cGAS activity in presence or absence of ISD.

(B) High salt extraction from nucleus can inhibit cGAS in vitro. Hela cell stably expressing Flag-tagged cGAS (Hela_FG-cGAS) was lysed in hypotonic buffer. Then hypotonic buffer supplemented with 0.5M NaCl was used to extract the nucleus (0.5M NaCl extract). The cGAS inhibitory effect of the 0.5M NaCl extract was evaluated (as control, hypotonic buffer with 0.5M NaCl was used)

(C-D) Putative cGAS inhibitor from nucleus high salt extract co-immunoprecipitate with cGAS. Hela_FG-cGAS cells were lysed in hypotonic buffer and cytosol protein was collected (s20), the nucleus was further extracted with hypotonic buffer supplemented with 1M NaCl (1M NaCl extract); both s20 and 1M NaCl extract were used for subsequent immunoprecipitation with M2 agarose beads in buffer with 0.4M NaCl or 1.0M NaCl respectively. Flag peptide containing buffer was used to elute FG-cGAS and its binding protein and the eluates, along with the starting materials were evaluated for cGAS activity. The amount of cGAS in starting materials and in IP eluates was evaluated by Western Blot (D).

(E) Putative cGAS inhibitor from nucleus cGAS IP can be eluted by buffer with 1M NaCl. Similar immunoprecipitation experiment as in (C) was performed, except that the IP was only performed in 1M NaCl buffer and that the beads were eluted with hypotonic buffer supplemented with 1M NaCl and BSA carrier protein.

(F) Putative cGAS inhibitor is sensitive to protease, but not RNase or DNase treatment. The IP eluates from E was either boiled at 95 degree for 5 minutes or treated with DNase, RNase, or Protease K at 37 degree for one hour. The cGAS inhibitory activity was evaluated.

To further confirm the theory above, we isolated cytosol (s20) and 1M NaCl extract from the nucleus, performed cGAS immunoprecipitation with buffer containing 0.4M NaCl and then eluted the beads with 1M NaCl buffer. Interestingly, we detected cGAS inhibitory activity from eluates of 1M NaCl extract immunoprecipitation but not eluates of s20 immunoprecipitation (Figure 3-8E). This indicates that we were able to enrich this putative cGAS inhibitor(s) from nuclear extract with immunoprecipitation and high salt (1M NaCl) elution.

We characterized the inhibitor(s) by heating and enzyme digestion tests (Figure 3-8F). We found that this putative inhibitor(s) was resistant to heat inactivation (95 degrees for 5 minutes), and it was also resistant to DNase and RNase treatment. The fact that protease K could kill the inhibitory effect proved that the inhibitory effect came from certain protein component(s).

Conclusions and discussion

In this project, we discovered that instead of simply being in the cytosol, the localization of cGAS changes dynamically during the cell cycle. With the majority of cGAS in the nucleus, it is intriguing that cGAS is not activated by chromatin. As previously reported, cytosolic chromatin (Gluck et al. 2017) and chromatin assembled in vitro (Mackenzie et al. 2017) can effectively activate cGAS. So there should be a mechanism to control the activity that cGAS in the nucleus, probably by the existence of an inhibitor that is associated with chromatin. As shown in Figure 3-8A, it is interesting to see that while cGAS in the nucleus bound with chromatin but was not activated, it can still be activated by ISD. This further indicates that the putative cGAS inhibitor is restricted to chromatin structure. In this case, as we added ISD into the reaction, the ISD would compete for cGAS binding with chromatin. When the cGAS protein bound with ISD, it was disassociated from chromatin and thus from the putative inhibitor, and that's why cGAS could be activated by ISD. In our experiments, we have also found that there were some fundamental biochemical differences between cytosolic cGAS and nuclear cGAS (data not shown), such as that nuclear cGAS could only be soluble in solutions

with salt concentration high than about 350mM NaCl and that nuclear cGAS appeared to have much larger molecular weight than cytosolic cGAS, even in buffer with detergent or with 1M NaCl. So it will be interesting to further characterize the nuclear cGAS, which may offer further clues on how cGAS behavior and activity are regulated in the nucleus.

From our observation, it seems that the only way for cGAS to be associated with chromatin/chromosome and enter the nucleus is through cell cycle when nuclear membrane breaks down. Though we do not currently have absolute perfect evidence (that would be to show that point mutations that abolish cGAS DNA binding can prevent cGAS from binding with chromatin/chromosome) to prove that the binding of cGAS and chromatin/chromosome is through DNA and the DNA binding domain on cGAS, it's very likely to be the case.

Considering the physiological function of cGAS being recruited to the nucleus during the cell cycle, there could be multiple possibilities. First of all, it could be a strategy for the cell to avoid unwanted activation of cGAS. During cell cycles, when nuclear membrane breaks down, nuclear chromosomal DNA is exposed to cGAS as a potential ligand. In this case, recruiting cGAS to the chromosome and then keep it inactive by certain chromosome binding cGAS inhibitor(s) could be an effective way to control cGAS activity. Another potential role of cGAS in the nucleus could be that cGAS may functions as an important regulator in the cell cycle and cell senescence, as reported by our colleagues and other researchers (Dou et al. 2017, Gluck et al. 2017, Yang et al. 2017). The DNA fragment generated by oxidative stress, telomere shortening, and tumor genomic instability could be sensed by cGAS and initiate responses, including promoting cell senescence. A third possibility is that cGAS may act as a nuclear DNA sensor. As the predominant cytosolic DNA sensor, it has long been proven that

it is responsible for eliciting the immune response against DNA virus including Herpes Simplex Virus. During the life cycles of HSV, following the entry of host cells, the viral capsid extrudes its genomic double-stranded DNA directly into the nucleus. It is still debating that how cGAS senses HSV DNA if it were only functional in the cytosol. One explanation could be that in some situations, the HSV particles might be defective and after these particles are taken up by macrophages or dendritic cells, their DNA would get exposed in the cytoplasm and thus recognized by cGAS. However, it is also possible that the cGAS in the nucleus, as we observed, could be activated by HSV genomic DNA. It would be interesting to further investigate how cGAS remains inactive while binding with the host chromatin but can be activated by viral DNA or self-generated damage DNA.

Material and methods

Cells and reagents

The THP1-Lucia™ ISG cell line was purchased from InvivoGen (Cat. Code: thpl-isg); Lentiviral infection and establishment of stable cell lines were described previously (Tanaka and Chen 2012); cGAS antibody was from Sigma, MAVS antibody was from Santa Cruz and ikba antibody was from Cell Signaling. ANTI-FLAG® M2 Affinity Gel was from Sigma. E. coli Ribosome was purchased from New England BioLabs. Benzonase was purchased from Sigma. RNases was purchased from ThermoFisher.

In vitro cGAMP synthesis assay

In 20 or 40uL reaction mix, the following components were added: 20 mM Tris-HCl (pH 7.5), 5mM MgCl₂, 0.2ug/ul BSA, 1mM ATP, 0.5mM GTP and 10ng/uL ISD or HT-DNA. L929 cytosol (s20) or 1.5 or 3ng of recombinant human cGAS was used as the source of cGAS activity. The reactions were incubated at 37 degrees for 30 minutes and then 95 degrees to heat inactivate. For reactions with cGAS inhibitor(s), the source of cGAS activity was first incubated with the putative inhibitor(s) for 15 minutes on ice, then DNA/ATP/GFP mix was added to initiate the reaction.

Quantification of cGAMP using THP-1 reporter cell

THP1-Lucia™ ISG cells were cultured in RPMI-1640 medium supplemented with 10% FBS and 50uM 2-Mercaptoethanol. For quantification of cGAMP, cells were pelleted and suspended to a final concentration of 5 million/mL in culture medium supplemented with 25ng/mL Perfringolysin O (PFO). Suspended cells were aliquoted as 50ul/well in 96-well cell culture plates and 5.5ul of the heated reaction mix or cGAMP standards. The cells were incubated in cell incubator overnight (at least 12 hours). For each reaction, 12ul of cell culture supernatant was mixed with 40uL of Lucia substrate and the luciferase activity was measured by a luminometer.

TLC assay of cGAS activity

Enzyme activity of recombinant full-length cGAS was tested with or without putative inhibitor in buffer containing 20mM Tris-HCl (pH 7.5), 5mM MgCl₂, and 0.2ug/mL BSA. cGAS (final concentration around 30nM) or an equal volume of water was incubated with

activating ligand DNA (final concentration 10ng/ul) in the presence of ATP, GTP, and trace amounts of [α -32P] ATP at 37 degrees for 30 minutes. Reactions were terminated by heating at 95 degrees for 5 minutes. One microliter of each reaction was used for TLC assay. When PEI-Cellulose F TLC plate (EMD Millipore) was used, the reaction products were separated with the use of 5mM NH₄HCO₃ in 15% H₂O and 85% Ethanol as solvent. Plates were dried and radiolabeled products were detected by imaging the exposed phosphor screen using a Typhoon phosphorimager (GE Healthcare).

Cell cycle synchronization

To arrest cells at M phase, split Hela cells by 1:4 one day before and treat the cell with 100ng/ml Nocodazole in the culture medium at following day for 14 hours. The chromosomes were visualized by live-cell staining and imaging using NucBlue™ Live ReadyProbes™ Reagent (ThermoFisher R37605). To arrest cells at G1/S phase, first treat the cells with 2mM Thymidine for 18 hours (cells were arrested at S phase), then remove Thymidine containing medium, wash with PBS, and add fresh culture medium to release cell cycle and culture for 9 hours. After releasing, perform the second block by adding 2mM Thymidine for 17 hours. Finally, remove Thymidine, wash with PBS, add back fresh medium and start tracking the synchronized cell cycle progress.

Cell lysis and extraction of different fractions

To separate cytosol protein and cell nucleus, cells were pelleted in tubes and then re-suspended with 3 volumes of hypotonic buffer (10mM Tris-HCl (pH 7.5), 10mM KCl, 3mM

MgCl₂) supplemented with cComplete™ Protease Inhibitor Cocktail (Roche). The cells were lysed either by douncing or by going through gauge 30 needles for 5 times. Then spin down at 5,000g for 10 minutes. The supernatant (s5) was further subjected to 20,000g to get cytosolic proteins (s20), the pellet (p5) was extensively washed by hypotonic buffer and labeled as nucleus. For cGAS sequential extraction, the hypotonic buffer lysate was subject to 20,000g centrifugation, the supernatant (s20) was labeled as cytosol and the pellet was suspended and extracted with RIPA buffer. After spin down, the supernatant was labeled and RIPA_extract and the pellet were boiled in 2x SDS loading buffer for subsequent analysis.

Immunoprecipitation and elution

Cells were collected as cell pellet and lysed in hypotonic buffer supplemented with 0.5% NP-40, the lysate was subjected to 5,000g centrifugation and the pellet (p5, labeled was nucleus) was washed and finally suspended in 1x volume of hypotonic buffer. The nucleus suspension was treated by Benzonase on ice for 30 minutes and then washed extensively using hypotonic buffer to remove residual Benzonase. Then hypotonic buffer supplemented with 1M NaCl was used to extract nuclear protein from the Benzonase digested nucleus (labeled as 1M NaCl extract). After extraction, the 1M NaCl extract was diluted with hypotonic buffer to reach a final salt concentration of 0.4M or 1M. Then ANTI-FLAG® M2 Affinity Gel was added to the diluted extract for immunoprecipitation at 4 degrees for 6 hours to overnight. After immunoprecipitation, the beads were washed with hypotonic buffer supplemented with 0.4M NaCl for 5 times. Then elution buffer (50mM Tris-HCl (pH7.5), 10mM KCl, 10%

120

Glycerol, 0.5mM DTT, and 0.1ug/ul BSA) supplemented with 1M NaCl or Flag peptide was used to elute proteins from the beads.

BIBLIOGRAPHY

- Abe, T., A. Harashima, T. Xia, H. Konno, K. Konno, A. Morales, J. Ahn, D. Gutman, and G. N. Barber. 2013. "STING recognition of cytoplasmic DNA instigates cellular defense." *Mol Cell* 50 (1):5-15. doi: 10.1016/j.molcel.2013.01.039.
- Ablasser, A., F. Bauernfeind, G. Hartmann, E. Latz, K. A. Fitzgerald, and V. Hornung. 2009. "RIG-I-dependent sensing of poly(dA:dT) through the induction of an RNA polymerase III-transcribed RNA intermediate." *Nat Immunol.* doi: ni.1779 [pii] 10.1038/ni.1779.
- Ablasser, A., M. Goldeck, T. Cavlar, T. Deimling, G. Witte, I. Rohl, K. P. Hopfner, J. Ludwig, and V. Hornung. 2013. "cGAS produces a 2'-5'-linked cyclic dinucleotide second messenger that activates STING." *Nature* 498 (7454):380-4. doi: 10.1038/nature12306.
- Ablasser, A., C. Hertrich, R. Wassermann, and V. Hornung. 2013. "Nucleic acid driven sterile inflammation." *Clin Immunol* 147 (3):207-15. doi: 10.1016/j.clim.2013.01.003.
- Ablasser, A., J. L. Schmid-Burgk, I. Hemmerling, G. L. Horvath, T. Schmidt, E. Latz, and V. Hornung. 2013. "Cell intrinsic immunity spreads to bystander cells via the intercellular transfer of cGAMP." *Nature* 503 (7477):530-4. doi: 10.1038/nature12640.
- Aderem, A. 2001. "Role of Toll-like receptors in inflammatory response in macrophages." *Crit Care Med* 29 (7 Suppl):S16-8.
- Aguirre, S., A. M. Maestre, S. Pagni, J. R. Patel, T. Savage, D. Gutman, K. Maringer, D. Bernal-Rubio, R. S. Shabman, V. Simon, J. R. Rodriguez-Madoz, L. C. Mulder, G. N. Barber, and A. Fernandez-Sesma. 2012. "DENV inhibits type I IFN production in infected cells by cleaving human STING." *PLoS Pathog* 8 (10):e1002934. doi: 10.1371/journal.ppat.1002934.
- Ahn, J., D. Gutman, S. Saijo, and G. N. Barber. 2012. "STING manifests self DNA-dependent inflammatory disease." *Proc Natl Acad Sci U S A* 109 (47):19386-91. doi: 10.1073/pnas.1215006109.
- Akira, S., and K. Takeda. 2004. "Toll-like receptor signalling." *Nat Rev Immunol* 4 (7):499-511. doi: 10.1038/nri1391.
- Akira, S., S. Uematsu, and O. Takeuchi. 2006. "Pathogen recognition and innate immunity." *Cell* 124 (4):783-801. doi: 10.1016/j.cell.2006.02.015.
- Almine, J. F., C. A. O'Hare, G. Dunphy, I. R. Haga, R. J. Naik, A. Atri, D. J. Connolly, J. Taylor, I. R. Kelsall, A. G. Bowie, P. M. Beard, and L. Unterholzner. 2017. "IFI16 and cGAS cooperate in the activation of STING during DNA sensing in human keratinocytes." *Nat Commun* 8:14392. doi: 10.1038/ncomms14392.
- Andrade, W. A., S. Agarwal, S. Mo, S. A. Shaffer, J. P. Dillard, T. Schmidt, V. Hornung, K. A. Fitzgerald, E. A. Kurt-Jones, and D. T. Golenbock. 2016. "Type I Interferon Induction by Neisseria gonorrhoeae: Dual Requirement of Cyclic GMP-AMP Synthase and Toll-like Receptor 4." *Cell Rep* 15 (11):2438-48. doi: 10.1016/j.celrep.2016.05.030.

- Andrade, W. A., A. Firon, T. Schmidt, V. Hornung, K. A. Fitzgerald, E. A. Kurt-Jones, P. Trieu-Cuot, D. T. Golenbock, and P. A. Kaminski. 2016. "Group B Streptococcus Degrades Cyclic-di-AMP to Modulate STING-Dependent Type I Interferon Production." *Cell Host Microbe* 20 (1):49-59. doi: 10.1016/j.chom.2016.06.003.
- Baetz, A., M. Frey, K. Heeg, and A. H. Dalpke. 2004. "Suppressor of cytokine signaling (SOCS) proteins indirectly regulate toll-like receptor signaling in innate immune cells." *J Biol Chem* 279 (52):54708-15. doi: 10.1074/jbc.M410992200.
- Barnes, B. J., M. J. Kellum, A. E. Field, and P. M. Pitha. 2002. "Multiple regulatory domains of IRF-5 control activation, cellular localization, and induction of chemokines that mediate recruitment of T lymphocytes." *Mol Cell Biol* 22 (16):5721-40.
- Barnes, B. J., P. A. Moore, and P. M. Pitha. 2001. "Virus-specific activation of a novel interferon regulatory factor, IRF-5, results in the induction of distinct interferon alpha genes." *The Journal of biological chemistry* 276 (26):23382-90.
- Barrat, F. J., and R. L. Coffman. 2008. "Development of TLR inhibitors for the treatment of autoimmune diseases." *Immunol Rev* 223:271-83. doi: 10.1111/j.1600-065X.2008.00630.x.
- Brentano, F., O. Schorr, R. E. Gay, S. Gay, and D. Kyburz. 2005. "RNA released from necrotic synovial fluid cells activates rheumatoid arthritis synovial fibroblasts via Toll-like receptor 3." *Arthritis Rheum* 52 (9):2656-65. doi: 10.1002/art.21273.
- Bridgeman, A., J. Maelfait, T. Davenne, T. Partridge, Y. Peng, A. Mayer, T. Dong, V. Kaever, P. Borrow, and J. Rehwinkel. 2015. "Viruses transfer the antiviral second messenger cGAMP between cells." *Science* 349 (6253):1228-32. doi: 10.1126/science.aab3632.
- Brunette, R. L., J. M. Young, D. G. Whitley, I. E. Brodsky, H. S. Malik, and D. B. Stetson. 2012. "Extensive evolutionary and functional diversity among mammalian AIM2-like receptors." *J Exp Med* 209 (11):1969-83. doi: 10.1084/jem.20121960.
- Burckstummer, T., C. Baumann, S. Bluml, E. Dixit, G. Durnberger, H. Jahn, M. Planyavsky, M. Bilban, J. Colinge, K. L. Bennett, and G. Superti-Furga. 2009. "An orthogonal proteomic-genomic screen identifies AIM2 as a cytoplasmic DNA sensor for the inflammasome." *Nat Immunol* 10 (3):266-72. doi: 10.1038/ni.1702.
- Burdette, D. L., K. M. Monroe, K. Sotelo-Troha, J. S. Iwig, B. Eckert, M. Hyodo, Y. Hayakawa, and R. E. Vance. 2011. "STING is a direct innate immune sensor of cyclic di-GMP." *Nature* 478 (7370):515-8. doi: 10.1038/nature10429.
- Burns, K., F. Martinon, C. Esslinger, H. Pahl, P. Schneider, J. L. Bodmer, F. Di Marco, L. French, and J. Tschopp. 1998. "MyD88, an adapter protein involved in interleukin-1 signaling." *J Biol Chem* 273 (20):12203-9.
- Cai, X., Y. H. Chiu, and Z. J. Chen. 2014. "The cGAS-cGAMP-STING pathway of cytosolic DNA sensing and signaling." *Mol Cell* 54 (2):289-96. doi: 10.1016/j.molcel.2014.03.040.
- Chang, L., and M. Karin. 2001. "Mammalian MAP kinase signalling cascades." *Nature* 410 (6824):37-40. doi: 10.1038/35065000.

- Chen, W., S. S. Lam, H. Srinath, Z. Jiang, J. J. Correia, C. A. Schiffer, K. A. Fitzgerald, K. Lin, and W. E. Royer, Jr. 2008. "Insights into interferon regulatory factor activation from the crystal structure of dimeric IRF5." *Nat Struct Mol Biol* 15 (11):1213-20. doi: 10.1038/nsmb.1496 nsmb.1496 [pii].
- Chiu, Y. H., J. B. Macmillan, and Z. J. Chen. 2009. "RNA polymerase III detects cytosolic DNA and induces type I interferons through the RIG-I pathway." *Cell* 138 (3):576-91. doi: S0092-8674(09)00714-4 [pii] 10.1016/j.cell.2009.06.015.
- Choe, J., M. S. Kelker, and I. A. Wilson. 2005. "Crystal structure of human toll-like receptor 3 (TLR3) ectodomain." *Science* 309 (5734):581-5. doi: 10.1126/science.1115253.
- Collins, A. C., H. Cai, T. Li, L. H. Franco, X. D. Li, V. R. Nair, C. R. Scharn, C. E. Stamm, B. Levine, Z. J. Chen, and M. U. Shiloh. 2015. "Cyclic GMP-AMP Synthase Is an Innate Immune DNA Sensor for Mycobacterium tuberculosis." *Cell Host Microbe* 17 (6):820-8. doi: 10.1016/j.chom.2015.05.005.
- Corrales, L., L. H. Glickman, S. M. McWhirter, D. B. Kanne, K. E. Sivick, G. E. Katibah, S. R. Woo, E. Lemmens, T. Banda, J. J. Leong, K. Metchette, T. W. Dubensky, Jr., and T. F. Gajewski. 2015. "Direct Activation of STING in the Tumor Microenvironment Leads to Potent and Systemic Tumor Regression and Immunity." *Cell Rep* 11 (7):1018-30. doi: 10.1016/j.celrep.2015.04.031.
- Crow, Y. J., B. E. Hayward, R. Parmar, P. Robins, A. Leitch, M. Ali, D. N. Black, H. van Bokhoven, H. G. Brunner, B. C. Hamel, P. C. Corry, F. M. Cowan, S. G. Frints, J. Klepper, J. H. Livingston, S. A. Lynch, R. F. Massey, J. F. Meritet, J. L. Michaud, G. Ponsot, T. Voit, P. Lebon, D. T. Bonthon, A. P. Jackson, D. E. Barnes, and T. Lindahl. 2006. "Mutations in the gene encoding the 3'-5' DNA exonuclease TREX1 cause Aicardi-Goutieres syndrome at the AGS1 locus." *Nat Genet* 38 (8):917-20. doi: 10.1038/ng1845.
- Cui, Y., H. Yu, X. Zheng, R. Peng, Q. Wang, Y. Zhou, R. Wang, J. Wang, B. Qu, N. Shen, Q. Guo, X. Liu, and C. Wang. 2017. "SENP7 Potentiates cGAS Activation by Relieving SUMO-Mediated Inhibition of Cytosolic DNA Sensing." *PLoS Pathog* 13 (1):e1006156. doi: 10.1371/journal.ppat.1006156.
- Der, S. D., A. Zhou, B. R. Williams, and R. H. Silverman. 1998. "Identification of genes differentially regulated by interferon alpha, beta, or gamma using oligonucleotide arrays." *Proc Natl Acad Sci U S A* 95 (26):15623-8.
- Diebold, S. S., T. Kaisho, H. Hemmi, S. Akira, and C. Reis e Sousa. 2004. "Innate antiviral responses by means of TLR7-mediated recognition of single-stranded RNA." *Science* 303 (5663):1529-31. doi: 10.1126/science.1093616.
- Diner, E. J., D. L. Burdette, S. C. Wilson, K. M. Monroe, C. A. Kellenberger, M. Hyodo, Y. Hayakawa, M. C. Hammond, and R. E. Vance. 2013. "The innate immune DNA sensor cGAS produces a noncanonical cyclic dinucleotide that activates human STING." *Cell Rep* 3 (5):1355-61. doi: 10.1016/j.celrep.2013.05.009.
- Dobbs, N., N. Burnaevskiy, D. Chen, V. K. Gonugunta, N. M. Alto, and N. Yan. 2015. "STING Activation by Translocation from the ER Is Associated with Infection

- and Autoinflammatory Disease." *Cell Host Microbe* 18 (2):157-68. doi: 10.1016/j.chom.2015.07.001.
- Dou, Z., K. Ghosh, M. G. Vizioli, J. Zhu, P. Sen, K. J. Wangensteen, J. Simithy, Y. Lan, Y. Lin, Z. Zhou, B. C. Capell, C. Xu, M. Xu, J. E. Kieckhafer, T. Jiang, M. Shoshkes-Carmel, Kmaa Tanim, G. N. Barber, J. T. Seykora, S. E. Millar, K. H. Kaestner, B. A. Garcia, P. D. Adams, and S. L. Berger. 2017. "Cytoplasmic chromatin triggers inflammation in senescence and cancer." *Nature* 550 (7676):402-406. doi: 10.1038/nature24050.
- Fernandes-Alnemri, T., J. W. Yu, P. Datta, J. Wu, and E. S. Alnemri. 2009. "AIM2 activates the inflammasome and cell death in response to cytoplasmic DNA." *Nature* 458 (7237):509-13. doi: 10.1038/nature07710.
- Fitzgerald, K. A., S. M. McWhirter, K. L. Faia, D. C. Rowe, E. Latz, D. T. Golenbock, A. J. Coyle, S. M. Liao, and T. Maniatis. 2003. "IKKepsilon and TBK1 are essential components of the IRF3 signaling pathway." *Nat Immunol* 4 (5):491-6. doi: 10.1038/ni921.
- Gall, A., P. Treuting, K. B. Elkon, Y. M. Loo, M. Gale, Jr., G. N. Barber, and D. B. Stetson. 2012. "Autoimmunity initiates in nonhematopoietic cells and progresses via lymphocytes in an interferon-dependent autoimmune disease." *Immunity* 36 (1):120-31. doi: 10.1016/j.jimmuni.2011.11.018.
- Gao, D., T. Li, X. D. Li, X. Chen, Q. Z. Li, M. Wight-Carter, and Z. J. Chen. 2015. "Activation of cyclic GMP-AMP synthase by self-DNA causes autoimmune diseases." *Proc Natl Acad Sci U S A* 112 (42):E5699-705. doi: 10.1073/pnas.1516465112.
- Gao, D., J. Wu, Y. T. Wu, F. Du, C. Aroh, N. Yan, L. Sun, and Z. J. Chen. 2013. "Cyclic GMP-AMP synthase is an innate immune sensor of HIV and other retroviruses." *Science* 341 (6148):903-6. doi: 10.1126/science.1240933.
- Gao, P., M. Ascano, Y. Wu, W. Barchet, B. L. Gaffney, T. Zillinger, A. A. Serganov, Y. Liu, R. A. Jones, G. Hartmann, T. Tuschl, and D. J. Patel. 2013. "Cyclic [G(2',5')pA(3',5')p] is the metazoan second messenger produced by DNA-activated cyclic GMP-AMP synthase." *Cell* 153 (5):1094-107. doi: 10.1016/j.cell.2013.04.046.
- Gao, P., M. Ascano, T. Zillinger, W. Wang, P. Dai, A. A. Serganov, B. L. Gaffney, S. Shuman, R. A. Jones, L. Deng, G. Hartmann, W. Barchet, T. Tuschl, and D. J. Patel. 2013. "Structure-function analysis of STING activation by c[G(2',5')pA(3',5')p] and targeting by antiviral DMXAA." *Cell* 154 (4):748-62. doi: 10.1016/j.cell.2013.07.023.
- Gentili, M., J. Kowal, M. Tkach, T. Satoh, X. Lahaye, C. Conrad, M. Boyron, B. Lombard, S. Durand, G. Kroemer, D. Loew, M. Dalod, C. Thery, and N. Manel. 2015. "Transmission of innate immune signaling by packaging of cGAMP in viral particles." *Science* 349 (6253):1232-6. doi: 10.1126/science.aab3628.
- Gluck, S., B. Guey, M. F. Gulen, K. Wolter, T. W. Kang, N. A. Schmacke, A. Bridgeman, J. Rehwinkel, L. Zender, and A. Ablasser. 2017. "Innate immune sensing of cytosolic chromatin fragments through cGAS promotes senescence." *Nat Cell Biol* 19 (9):1061-1070. doi: 10.1038/ncb3586.

- Goubau, D., S. Deddouche, and C. Reis e Sousa. 2013. "Cytosolic sensing of viruses." *Immunity* 38 (5):855-69. doi: 10.1016/j.immuni.2013.05.007.
- Graham, R. R., S. V. Kozyrev, E. C. Baechler, M. V. Reddy, R. M. Plenge, J. W. Bauer, W. A. Ortmann, T. Koeuth, M. F. Gonzalez Escribano, B. Pons-Estel, M. Petri, M. Daly, P. K. Gregersen, J. Martin, D. Altshuler, T. W. Behrens, and M. E. Alarcon-Riquelme. 2006. "A common haplotype of interferon regulatory factor 5 (IRF5) regulates splicing and expression and is associated with increased risk of systemic lupus erythematosus." *Nat Genet* 38 (5):550-5. doi: ng1782 [pii] 10.1038/ng1782.
- Groom, J. R., C. A. Fletcher, S. N. Walters, S. T. Grey, S. V. Watt, M. J. Sweet, M. J. Smyth, C. R. Mackay, and F. Mackay. 2007. "BAFF and MyD88 signals promote a lupuslike disease independent of T cells." *J Exp Med* 204 (8):1959-71. doi: 10.1084/jem.20062567.
- Hancock, R. E., and M. G. Scott. 2000. "The role of antimicrobial peptides in animal defenses." *Proc Natl Acad Sci U S A* 97 (16):8856-61.
- Hansen, K., T. Prabakaran, A. Laustsen, S. E. Jorgensen, S. H. Rahbaek, S. B. Jensen, R. Nielsen, J. H. Leber, T. Decker, K. A. Horan, M. R. Jakobsen, and S. R. Paludan. 2014. "Listeria monocytogenes induces IFN β expression through an IFI16-, cGAS- and STING-dependent pathway." *EMBO J* 33 (15):1654-66. doi: 10.15252/embj.201488029.
- Heil, F., H. Hemmi, H. Hochrein, F. Ampenberger, C. Kirschning, S. Akira, G. Lipford, H. Wagner, and S. Bauer. 2004. "Species-specific recognition of single-stranded RNA via toll-like receptor 7 and 8." *Science* 303 (5663):1526-9. doi: 10.1126/science.1093620.
- Hemmi, H., O. Takeuchi, T. Kawai, T. Kaisho, S. Sato, H. Sanjo, M. Matsumoto, K. Hoshino, H. Wagner, K. Takeda, and S. Akira. 2000. "A Toll-like receptor recognizes bacterial DNA." *Nature* 408 (6813):740-5. doi: 10.1038/35047123.
- Hiscott, J., R. Lin, P. Nakhaei, and S. Paz. 2006. "MasterCARD: a priceless link to innate immunity." *Trends in molecular medicine* 12 (2):53-6. doi: 10.1016/j.molmed.2005.12.003.
- Ho, S. S., W. Y. Zhang, N. Y. Tan, M. Khatoo, M. A. Suter, S. Tripathi, F. S. Cheung, W. K. Lim, P. H. Tan, J. Ngeow, and S. Gasser. 2016. "The DNA Structure-Specific Endonuclease MUS81 Mediates DNA Sensor STING-Dependent Host Rejection of Prostate Cancer Cells." *Immunity* 44 (5):1177-89. doi: 10.1016/j.immuni.2016.04.010.
- Holm, C. K., S. B. Jensen, M. R. Jakobsen, N. Cheshenko, K. A. Horan, H. B. Moeller, R. Gonzalez-Dosal, S. B. Rasmussen, M. H. Christensen, T. O. Yarovinsky, F. J. Rixon, B. C. Herold, K. A. Fitzgerald, and S. R. Paludan. 2012. "Virus-cell fusion as a trigger of innate immunity dependent on the adaptor STING." *Nat Immunol* 13 (8):737-43. doi: 10.1038/ni.2350.
- Honda, K., and T. Taniguchi. 2006. "IRFs: master regulators of signalling by Toll-like receptors and cytosolic pattern-recognition receptors." *Nat Rev Immunol* 6 (9):644-58. doi: nri1900 [pii] 10.1038/nri1900.

- Hornung, V., A. Ablasser, M. Charrel-Dennis, F. Bauernfeind, G. Horvath, D. R. Caffrey, E. Latz, and K. A. Fitzgerald. 2009. "AIM2 recognizes cytosolic dsDNA and forms a caspase-1-activating inflammasome with ASC." *Nature* 458 (7237):514-8. doi: 10.1038/nature07725.
- Hornung, V., J. Ellegast, S. Kim, K. Brzozka, A. Jung, H. Kato, H. Poeck, S. Akira, K. K. Conzelmann, M. Schlee, S. Endres, and G. Hartmann. 2006. "5'-Triphosphate RNA is the ligand for RIG-I." *Science* 314 (5801):994-7. doi: 10.1126/science.1132505.
- Hoshino, K., T. Sugiyama, M. Matsumoto, T. Tanaka, M. Saito, H. Hemmi, O. Ohara, S. Akira, and T. Kaisho. 2006. "IkappaB kinase-alpha is critical for interferon-alpha production induced by Toll-like receptors 7 and 9." *Nature* 440 (7086):949-53. doi: nature04641 [pii] 10.1038/nature04641.
- Hu, M. M., Q. Yang, X. Q. Xie, C. Y. Liao, H. Lin, T. T. Liu, L. Yin, and H. B. Shu. 2016. "Sumoylation Promotes the Stability of the DNA Sensor cGAS and the Adaptor STING to Regulate the Kinetics of Response to DNA Virus." *Immunity* 45 (3):555-569. doi: 10.1016/j.immuni.2016.08.014.
- Ikushima, H., H. Negishi, and T. Taniguchi. 2013. "The IRF Family Transcription Factors at the Interface of Innate and Adaptive Immune Responses." *Cold Spring Harb Symp Quant Biol* 78:105-116. doi: 10.1101/sqb.2013.78.020321.
- Ishii, K. J., T. Kawagoe, S. Koyama, K. Matsui, H. Kumar, T. Kawai, S. Uematsu, O. Takeuchi, F. Takeshita, C. Coban, and S. Akira. 2008. "TANK-binding kinase-1 delineates innate and adaptive immune responses to DNA vaccines." *Nature* 451 (7179):725-9. doi: 10.1038/nature06537.
- Ishikawa, H., and G. N. Barber. 2008. "STING is an endoplasmic reticulum adaptor that facilitates innate immune signalling." *Nature* 455 (7213):674-8. doi: 10.1038/nature07317.
- Ishikawa, H., Z. Ma, and G. N. Barber. 2009. "STING regulates intracellular DNA-mediated, type I interferon-dependent innate immunity." *Nature* 461 (7265):788-92. doi: 10.1038/nature08476.
- Israel, A. 2010. "The IKK complex, a central regulator of NF-kappaB activation." *Cold Spring Harbor perspectives in biology* 2 (3):a000158. doi: 10.1101/cshperspect.a000158.
- Jakob, T., P. S. Walker, A. M. Krieg, M. C. Udey, and J. C. Vogel. 1998. "Activation of cutaneous dendritic cells by CpG-containing oligodeoxynucleotides: a role for dendritic cells in the augmentation of Th1 responses by immunostimulatory DNA." *J Immunol* 161 (6):3042-9.
- Jiang, X., L. N. Kinch, C. A. Brautigam, X. Chen, F. Du, N. V. Grishin, and Z. J. Chen. 2012. "Ubiquitin-induced oligomerization of the RNA sensors RIG-I and MDA5 activates antiviral innate immune response." *Immunity* 36 (6):959-73. doi: 10.1016/j.immuni.2012.03.022.
- Kaminski, J. J., S. A. Schattgen, T. C. Tzeng, C. Bode, D. M. Klinman, and K. A. Fitzgerald. 2013. "Synthetic oligodeoxynucleotides containing suppressive

- TTAGGG motifs inhibit AIM2 inflammasome activation." *J Immunol* 191 (7):3876-83. doi: 10.4049/jimmunol.1300530.
- Kawai, T., and S. Akira. 2007. "Signaling to NF-kappaB by Toll-like receptors." *Trends Mol Med* 13 (11):460-9. doi: 10.1016/j.molmed.2007.09.002.
- Kawai, T., and S. Akira. 2010. "The role of pattern-recognition receptors in innate immunity: update on Toll-like receptors." *Nat Immunol* 11 (5):373-84. doi: 10.1038/ni.1863.
- Kawai, T., K. Takahashi, S. Sato, C. Coban, H. Kumar, H. Kato, K. J. Ishii, O. Takeuchi, and S. Akira. 2005. "IPS-1, an adaptor triggering RIG-I- and Mda5-mediated type I interferon induction." *Nat Immunol* 6 (10):981-8.
- Kim, H. M., B. S. Park, J. I. Kim, S. E. Kim, J. Lee, S. C. Oh, P. Enkhbayar, N. Matsushima, H. Lee, O. J. Yoo, and J. O. Lee. 2007. "Crystal structure of the TLR4-MD-2 complex with bound endotoxin antagonist Eritoran." *Cell* 130 (5):906-17. doi: 10.1016/j.cell.2007.08.002.
- Kim, T., S. Pazhoor, M. Bao, Z. Zhang, S. Hanabuchi, V. Facchinetti, L. Bover, J. Plumas, L. Chaperot, J. Qin, and Y. J. Liu. 2010. "Aspartate-glutamate-alanine-histidine box motif (DEAH)/RNA helicase A helicases sense microbial DNA in human plasmacytoid dendritic cells." *Proc Natl Acad Sci U S A* 107 (34):15181-6. doi: 10.1073/pnas.1006539107.
- Komuro, A., and C. M. Horvath. 2006. "RNA- and virus-independent inhibition of antiviral signaling by RNA helicase LGP2." *J Virol* 80 (24):12332-42. doi: 10.1128/JVI.01325-06.
- Konno, H., K. Konno, and G. N. Barber. 2013. "Cyclic dinucleotides trigger ULK1 (ATG1) phosphorylation of STING to prevent sustained innate immune signaling." *Cell* 155 (3):688-98. doi: 10.1016/j.cell.2013.09.049.
- Krausgruber, T., K. Blazek, T. Smallie, S. Alzabin, H. Lockstone, N. Sahgal, T. Hussell, M. Feldmann, and I. A. Udalova. 2011. "IRF5 promotes inflammatory macrophage polarization and TH1-TH17 responses." *Nat Immunol* 12 (3):231-8. doi: 10.1038/ni.1990
- ni.1990 [pii].
- Lafyatis, R., and M. York. 2009. "Innate immunity and inflammation in systemic sclerosis." *Curr Opin Rheumatol* 21 (6):617-22. doi: 10.1097/BOR.0b013e32832fd69e.
- Lau, L., E. E. Gray, R. L. Brunette, and D. B. Stetson. 2015. "DNA tumor virus oncogenes antagonize the cGAS-STING DNA-sensing pathway." *Science* 350 (6260):568-71. doi: 10.1126/science.aab3291.
- Lazear, H. M., A. Lancaster, C. Wilkins, M. S. Suthar, A. Huang, S. C. Vick, L. Clepper, L. Thackray, M. M. Brassil, H. W. Virgin, J. Nikolich-Zugich, A. V. Moses, M. Gale, Jr., K. Fruh, and M. S. Diamond. 2013. "IRF-3, IRF-5, and IRF-7 coordinately regulate the type I IFN response in myeloid dendritic cells downstream of MAVS signaling." *PLoS Pathog* 9 (1):e1003118. doi: 10.1371/journal.ppat.1003118
- PPATHOGENS-D-12-01922 [pii].

- Lazzari, E., and C. A. Jefferies. 2014. "IRF5-mediated signaling and implications for SLE." *Clinical immunology* 153 (2):343-352. doi: 10.1016/j.clim.2014.06.001.
- Li, T., H. Cheng, H. Yuan, Q. Xu, C. Shu, Y. Zhang, P. Xu, J. Tan, Y. Rui, P. Li, and X. Tan. 2016. "Antitumor Activity of cGAMP via Stimulation of cGAS-cGAMP-STING-IRF3 Mediated Innate Immune Response." *Sci Rep* 6:19049. doi: 10.1038/srep19049.
- Li, X. D., and Z. J. Chen. 2012. "Sequence specific detection of bacterial 23S ribosomal RNA by TLR13." *eLife* 1:e00102. doi: 10.7554/eLife.00102.
- Li, X. D., J. Wu, D. Gao, H. Wang, L. Sun, and Z. J. Chen. 2013. "Pivotal roles of cGAS-cGAMP signaling in antiviral defense and immune adjuvant effects." *Science* 341 (6152):1390-4. doi: 10.1126/science.1244040.
- Li, X., C. Shu, G. Yi, C. T. Chaton, C. L. Shelton, J. Diao, X. Zuo, C. C. Kao, A. B. Herr, and P. Li. 2013. "Cyclic GMP-AMP synthase is activated by double-stranded DNA-induced oligomerization." *Immunity* 39 (6):1019-31. doi: 10.1016/j.jimmuni.2013.10.019.
- Lien, C., C. M. Fang, D. Huso, F. Livak, R. Lu, and P. M. Pitha. 2010. "Critical role of IRF-5 in regulation of B-cell differentiation." *Proceedings of the National Academy of Sciences of the United States of America* 107 (10):4664-8. doi: 10.1073/pnas.0911193107.
- Liu, F., Y. Xia, A. S. Parker, and I. M. Verma. 2012. "IKK biology." *Immunological reviews* 246 (1):239-53. doi: 10.1111/j.1600-065X.2012.01107.x.
- Liu, S., X. Cai, J. Wu, Q. Cong, X. Chen, T. Li, F. Du, J. Ren, Y. T. Wu, N. V. Grishin, and Z. J. Chen. 2015. "Phosphorylation of innate immune adaptor proteins MAVS, STING, and TRIF induces IRF3 activation." *Science* 347 (6227):aaa2630. doi: 10.1126/science.aaa2630.
- Ma, Z., S. R. Jacobs, J. A. West, C. Stopford, Z. Zhang, Z. Davis, G. N. Barber, B. A. Glaunsinger, D. P. Dittmer, and B. Damania. 2015. "Modulation of the cGAS-STING DNA sensing pathway by gammaherpesviruses." *Proc Natl Acad Sci U S A* 112 (31):E4306-15. doi: 10.1073/pnas.1503831112.
- Mackenzie, K. J., P. Carroll, C. A. Martin, O. Murina, A. Fluteau, D. J. Simpson, N. Olova, H. Sutcliffe, J. K. Rainger, A. Leitch, R. T. Osborn, A. P. Wheeler, M. Nowotny, N. Gilbert, T. Chandra, M. A. M. Reijns, and A. P. Jackson. 2017. "cGAS surveillance of micronuclei links genome instability to innate immunity." *Nature* 548 (7668):461-465. doi: 10.1038/nature23449.
- Meylan, E., J. Curran, K. Hofmann, D. Moradpour, M. Binder, R. Bartenschlager, and J. Tschoopp. 2005. "Cardif is an adaptor protein in the RIG-I antiviral pathway and is targeted by hepatitis C virus." *Nature* 437 (7062):1167-72.
- Miceli-Richard, C., E. Comets, P. Loiseau, X. Puechal, E. Hachulla, and X. Mariette. 2007. "Association of an IRF5 gene functional polymorphism with Sjogren's syndrome." *Arthritis Rheum* 56 (12):3989-94. doi: 10.1002/art.23142.
- Morita, M., G. Stamp, P. Robins, A. Dulic, I. Rosewell, G. Hrvnak, G. Daly, T. Lindahl, and D. E. Barnes. 2004. "Gene-targeted mice lacking the Trex1 (DNase III) 3'-->5' DNA exonuclease develop inflammatory myocarditis." *Mol Cell Biol* 24 (15):6719-27. doi: 10.1128/MCB.24.15.6719-6727.2004.

- Mukai, K., H. Konno, T. Akiba, T. Uemura, S. Waguri, T. Kobayashi, G. N. Barber, H. Arai, and T. Taguchi. 2016. "Activation of STING requires palmitoylation at the Golgi." *Nat Commun* 7:11932. doi: 10.1038/ncomms11932.
- Muruve, D. A., V. Petrilli, A. K. Zaiss, L. R. White, S. A. Clark, P. J. Ross, R. J. Parks, and J. Tschopp. 2008. "The inflammasome recognizes cytosolic microbial and host DNA and triggers an innate immune response." *Nature* 452 (7183):103-7. doi: 10.1038/nature06664.
- Noppert, S. J., K. A. Fitzgerald, and P. J. Hertzog. 2007. "The role of type I interferons in TLR responses." *Immunol Cell Biol* 85 (6):446-57. doi: 7100099 [pii] 10.1038/sj.icb.7100099.
- O'Connell, R. M., S. K. Saha, S. A. Vaidya, K. W. Bruhn, G. A. Miranda, B. Zarnegar, A. K. Perry, B. O. Nguyen, T. F. Lane, T. Taniguchi, J. F. Miller, and G. Cheng. 2004. "Type I interferon production enhances susceptibility to Listeria monocytogenes infection." *J Exp Med* 200 (4):437-45. doi: 10.1084/jem.20040712.
- O'Neill, L. A., and A. G. Bowie. 2007. "The family of five: TIR-domain-containing adaptors in Toll-like receptor signalling." *Nat Rev Immunol* 7 (5):353-64. doi: 10.1038/nri2079.
- Okabe, Y., K. Kawane, S. Akira, T. Taniguchi, and S. Nagata. 2005. "Toll-like receptor-independent gene induction program activated by mammalian DNA escaped from apoptotic DNA degradation." *J Exp Med* 202 (10):1333-9. doi: 10.1084/jem.20051654.
- Oldenburg, M., A. Kruger, R. Ferstl, A. Kaufmann, G. Nees, A. Sigmund, B. Bathke, H. Lauterbach, M. Suter, S. Dreher, U. Koedel, S. Akira, T. Kawai, J. Buer, H. Wagner, S. Bauer, H. Hochrein, and C. J. Kirschning. 2012. "TLR13 recognizes bacterial 23S rRNA devoid of erythromycin resistance-forming modification." *Science* 337 (6098):1111-5. doi: 10.1126/science.1220363.
- Orzalli, M. H., N. A. DeLuca, and D. M. Knipe. 2012. "Nuclear IFI16 induction of IRF-3 signaling during herpesviral infection and degradation of IFI16 by the viral ICP0 protein." *Proc Natl Acad Sci U S A* 109 (44):E3008-17. doi: 10.1073/pnas.1211302109.
- Roberts, T. L., A. Idris, J. A. Dunn, G. M. Kelly, C. M. Burnton, S. Hodgson, L. L. Hardy, V. Garceau, M. J. Sweet, I. L. Ross, D. A. Hume, and K. J. Stacey. 2009. "HIN-200 proteins regulate caspase activation in response to foreign cytoplasmic DNA." *Science* 323 (5917):1057-60. doi: 10.1126/science.1169841.
- Romling, U., M. Y. Galperin, and M. Gomelsky. 2013. "Cyclic di-GMP: the first 25 years of a universal bacterial second messenger." *Microbiol Mol Biol Rev* 77 (1):1-52. doi: 10.1128/MMBR.00043-12.
- Santaguida, S., A. Richardson, D. R. Iyer, O. M'Saad, L. Zasadil, K. A. Knouse, Y. L. Wong, N. Rhind, A. Desai, and A. Amon. 2017. "Chromosome Mis-segregation Generates Cell-Cycle-Arrested Cells with Complex Karyotypes that Are Eliminated by the Immune System." *Dev Cell* 41 (6):638-651 e5. doi: 10.1016/j.devcel.2017.05.022.

- Satoh, T., H. Kato, Y. Kumagai, M. Yoneyama, S. Sato, K. Matsushita, T. Tsujimura, T. Fujita, S. Akira, and O. Takeuchi. 2010. "LGP2 is a positive regulator of RIG-I- and MDA5-mediated antiviral responses." *Proc Natl Acad Sci U S A* 107 (4):1512-7. doi: 10.1073/pnas.0912986107.
- Schoggins, J. W., D. A. MacDuff, N. Imanaka, M. D. Gainey, B. Shrestha, J. L. Eitson, K. B. Mar, R. B. Richardson, A. V. Ratushny, V. Litvak, R. Dabelic, B. Manicassamy, J. D. Aitchison, A. Aderem, R. M. Elliott, A. Garcia-Sastre, V. Racaniello, E. J. Snijder, W. M. Yokoyama, M. S. Diamond, H. W. Virgin, and C. M. Rice. 2014. "Pan-viral specificity of IFN-induced genes reveals new roles for cGAS in innate immunity." *Nature* 505 (7485):691-5. doi: 10.1038/nature12862.
- Seo, G. J., A. Yang, B. Tan, S. Kim, Q. Liang, Y. Choi, W. Yuan, P. Feng, H. S. Park, and J. U. Jung. 2015. "Akt Kinase-Mediated Checkpoint of cGAS DNA Sensing Pathway." *Cell Rep* 13 (2):440-9. doi: 10.1016/j.celrep.2015.09.007.
- Seth, R. B., L. Sun, C. K. Ea, and Z. J. Chen. 2005. "Identification and characterization of MAVS, a mitochondrial antiviral signaling protein that activates NF-kappaB and IRF 3." *Cell* 122 (5):669-82. doi: S0092-8674(05)00816-0 [pii] 10.1016/j.cell.2005.08.012.
- Sharma, S., B. R. tenOever, N. Grandvaux, G. P. Zhou, R. Lin, and J. Hiscott. 2003. "Triggering the interferon antiviral response through an IKK-related pathway." *Science* 300 (5622):1148-51. doi: 10.1126/science.1081315 1081315 [pii].
- Sparwasser, T., E. S. Koch, R. M. Vabulas, K. Heeg, G. B. Lipford, J. W. Ellwart, and H. Wagner. 1998. "Bacterial DNA and immunostimulatory CpG oligonucleotides trigger maturation and activation of murine dendritic cells." *Eur J Immunol* 28 (6):2045-54. doi: 10.1002/(SICI)1521-4141(199806)28:06<2045::AID-IMMU2045>3.0.CO;2-8.
- Storek, K. M., N. A. Gertsvolf, M. B. Ohlson, and D. M. Monack. 2015. "cGAS and Ifi204 cooperate to produce type I IFNs in response to Francisella infection." *J Immunol* 194 (7):3236-45. doi: 10.4049/jimmunol.1402764.
- Su, C., and C. Zheng. 2017. "Herpes Simplex Virus 1 Abrogates the cGAS/STING-Mediated Cytosolic DNA-Sensing Pathway via Its Virion Host Shutoff Protein, UL41." *J Virol* 91 (6). doi: 10.1128/JVI.02414-16.
- Sun, L., J. Wu, F. Du, X. Chen, and Z. J. Chen. 2013. "Cyclic GMP-AMP synthase is a cytosolic DNA sensor that activates the type I interferon pathway." *Science* 339 (6121):786-91. doi: 10.1126/science.1232458.
- Sun, S., N. L. Rao, J. Venable, R. Thurmond, and L. Karlsson. 2007. "TLR7/9 antagonists as therapeutics for immune-mediated inflammatory disorders." *Inflamm Allergy Drug Targets* 6 (4):223-35.
- Sun, W., Y. Li, L. Chen, H. Chen, F. You, X. Zhou, Y. Zhou, Z. Zhai, D. Chen, and Z. Jiang. 2009. "ERIS, an endoplasmic reticulum IFN stimulator, activates innate immune signaling through dimerization." *Proc Natl Acad Sci U S A* 106 (21):8653-8. doi: 10.1073/pnas.0900850106.
- Takaoka, A., Z. Wang, M. K. Choi, H. Yanai, H. Negishi, T. Ban, Y. Lu, M. Miyagishi, T. Kodama, K. Honda, Y. Ohba, and T. Taniguchi. 2007. "DAI (DLM-1/ZBP1) is

- a cytosolic DNA sensor and an activator of innate immune response." *Nature* 448 (7152):501-5. doi: 10.1038/nature06013.
- Takaoka, A., H. Yanai, S. Kondo, G. Duncan, H. Negishi, T. Mizutani, S. Kano, K. Honda, Y. Ohba, T. W. Mak, and T. Taniguchi. 2005. "Integral role of IRF-5 in the gene induction programme activated by Toll-like receptors." *Nature* 434 (7030):243-9. doi: 10.1038/nature03308.
- Tamura, T., H. Yanai, D. Savitsky, and T. Taniguchi. 2008. "The IRF family transcription factors in immunity and oncogenesis." *Annu Rev Immunol* 26:535-84. doi: 10.1146/annurev.immunol.26.021607.090400.
- Tanaka, Y., and Z. J. Chen. 2012. "STING specifies IRF3 phosphorylation by TBK1 in the cytosolic DNA signaling pathway." *Sci Signal* 5 (214):ra20. doi: 10.1126/scisignal.2002521
- 5/214/ra20 [pii].
- Tsuchida, T., J. Zou, T. Saitoh, H. Kumar, T. Abe, Y. Matsuura, T. Kawai, and S. Akira. 2010. "The ubiquitin ligase TRIM56 regulates innate immune responses to intracellular double-stranded DNA." *Immunity* 33 (5):765-76. doi: 10.1016/j.immuni.2010.10.013.
- Unterholzner, L., S. E. Keating, M. Baran, K. A. Horan, S. B. Jensen, S. Sharma, C. M. Sirois, T. Jin, E. Latz, T. S. Xiao, K. A. Fitzgerald, S. R. Paludan, and A. G. Bowie. 2010. "IFI16 is an innate immune sensor for intracellular DNA." *Nat Immunol* 11 (11):997-1004. doi: 10.1038/ni.1932.
- Wang, C., L. Deng, M. Hong, G. R. Akkaraju, J. Inoue, and Z. J. Chen. 2001. "TAK1 is a ubiquitin-dependent kinase of MKK and IKK." *Nature* 412 (6844):346-51. doi: 10.1038/35085597.
- Wang, H., S. Hu, X. Chen, H. Shi, C. Chen, L. Sun, and Z. J. Chen. 2017. "cGAS is essential for the antitumor effect of immune checkpoint blockade." *Proc Natl Acad Sci U S A* 114 (7):1637-1642. doi: 10.1073/pnas.1621363114.
- Wang, Q., L. Huang, Z. Hong, Z. Lv, Z. Mao, Y. Tang, X. Kong, S. Li, Y. Cui, H. Liu, L. Zhang, X. Zhang, L. Jiang, C. Wang, and Q. Zhou. 2017. "The E3 ubiquitin ligase RNF185 facilitates the cGAS-mediated innate immune response." *PLoS Pathog* 13 (3):e1006264. doi: 10.1371/journal.ppat.1006264.
- Wang, Q., X. Liu, Y. Cui, Y. Tang, W. Chen, S. Li, H. Yu, Y. Pan, and C. Wang. 2014. "The E3 ubiquitin ligase AMFR and INSIG1 bridge the activation of TBK1 kinase by modifying the adaptor STING." *Immunity* 41 (6):919-33. doi: 10.1016/j.immuni.2014.11.011.
- Wang, Y., Q. Lian, B. Yang, S. Yan, H. Zhou, L. He, G. Lin, Z. Lian, Z. Jiang, and B. Sun. 2015. "TRIM30alpha Is a Negative-Feedback Regulator of the Intracellular DNA and DNA Virus-Triggered Response by Targeting STING." *PLoS Pathog* 11 (6):e1005012. doi: 10.1371/journal.ppat.1005012.
- Wassermann, R., M. F. Gulen, C. Sala, S. G. Perin, Y. Lou, J. Rybniker, J. L. Schmid-Burgk, T. Schmidt, V. Hornung, S. T. Cole, and A. Ablasser. 2015. "Mycobacterium tuberculosis Differentially Activates cGAS- and Inflammasome-Dependent Intracellular Immune Responses through ESX-1." *Cell Host Microbe* 17 (6):799-810. doi: 10.1016/j.chom.2015.05.003.

- Woo, S. R., M. B. Fuertes, L. Corrales, S. Spranger, M. J. Furdyna, M. Y. Leung, R. Duggan, Y. Wang, G. N. Barber, K. A. Fitzgerald, M. L. Alegre, and T. F. Gajewski. 2014. "STING-dependent cytosolic DNA sensing mediates innate immune recognition of immunogenic tumors." *Immunity* 41 (5):830-42. doi: 10.1016/j.jimmuni.2014.10.017.
- Wu, J. J., W. Li, Y. Shao, D. Avey, B. Fu, J. Gillen, T. Hand, S. Ma, X. Liu, W. Miley, A. Konrad, F. Neipel, M. Sturzl, D. Whitby, H. Li, and F. Zhu. 2015. "Inhibition of cGAS DNA Sensing by a Herpesvirus Virion Protein." *Cell Host Microbe* 18 (3):333-44. doi: 10.1016/j.chom.2015.07.015.
- Wu, J., L. Sun, X. Chen, F. Du, H. Shi, C. Chen, and Z. J. Chen. 2013. "Cyclic GMP-AMP is an endogenous second messenger in innate immune signaling by cytosolic DNA." *Science* 339 (6121):826-30. doi: 10.1126/science.1229963.
- Xia, P., B. Ye, S. Wang, X. Zhu, Y. Du, Z. Xiong, Y. Tian, and Z. Fan. 2016. "Glutamylation of the DNA sensor cGAS regulates its binding and synthase activity in antiviral immunity." *Nat Immunol* 17 (4):369-78. doi: 10.1038/ni.3356.
- Xu, L. G., Y. Y. Wang, K. J. Han, L. Y. Li, Z. Zhai, and H. B. Shu. 2005. "VISA Is an Adapter Protein Required for Virus-Triggered IFN-beta Signaling." *Mol Cell* 19 (6):727-40.
- Yamamoto, S., T. Yamamoto, and T. Tokunaga. 2000. "The discovery of immunostimulatory DNA sequence." *Springer Semin Immunopathol* 22 (1-2):11-9.
- Yang, H., H. Wang, J. Ren, Q. Chen, and Z. J. Chen. 2017. "cGAS is essential for cellular senescence." *Proc Natl Acad Sci U S A* 114 (23):E4612-E4620. doi: 10.1073/pnas.1705499114.
- Yang, P., H. An, X. Liu, M. Wen, Y. Zheng, Y. Rui, and X. Cao. 2010. "The cytosolic nucleic acid sensor LRRFIP1 mediates the production of type I interferon via a beta-catenin-dependent pathway." *Nat Immunol* 11 (6):487-94. doi: 10.1038/ni.1876.
- Yang, Y. G., T. Lindahl, and D. E. Barnes. 2007. "Trex1 exonuclease degrades ssDNA to prevent chronic checkpoint activation and autoimmune disease." *Cell* 131 (5):873-86. doi: 10.1016/j.cell.2007.10.017.
- Yoh, S. M., M. Schneider, J. Seifried, S. Soonthornvacharin, R. E. Akleh, K. C. Olivieri, P. D. De Jesus, C. Ruan, E. de Castro, P. A. Ruiz, D. Germanaud, V. des Portes, A. Garcia-Sastre, R. Konig, and S. K. Chanda. 2015. "PQBP1 Is a Proximal Sensor of the cGAS-Dependent Innate Response to HIV-1." *Cell* 161 (6):1293-1305. doi: 10.1016/j.cell.2015.04.050.
- Yoneyama, M., and T. Fujita. 2007. "Function of RIG-I-like receptors in antiviral innate immunity." *J Biol Chem* 282 (21):15315-8. doi: 10.1074/jbc.R700007200.
- Yoneyama, M., M. Kikuchi, K. Matsumoto, T. Imaizumi, M. Miyagishi, K. Taira, E. Foy, Y. M. Loo, M. Gale, Jr., S. Akira, S. Yonehara, A. Kato, and T. Fujita. 2005. "Shared and unique functions of the DExD/H-box helicases RIG-I, MDA5, and LGP2 in antiviral innate immunity." *J Immunol* 175 (5):2851-8.

- Yoneyama, M., M. Kikuchi, T. Natsukawa, N. Shinobu, T. Imaizumi, M. Miyagishi, K. Taira, S. Akira, and T. Fujita. 2004. "The RNA helicase RIG-I has an essential function in double-stranded RNA-induced innate antiviral responses." *Nat Immunol* 5 (7):730-7. doi: 10.1038/ni1087.
- Yoshida, H., Y. Okabe, K. Kawane, H. Fukuyama, and S. Nagata. 2005. "Lethal anemia caused by interferon-beta produced in mouse embryos carrying undigested DNA." *Nat Immunol* 6 (1):49-56. doi: 10.1038/ni1146.
- Zhang, J., M. M. Hu, Y. Y. Wang, and H. B. Shu. 2012. "TRIM32 protein modulates type I interferon induction and cellular antiviral response by targeting MITA/STING protein for K63-linked ubiquitination." *J Biol Chem* 287 (34):28646-55. doi: 10.1074/jbc.M112.362608.
- Zhang, X., T. W. Brann, M. Zhou, J. Yang, R. M. Oguariri, K. B. Lidie, H. Imamichi, D. W. Huang, R. A. Lempicki, M. W. Baseler, T. D. Veenstra, H. A. Young, H. C. Lane, and T. Imamichi. 2011. "Cutting edge: Ku70 is a novel cytosolic DNA sensor that induces type III rather than type I IFN." *J Immunol* 186 (8):4541-5. doi: 10.4049/jimmunol.1003389.
- Zhang, X., H. Shi, J. Wu, X. Zhang, L. Sun, C. Chen, and Z. J. Chen. 2013. "Cyclic GMP-AMP containing mixed phosphodiester linkages is an endogenous high-affinity ligand for STING." *Mol Cell* 51 (2):226-35. doi: 10.1016/j.molcel.2013.05.022.
- Zhang, X., J. Wu, F. Du, H. Xu, L. Sun, Z. Chen, C. A. Brautigam, X. Zhang, and Z. J. Chen. 2014. "The cytosolic DNA sensor cGAS forms an oligomeric complex with DNA and undergoes switch-like conformational changes in the activation loop." *Cell Rep* 6 (3):421-30. doi: 10.1016/j.celrep.2014.01.003.
- Zhang, Y., L. Yeruva, A. Marinov, D. Prantner, P. B. Wysocki, V. Lupashin, and U. M. Nagarajan. 2014. "The DNA sensor, cyclic GMP-AMP synthase, is essential for induction of IFN-beta during Chlamydia trachomatis infection." *J Immunol* 193 (5):2394-404. doi: 10.4049/jimmunol.1302718.
- Zhang, Z., B. Yuan, M. Bao, N. Lu, T. Kim, and Y. J. Liu. 2011. "The helicase DDX41 senses intracellular DNA mediated by the adaptor STING in dendritic cells." *Nat Immunol* 12 (10):959-65. doi: 10.1038/ni.2091.
- Zhong, B., Y. Yang, S. Li, Y. Y. Wang, Y. Li, F. Diao, C. Lei, X. He, L. Zhang, P. Tien, and H. B. Shu. 2008. "The adaptor protein MITA links virus-sensing receptors to IRF3 transcription factor activation." *Immunity* 29 (4):538-50. doi: 10.1016/j.jimmuni.2008.09.003.
- Zhong, B., L. Zhang, C. Lei, Y. Li, A. P. Mao, Y. Yang, Y. Y. Wang, X. L. Zhang, and H. B. Shu. 2009. "The ubiquitin ligase RNF5 regulates antiviral responses by mediating degradation of the adaptor protein MITA." *Immunity* 30 (3):397-407. doi: 10.1016/j.jimmuni.2009.01.008.